WCH-46
Rev. 0

Geologic Atlas Series

Late Pleistocene- and Holocene-Age

Columbia River Sediments and Bedforms: Hanford Reach Area, Washington – Part 2

E0507029

Late Pleistocene- and Holocene-Age Columbia River Sediments and Bedforms: Hanford Reach Area, Washington Part 2

Geologic Atlas Series

K. R. Fecht
T. E. Marceau

Washington Closure Hanford
Richland, Washington

March 2006

PREFACE

This report presents the results of a geologic study conducted on the lower slopes of the Columbia River Valley in south-central Washington. The study was designed to investigate glaciofluvial and fluvial sediments and bedforms that are present in the river valley and formed subsequent to Pleistocene large-scale cataclysmic flooding of the region. The purpose of the study was to:

- Identify and describe Holocene fluvial bedforms and landforms of the Columbia River in the Pasco Basin
- Reconstruct the post-glacial river history
- Evaluate the stability of the river channel along the Hanford Reach.

The study was developed in 1999 to help preserve and protect cultural resources of the Hanford Reach that would be encountered during environmental cleanup and restoration of the Hanford Site. The results of the study are being used by environmental scientists to plan cleanup work in and around culturally sensitive areas where intrusive activities will be required to investigate or remediate contaminated soils and sediments. The report also identifies the landforms along the river that have been potentially inundated by floodwaters that contained contaminants from Hanford Site operations. This information supports human health and ecological risk assessment of the shoreline areas along the Hanford Reach.

The results of the study are being published in a three-part series. This report is the second (Part 2) in the series. Part 1, which includes Chapters 1 through 3, was published in 2004 and presents background information regarding the study area and a general description of the sedimentary bedforms and geomorphic landforms encountered during the field investigations. The first report (BHI-01648) was titled *Late Pleistocene- and Holocene-Age Columbia River Sediments and Bedforms: Hanford Reach Area, Washington – Part 1*.

The Part 2 report is divided into three principal chapters and a summary and conclusion section. The first chapter (Chapter 4) provides a discussion of sedimentology and interpretation of bedforms and landforms mapped in the study area. Chapter 5 presents a discussion of the age of sedimentary deposits in the study area based on tephrochronology and radiocarbon dating methods. Chapter 6 includes a discussion of the evolutionary history of the Columbia River in the Pasco Basin from post-cataclysmic flooding up to the present-day river, as well as an evaluation of the stability of the river channel.

The final part (Part 3) of the study will include geologic maps of the lower elevations of the river valley in the Pasco Basin from Sentinel Gap (RM 410) downstream to the confluence of the Snake River at Kennewick (RM 325). The maps will be published in a separate report.

The three-part series is being published separately as a result of prime contractor changes at the U.S. Department of Energy's (DOE-RL) Hanford Site, and contractor work scope assignments by DOE-RL. For further information on the study, see Chapter 1 of Part 1.

CONTENTS

APPENDIX

TABLES

ACKNOWLEDGMENTS

Many individuals and organizations have contributed to this study and are acknowledged in Part 1 of the atlas. In addition the authors would like to specifically recognize those individuals who have directly contributed in the development Part 2. We thank Jim Sharpe for reviewing the atlas and providing useful comments that improved the overall atlas. We gratefully acknowledge Jan Boldt, Leslie Brown, and Marcie Jacques of Washington Closure Hanford's Publications group who have worked diligently in compiling several drafts and preparing the final atlas.

4.0 INTERPRETATIONS OF GEOMORPHOLOGIC LANDFORMS AND SEDIMENTARY BEDFORMS

This chapter presents (1) the characteristics and configuration of geomorphic features that make up the landscape of the Columbia River Valley, and (2) the nature and characteristics of the bedforms of late- and post-glacial sediments. The first section (Section 4.1) describes large-scale geomorphic features that form the diverse landscape of the river valley. Section 4.2 addresses lithofacies of fluvial clastic sediments that have been identified in the river valley based on their primary depositional characteristics. Section 4.3 discusses the sedimentary bedforms based on the architectural elements. Section 4.4 presents a summary of bedforms associated with a set of downward-stepping terraces that make up the low elevations of the river valley.

4.1 OVERVIEW OF LARGE-SCALE LANDFORMS IN THE PASCO BASIN

Large-scale landforms have created a landscape of a gently sloping, concave-shaped river valley bounded by anticlinal ridges. The middle and lower slopes of the valley landscape are interrupted by a variety of small-scale fluvial landforms such as terrace benches and steps, bars, and channelways. In the semiarid environment of south-central Washington, these landform patterns are readily distinguished in the field, on aerial photographs and, the large-scale features, on 1:24,000 scale topographic maps since the upper-bounding surface of the geomorphic features are well exposed. The landforms are only locally obscured with a thin veneer of surficial sediments. Vegetation over much of the river valley is sparse.

Large-scale landforms within the river valley include the laterally extensive features that typically form distinctive elements in 1:24,000 scale topographic maps. The large-scale landforms as defined in this atlas form distinct geomorphic patterns based on topographic relief characteristics, position in the river valley, and rock/sediment type. Large-scale landforms are divided into five relief generations that generally decrease in age from the higher elevations of the ridge terrain down slope into the lower elevation of the modern Columbia River. The relief generations are described below and presented in map view in Figure 4-1.

Relief Generation I: Miocene orogenic structures – Relief Generation I includes Miocene orogenic structures of anticlinal ridges, synclinal troughs, and associated faults of the Yakima Fold Belt and the broad subsidence of the Columbia Basin (Reidel et al. 1994). Structural deformation has been ongoing in south-central Washington since at least the onset of Columbia River basalt volcanism. Over the past 12 million years, the average long-term uplift and basin subsidence rates have both been approximately 40 m per million years (Reidel et al. 1994). The anticlinal ridges have locally aggraded a thin veneer of sediments, whereas the synclinal troughs have accumulated thick sequences of fluvial, lacustrine, and glaciofluvial sediments. Sediment thickness in the synclines ranges from several meters up to about 300 m.

4.1 OVERVIEW OF LARGE-SCALE LANDFORMS IN THE PASCO BASIN

Relief Generation II: Late Pliocene epeirogenic surface – The second relief generation is a late Pliocene surface that consists of an old surface of the Ringold Formation and forms an elevated terrace with remnants present on the margins of the river valley. The Ringold sequence is associated with aggradation of fluvial and lacustrine sediments followed by rapid incision into this sedimentary sequence due to a regional base level change (Newcomb et al. 1972). The terrace tread is capped by a superimposed petrocalcic horizon and a thin section of post-Ringold sediments. Ringold sediments accumulated in a subsiding basin in which the older Ringold paleotopographic surfaces are deformed and appear generally conformable to the underlying Columbia River basalt.

The upper portion of the Ringold sediments north and east of the modern-day Columbia River are relatively undeformed (PSPL 1982). Relief Generation II is divided into several subsets that can be mapped in the river valley. These subdivisions are presented in Table 4-1 and depicted in Figure 4-1.

Relief Generation III: Pleistocene glaciofluvial cataclysmic flood surfaces – This relief generation includes large-scale Pleistocene bars and elevated channelways that resulted from numerous large-scale cataclysmic outburst glaciofluvial floods. The floods inundated south-central Washington and the lower Columbia River valley, including the study area (Bretz et al. 1956, Baker 1973, Waitt 1980), primarily from ancient Glacial Lake Missoula. Flood bars represent repeated sediment aggradation from numerous cataclysmic floods over several glacial periods (Bjornstad et al. 2001). The elevated channelways were formed by floodwaters eroding into ancient valleys and across low-elevation divides. Subdivisions of this relief generation are presented in Table 4-1 and shown in Figure 4-1.

Relief Generation IV: Late Pleistocene glaciofluvial/Early Holocene fluvial surfaces – This generation includes multiple late Pleistocene glaciofluvial and early Holocene fluvial surfaces. The discharges are the result of meltwater runoff and small-scale outburst floods during retreat of the Cordilleran Ice Sheet (i.e., post-cataclysmic flooding of the river valley) and post-glacial fluvial river floods. Runoff that occurred in this generation was significantly less than large-scale outburst floods, but much greater than modern river conditions.

Relief Generation V: Middle and Late Holocene modern river condition surfaces – This relief generation includes geomorphic surfaces that are associated with runoff conditions much like conditions in the present-day Columbia River. Surfaces of this relief generation include middle and late Holocene surficial deposits of mainstream and tributary bedform surfaces and the present-day river channel and floodplain (Table 4-1 and Figure 4-1). The surfaces also include minor sidestream alluvium, eolian dunes, sheets, and streaks, and colluvial sediments and landforms.

In the subsurface of the Pasco Basin, paleotopographic surfaces form synclinal troughs and are presented in cross section that transects the river valley (Figure 4-2). Older paleotopographic surfaces tend to be concave in shape and reflect sediment aggradation during subsidence of the synclinal areas and uplift of the anticlinal ridges.

Syndepositional folding is most evident in paleotopographic surfaces of pre-Pleistocene age. Surfaces generally decrease in age upward in stratigraphic section.

Table 4-1. Relief generations and subdivisions of the Columbia River Valley of south-central Washington.

Generation I – Miocene orogenic structures
1. Structural uplift of Columbia River basalt and interbedded Ellensburg sediments that form basaltic ridges of the Yakima Fold Belt
2. Subsidence of synclinal valleys (Wahluke, Cold Creek, and Pasco synclines) forming the Pasco Basin subbasin in the central Columbia Basin
Generation II – Late Pliocene Ringold surface
3. Basin-wide sediment aggradation by Columbia River and major tributaries (Clearwater-Salmon and Yakima Rivers)
4. Local sediment aggradation by sidestreams, largest sediment contributions by Wahluke, Cold/Dry, Amon, and Zintel Creeks. Sidestreams entering the right bank of the Columbia River in the Priest Rapids segment aggraded minor sediment in the creek beds, but mainly discharged sediment load into mainstream fluvial system
Generation III – Glaciofluvial cataclysmic flood surface from periodic glacial outburst floods during the Pleistocene (degradation of valley floor due to glacial outburst floods during the Pleistocene and major river rejuvenation from late Pliocene and to possibly the early Pleistocene)
5. Upland loess sheets on basaltic ridges occurring above outburst flood level – source material is mainly outburst flood deposits from valley floor
6. Interbedded sand/silt facies of outburst flood deposits along basin margin and backflooded valleys
7. Sand-dominated facies of outburst flood deposits found on large-scale bar landforms located in intermediate position between interbedded sand/silt facies and gravel-dominated facies (e.g., distal parts of Priest Rapids, Cold Creek, Esquatzel, Kennewick bars)
8. Gravel-dominated facies of outburst flood deposits associated with large-sacle bar landforms (proximal parts Priest Rapids, Cold Creek, Esquatzel, Kennewick bars)
9. Gravel-dominated facies of outburst flood deposits in channelways
10. Landslides formed as a result of outburst floodings
11. Scabland-scoured erosional surfaces on basaltic ridge from outburst flooding
Generation IV – Late Pleistocene runoff glaciofluvial and fluvial deposits
12. Multichannel, braided mainstream alluvial deposits
13. Single channel, braided mainstream alluvial deposits
14. Single channel, straight mainstream alluvial deposits with downward stepping terrace steps
15. Single channel, straight and meandering sidestream alluvial deposits with local alluvial fan debris
16. Eolian sand dunes, sheets, and streaks
17. Colluvial debris and slopewash
Generation V – Present-day surficial deposits
18. Straight channel, mainstream alluvial deposits in channelways, overbank areas, and island/bar complexes
19. Sidestream channel gravel and sand and overband alluvium
20. Eolian sand dunes, sheets, and streaks
21. Irrigation-induced and undercut block landslide debris

4.2 LITHOFACIES OF FLUVIAL CLASTIC SEDIMENTS

This section identifies the lithofacies observed in fluvial clastic sediments of the lower relief generations (Relief Generations IV and V) of the landscape. The lithofacies are interpreted based on grain size, bedding characteristics, composition, and sedimentation, and follow the lithofacies classification of Miall (1978, 1996) (see Appendix A, Part 1). The lithofacies are presented in terms of their dominant grain size that are gravel-dominated facies, sand-dominated facies, and fine-grained facies (Sections 4.2.1 through 4.2.3).

The lithofacies descriptions are based on observations of vertical exposures as part of field mapping, interpretation of borehole logs and cuttings, and interpretation of ground-penetrating radar surveys. The field descriptions are complemented with granulometric data from analyses of samples collected from fluvial sediments exposed in the two lowest relief generations. Samples were collected by the authors over several years. Sample sites were selected from natural and anthropogenic exposures that consisted of various lithofacies within main channel and overbank fluvial environments. The samples were not collected systematically within lithofacies, and therefore textural parameters are not necessarily diagnostic of sediments that accumulated in the Columbia River valley during late glacial and post-glacial times. However, the textural parameters are considered representative of lithofacies and architectural elements.

4.2.1 Gravel Facies

Gravel bedforms result from deposition of clasts by tractive forces and molding of the stream bed through hydrodynamic processes. These forces and processes acting in the river valley have formed five distinctive gravel-dominated lithofacies:

Clast-supported, horizontally stratified gravel with felsic matrix (Lithofacies Ghf) – This lithofacies consists of clast-supported pebble-to-cobble gravel with crude to moderately well-developed horizontal stratification. The matrix of gravel units and occasional sand lenses is primarily composed of medium to fine-grained felsic (i.e., quartzofeldspathic) sands throughout most of the Hanford Reach. Lithofacies Ghf is the dominant gravel lithofacies of the lower fluvial terraces and modern Columbia River (i.e., Relief Generation V) along the Hanford Reach and much of the southern Pasco Basin. The lithofacies is observed in natural exposures along the riverbanks and margins of fluvial bars and islands. The lithofacies is also observed in abandoned trenches at mining, agricultural, and industrial sites that were excavated into the channelways along the reach from Sentinel Gap (RM 410) to Richland (RM 335).

The texture of the gravel and sand within lithofacies Ghf varies vertically in exposures. The variation primarily occurs in the gravel fraction where clasts vary from pebble to pebble-to-cobble to cobble. The texture of the sand matrix changes, not so much in the size of the particles, but the percentage of sand (i.e., overall weight percent of the sand fraction). The texture variations create the horizontal stratification in the exposures. The stratification is the result of changes in traction currents and transport rates along the stream bed (Miall 1996).

Several exposures of lithofacies Ghf have gravel clast with a preferred orientation. The long and intermediate axes of gravel clasts are oriented upstream (Figure 3-9, Part 1). This gravel structure is termed “imbrication.”

4.2 LITHOFACIES OF FLUVIAL CLASTIC SEDIMENTS

4.2.1 Gravel Facies

Clast-supported, horizontally stratified gravel with basaltic matrix (Lithofacies Ghb) – This lithofacies consists of clast-supported pebble-to-cobble gravel with moderately to well-developed horizontal stratification. The matrix of gravel units is primarily very coarse to medium sand with the composition of the sand consisting of a high concentration of basalt and lesser amounts of quartz, feldspar, and other lithic fragments. Lithofacies Ghb is commonly associated with Relief Generations III and IV. Basaltic sandy gravel locally occurs in Relief Generation V as minor lenses deposited where ephemeral side-streams discharge into the Columbia River (RM 393 to RM 406). The lenses in Relief Generation V are distinguished from the mainstream Lithofacies Ghb by the angular to subrounded gravel clasts compared to mainly subrounded clasts in Relief Generations III and IV. The lithofacies Ghb has been interpreted from ground-penetrating radar data from surveys conducted in the northern part of the Hanford Site. The lithofacies is observed in channel bedforms as tabular sedimentary clastic bodies. These features are commonly truncated by other channels eroded into the riverbed and subsequently filled with another deposit of gravel (Ghb or Ghf) or sand (Gps or Gpl) lithofacies. The textural variations observed in this lithofacies are similar to those described in lithofacies Ghf.

Trough cross-bedded gravel (Lithofacies Gt) – The lithofacies has broad, shallow trough-shaped structures and consist mostly of pebble gravel, with a matrix of mainly quartzofeldspathic sands. The trough structures are less than 45 cm deep and several meters wide. This lithofacies is infrequently observed in the study area and occurs as gravel fill in cross channels associated with mid-channel and bank-attached gravel bars and islands (Relief Generation V) mainly between “the Horn” (RM 375) and the F-Slough (RM 367) and in the northern portion of Savage Island (RM 359).

Planar cross-bedded gravel with large-scale sets (Lithofacies Gpl) – This lithofacies contains planer sets of planar cross beds of gravel sheets. The sets are greater than 30 cm in thickness, typically 1 to 1.5 m thick. The foresets have dips of 28 to 36 degrees and are oriented with dips trending in a down-current direction with a similar direction as the modern Columbia River. Large-scale cross beds are commonly exposed in excavations trenched into channel and bar segments in Relief Generations III and IV. Lithofacies Gpl has also been interpreted from ground-penetrating radar data collected from traverses across several channel and bar-shaped landforms. The gravel clasts vary in size from cobble-to-pebble with occasional boulders that are a remnant glaciofluvial lag from Relief Generation III. The matrix of the gravel is sand and silty sand. The sand composition is highly variable, with up to 95% basalt. The remainder of the sand matrix consists of quartz, feldspar, and other lithic fragments. The silt composition is commonly quartz and feldspar with only minor amounts of basalt in the coarse silt fraction.

Planar cross-bedded small-scale sets (Lithofacies Gps) – This lithofacies contains sets of planar cross-bedded gravel sheets with small-scale sets that obtain thicknesses of about 30 cm. Foresets dip about 30 degrees, with dips traveling in a similar direction to the modern Columbia River. Planar cross beds were observed in the left channel of the river at Locke Island, downstream from the channel constriction created by the encroachment of the Locke Island landslide complex into the river channel (Relief Generation V). The cross beds consist of pebble-size gravel with a matrix of quartzofeldspathic medium- to fine-grained sands. The cross-bedded gravel sheet formed in an area of flow expansion where the channel changes abruptly from a riffle to a pool, creating an environment favorable for the growth of foresets. Other lithofacies Gps are interpreted by the external expression of the bedform with downstream-dipping slip faces.

4.2 LITHOFACIES OF FLUVIAL CLASTIC SEDIMENTS

4.2.2 Sand Facies

Sand-dominated lithofacies form during sediment deposition in which particles being transported by saltation and in suspension are interrupted by a decrease in stream competency. There are three major types of sand lithofacies that have been observed in the river valley: horizontally bedded sands, low-angle cross-bedded sands, and dune forms. Dunes are present, but are only rarely exposed as minor discontinuous lenses interbedded with the major sand lithofacies. The dunes occur along modern-day riverbanks and within secondary channelways on modern-day island/bar complexes.

Horizontally bedded sands (Lithofacies Sh) – This lithofacies is characterized by horizontal, parallel laminations of primarily fine-grained, quartzofeldspathic sand (Relief Generations III, IV, and V). In the northwestern portion of the study area along the right bank (RM 393 to RM 406) this lithofacies contains basaltic sand due to the influx of basaltic-laden sediments into mainstream fluvial deposits by ephemeral side streams (Relief Generation V). Basaltic-laden sediments are common to Relief Generations III and IV. Beds vary from 5 to 45 cm in thickness with individual beds traceable along exposures for many tens of meters. There is little evidence of erosion or scour of the underlying bedding surfaces. The beds form multistory sand sequences up to about 4 m thick and commonly occur on several fluvial terraces (Relief Generations IV and V), as well as up to 20 m thick on glaciofluvial terrain (Relief Generation III). Massive to poorly bedded eolian units commonly cap individual fluvial sand units and the multistory sequences, indicating time breaks between fluvial flood events. Lithofacies Sh is commonly found within sand ridges that trend parallel to and at the edge of the channel system, and cap the gravel macroforms on bank-attached and mid-channel islands.

Low-angle, cross-bedded sand (Lithofacies Sl) – This lithofacies contains low-angle cross beds that generally dip 5 to 10 degrees. The cross-bedding is oriented downstream, making cross beds good paleocurrent indicators for reconstructing the fluvial history of the river. This lithofacies is commonly found at the downstream end of most bank-attached and mid-channel islands (Relief Generation V).

Lithofacies Sl forms vertical and downstream accretionary bedforms on mid-channel and bank-attached island/bar complexes in the river channel. Lithofacies Sl is not often preserved on active gravel bars, since these bedforms are a transient feature that are eroded off the bars and transported downstream during high-stage flow.

Massive sand (Lithofacies Sm) – Lithofacies Sm is associated with sand bodies where the original texture has been modified by post-depositional surficial processes. The massive sands appear to be the product of bioturbation that has destroyed the primary internal structures with only the bedding surfaces discernable in exposures. Bedding thickness is similar to the other major sand lithofacies Sh and Sl. This lithofacies is primarily in Relief Generation IV and V.

Basaltic plane cross-bedded sand (Lithofacies Spb) – This lithofaces consists of cross-bedded sand that form two-dimensional dunes. The dips of the foreset beds range from 20 to 30 degrees. The grain size in cross-bed sets is typically coarse to very coarse sand with the composition high in basalt. The upper and lower bounding surfaces are very sharp. Lithofacies Spb is commonly observed in Relief Generations III and IV. Beds are commonly 30 to 100 cm thick.

Felsic plane cross-bedded sand (Lithofacies Spf) – Lithofacies Spf is similar to lithofaces Spb, except the sands are mostly felsic (i.e., quartz and feldspar) and the bedding thickness ranges up to about 40 cm (Relief Generation V).

4.2 LITHOFACIES OF FLUVIAL CLASTIC SEDIMENTS

4.2.3 Fine-Grained Fluvial Facies

The fine-grained clastic sediments are typically deposited from the suspended load of streams and require low-energy environments for deposition. Within the study area, these lower energy environments include floodplains, secondary channelways, and abandoned channelways.

Several fluvial lithofacies of fine-grained sediments have been observed within exposures found within Relief Generations IV and V.

Laminated sand, silt, and mud (Lithofacies Fl) – This lithofacies consists of thin lenses of laminated mud, silt, and fine- to very-fine-grained sand. The lenses are slightly undulating with plant roots and bioturbation occasionally intermixed with eolian sand lenses/beds. The typical thickness of the lithofacies is a few centimeters up to about 1.5 m. This lithofacies is commonly deposited in the low-energy environments such as within slough areas adjacent to secondary channels associated with bank-attached islands (e.g., F-Slough [RM 367] and Hanford Townsite [RM 363]).

Massive mud and silt (Lithofacies Fm) – This lithofacies contains massive beds of mud silt and sand. This massive mud and silt lens is several centimeters thick and occasionally found in distal areas associated with ponding in high-stage flow. The lithofacies is associated with lithofacies Fl and found in the same low-energy environments. Desiccation cracks are occasionally observed in upper bounding surfaces.

Silt and mud (Lithofacies Fsm) – Lithofacies Fsm forms massive mud and silt beds, but does not contain sand lenses. Lithofacies Fsm has similar thickness as Lithofacies Fm. It was also deposited in similar low-energy environments as Lithofacies Fm.

4.3 ARCHITECTURAL ELEMENTS ASSOCIATED WITH COLUMBIA RIVER SEDIMENTS

The fluvial architectural elements define the primary depositional macroforms or bedforms identified in the river valley. The elements are composed of distinct facies assemblages that have well-defined bounding surfaces and mappable geomorphic form. The lithofacies assemblages that form architectural elements are based on the descriptions presented in Section 4.2. The bounding surfaces and geometry of the elements were identified in the field as part of the mapping study supplemented by examination of several excavations constructed into bedforms and ground-penetrating radar profiles of surveys over the surface of bedforms. The locations of supplementary areas were selected to include main channel and overbank environments. The architectural elements defined in this study are presented in Table 4-2 along with the major lithofacies assemblages identified in the element.

Architectural elements within lower elevations of the study area are discussed in terms of channel and overbank environments. The architectural elements in channel environments include CHL, CHM, GBL, GBM, SB, DA, and CH(FF). Channel elements in this report are subdivided into two groups based on the scale of the bedforms. Bedforms of CHL and GBL are much larger in overall surface area and thickness than other channel elements. These two elements are associated with Pleistocene cataclysmic glaciofluvial flooding from outburst floods (Relief Generations III and IV). The large-scale bedforms reflect flow rates and water volumes that far exceeded those riverine elements investigated in the study area during post-glacial times.

Table 4-2. Architectural elements of late Pleistocene and glaciofluvial and Holocene fluvial sediments.

Element	Symbol	Major Facies	Geometry and Relationships	Interpretation
Channels – large scale	CHL	Ghl with Gpl, Spb	Sheets; often 15 m thick with tails, several km wide; stacked bedforms	Cataclysmic glaciofluvial channel deposits
Channels – moderate scale	CHM	Ghf with Gps, Gt, Spf	Lens and sheets; up to 5 m thick with tails; up to 1 km wide; multi-story	Entrenched fluvial channel deposits
Gravel bars – large scale	GBL	Gpl, Spb	Lens; >5 m thick; >500 m wide and >1,000 long; multi-story	Braided glaciofluvial channel deposits
Gravel bars – moderate scale	GBM	Gps	Lens; 1 to 5 m thick with tails; up to 100 m wide and 500 m long; multi-story	Braided fluvial channel deposits
Sandy bedforms	SB	Sh, Sm	Sheets; <1 m thick; lies on CHM	Transient transverse bar deposits (deposited in less than bank full flow)
Downstream – accretion bedforms	DA	Fs, Fsm	Tubular; up to 4 m thick; up to 700 m wide and occasionally over 1,500 m in length; multi-story; lies on and interbedded with CHM	Mid-channel and bank-attached bars
Overbank Fines	FF	Fm, Fsm	Sheets; up to 1.5 m thick; typically <100 m wide; interbedded with LV	Overbank sheet flow and floodplain ponds
Levee	LV	Sh, Fl, Fm, Fsm	Wedge; up to 3 m thick; up to 40 m wide and variable length (30 m to several km); interbedded with FF; overlies CHM	Overbank flooding adjacent to channel
Crevasse channel	CR	Sh with Fsm (?)	Lens; <2 m thick; 1 to 2 m wide and less than 40 m long	Breach in main channel margin
Crevasse splay	CS	Fm, Fsm	Lens; <1 m thick; estimated at 30 m wide by 40 m long	Delta-like progradation from crevasse channel into floodplain
Abandoned channel	CH(FF)	Fs, Fsm	Ribbon; <1.5 m thick, up to 100 m wide; overlies CHF	Product of chute or neck cutoff

4.3 ARCHITECTURAL ELEMENTS ASSOCIATED WITH COLUMBIA RIVER SEDIMENTS

Bedforms of CHM, GBM, SB, DA, and CH(FF) were commonly encountered in fluvial channel environments. CHM is highly variable in shape. GBM, SB, and DA are associated with bar and island complexes. CH(FF) is found as fine-grained capping plugs in abandoned channelways. GBM is the most common element in Relief Generation IV based on examination of surface morphologies in aerial photos and geologic maps, exposures in constructed excavations, and ground-penetrating radar profiles. CHM is the most common element exposed in Relief Generation V. CHM, GBM, SB, DA, and CH(FF) have been locally observed in sediments associated with Relief Generations III and IV, but are the common elements of fluvial environments in Relief Generation V.

The overbank environment is dominated by two architectural elements, FF and LV, and is found in Relief Generation V. The lateral boundary conditions between the channel and overbank elements are typically sharp with no observed interbedding relationships. The friable fine-grained texture of overbank material is easily eroded by stream power in the main channel environments. In localities where FF and LV are present, the two elements are often interbedding observed in the overbank environment proximal to the channel deposits. The two elements are distinguished in the field based on the geometry of bedforms. FF is found as broad thin sheets. LV forms thin sand wedges and narrow ridges. Other overbank elements have been identified in the study area, but the elements are smaller in scale (e.g., crevasse channel and crevasse splay) and are not discussed in this report.

4.4 COLUMBIA RIVER TERRACES

The field reconnaissance of the Hanford Reach segment of the Columbia River Valley revealed a flight of late-glacial and post-glacial downward-stepping terraces that vary in length, width, and height, and differ in geomorphic character (Figure 4-3). The terraces were defined based on an analysis of topographic maps and aerial photographs of the modern river valley, followed by walking out fluvial geomorphic landforms identified from the maps and photographs. Sediments were sampled from cutbanks and other exposures for textural analysis. Volcanic ash locations were identified and samples collected for analysis of the specific eruption and to aid in dating ash-bearing terraces (Section 5.1). Organic material (i.e., shell, bones, charcoal, and wood) was collected for absolute age date (Section 5.2). The terraces and other alluvial features (channel, bar, and overbank features) and sample locations were delineated on base maps using U.S. Geological Survey 1:24,000 topographic maps. Aerial photographs, topographic features, and global positioning measurements aided in accurately locating terrace landforms and sample locations on base maps.

The correlation of remnant terrace segments on the topographic base maps was based on the following:

- Results of inspection of aerial photographs
- Survey measurements using global positioning systems
- Presence of marker horizons (i.e., volcanic ash tephra)
- Absolute age by carbon-14 dating (including specific volcanic ashes with known dates of eruption)
- Relative stage of soil pedogenesis.

4.4 COLUMBIA RIVER TERRACES

Within the Pasco Basin numerous terraces have been identified and mapped primarily as part of regional studies supporting the siting, construction, and operation of nuclear facilities on the U.S. Department of Energy Hanford Site. Many of the terraces that were mapped in these studies are Pleistocene depositional bars or erosional landforms (e.g., WCC 1981). Younger terrace remnants were also identified in archaeological studies along the Columbia River (Chatters et al. 1992). Figure 4-4 summarizes many of the terraces in or adjacent to the study, including terraces addressed in this study.

Seven lower river valley terraces were identified and mapped along the Columbia River Valley. Only paired terraces that are Holocene age or the youngest Pleistocene terraces are described in detail in this atlas. Unpaired terraces in the study area are generally small in aerial extent and typically isolated to areas near ancient river bends. The topographic position and relationship to main terraces for unpaired terraces are briefly discussed.

In this atlas the terraces are named based on an alphanumeric system. The first symbol is a letter that designates the geologic epoch: "P" for Pleistocene-age terraces and "H" for Holocene-age terraces. The second symbol is a number that designates the terrace within an epoch, starting with "1" as the oldest mapped terrace and increasing sequentially to the youngest terrace. The terraces are differentiated into six Holocene-age terraces (H-1 through H-6) and the youngest Pleistocene-age terrace (P-1). Terraces older than P-1 are designated P-X. A summary description of each terrace from oldest to youngest is provided in the following sections.

4.4.1 Pleistocene Terraces

Numerous late-Pleistocene terrace landforms have been identified in the Columbia Basin (WCC 1981). This report addresses only the youngest Pleistocene terrace with remnants that are extensively exposed from Sentinel Gap (RM 410) down to the north end of Richland (RM 345). This terrace is interpreted to represent a period of high flow rates from runoff of glacial meltwater that post-dates the last large-scale cataclysmic flooding from Glacial Lake Missoula.

P-1 Terrace. The P-1 Terrace represents a series of remnant terraces about 22 m above the normal level of the modern Columbia River. In Relief Generation III, the tread is relatively flat and free of secondary landforms (e.g., channels and bars). The margins of the terrace in many locations are well defined with steep to moderately steep descending escarpments to one of the lower Holocene terrace benches and gently to moderately steep ascending escarpments up into the lower valley. The sediment cover on the tread is highly basaltic sandy granule gravel to sandy cobble-boulder gravel. The terrace remnants merge south of RM 385 with several abandoned channelways of an ancient river valley. In the merger area, the upriver end of the southernmost abandoned channelways is partially filled with gravel as the channelways became plugged when the river discharge was reduced and the river migrated to the northern channelways. Downstream from the merger area, the abandoned channelways contained several secondary landforms not observed in the remnant terraces. These secondary landforms included large-scale current ripples, bank-attached and mid-channel bars (including longitudinal and transverse bar bedforms), and secondary channelways. The terraces and abandoned channelways bifurcate around several large land masses north and south of Gable Mountain before merging into a broad, single channelway from near the Wye Barricade area (9 km west of RM 353) to the downstream boundary north of Richland (RM 345). South of RM 345, the terrace loses definition where it intersects with the lower Yakima River Valley.

4.4 COLUMBIA RIVER TERRACES

4.4.2 Holocene Terraces

Several small (Figure 4-3), isolated terraces were observed between the P-1 and H-1 Terraces. Along the margins of this northern channel these small, isolated terraces occur on the inside of the river bend in the "horn" area of the Hanford Reach. The margins of these small terraces are well defined with steep scarps.

At the end of the Pleistocene, the Columbia River changed from a multichannel river between RM 353 and RM 385 to a single channel defined by the northernmost channel of the late Pleistocene channelway network. With the formation of a single channel along the 51-km (32-mi) segment, the Columbia River formed a single channel along the entire 124-km (77-mi) reach of the study area, with only minor interruption of secondary channels associated with bank-attached and mid-channel bars.

The sediments in these terraces mark a change in the compositional assemblages of the sand fraction transported and deposited by the Columbia River. Basalt dominated the composition in the sand fraction of glaciofluvial sediments in Pleistocene landforms in much of the Hanford Reach. In the earliest Holocene terraces, the sand fraction composition returned to predominantly quartzofeldspathic sands, which was characteristic of the Columbia River sands during preglacial times (see Fecht et al. 1987).

Several point-bar deposits were identified in the study area that are remnants of the earliest Holocene river channel. These remnants formed prior to the H-1 Terrace. These terrace remnants are limited in aerial extent, and are unpaired, erosional terraces primarily located in the Columbia horn region (e.g., in and around 100-D Area) of the study area. These small terrace remnants are discussed further in the "Horn" river segment (Section 3.1, Part 1). Most of these small terrace remnants are obscured beneath eolian sand sheets and dune colonies and were only recently encountered during borehole drilling operations and construction activities in support of environmental restoration at the U.S. Department of Energy's Hanford Site.

H-1 Terrace. The H-1 Terrace is the oldest of the extensive terraces in the Holocene terrace system. The H-1 Terrace consists of a series of terrace remnants that are characterized by a broad, undulating, gently sloping, pebble-to-cobble gravel clast landform with a tread that occasionally contains low-amplitude channel and bar bedforms. The terrace represents the main river channel of an ancient Columbia River. The H-1 Terrace lies about 12 m above the low water level of the Columbia River and about 2 m above the H-2 Terrace. The remnants of the H-1 Terrace have poorly defined margins in areas with gentle lower valley slopes but is well defined in areas with moderately steep slopes. In many areas the terrace margins and treads are masked by eolian dune colonies that veneer many parts of the Hanford Reach.

H-2 Terrace. The H-2 Terrace has many of the same characteristics of the H-1 Terrace with broad, undulating, gently sloping, gravelly tread. The H-2 Terrace contains more abundant low-amplitude channel and bar geomorphic bedforms than are present with the H-1 Terrace. Like the H-1 Terrace, the H-2 Terrace represents an ancient river channel of the Columbia River. The H-2 Terrace lies about 4 m above the H-3 Terrace. The H-2 Terrace remnants have poorly defined margins due to the gentle slopes at the boundaries of the terraces. In places the terrace margins and treads are obscured beneath eolian dune colonies covering much of the Hanford Reach area.

4.4 COLUMBIA RIVER TERRACES

4.4.2 Holocene Terraces

H-3 Terrace. The H-3 Terrace is a prominent terrace in the upstream portion of the study area between Priest Rapids Dam and Vernita Bridge (RM 395 to RM 388) and between Bateman Island (RM 334) and the end of the study area (RM 325). Kennewick Man was eroded from near the base of the H-3 Terrace. On the left bank of the river from Vernita Bridge to the Wahluke Ferry Landing across from 100-D Area (RM 378), the H-3 Terrace is partially hidden behind the H-4 Terrace. The tread of the H-3 Terrace is only at a slightly higher elevation (about 1.6 km [1 mi)] than the tread of the H-4 Terrace. The position and similar topographic relief often obscures the H-3 Terrace. In addition, eolian sand sheets and dune colonies commonly cover the surface of the two terraces.

The H-3 Terrace is a compact sequence of fine-grained sediments including a thin, fine-sand base, thick silty sand middle section, and compact sand cap. The fine sand base is an alluvial deposit that commonly consists of three or four stories of plane-laminated fine sand. The thick middle sequence consists of remnants of multistory, plane-laminated beds that vary between normally graded beds and beds with fine sand lenses capped by silty sand stringers. Bed thickness generally ranges between 15 to 40 cm. The upper sand cap is a massive fine-grained sand unit that in several localities contains a distinctive volcanic ash (Mazama ash, see Section 5.1) horizon interbedded with the sand near the top of the cap unit. The sand cap is interpreted to be eolian in origin, but heavy bioturbation has destroyed any primary bedding structures that could be used to determine origin. The ash appears to be mostly from airfall with only minor reworking by fluvial processes. The ash is present in numerous locations in remnants of the H-3 Terrace and in fine sandy plugs in abandoned side channels from above Priest Rapids Dam (RM 395) to Kennewick (RM 330). The river margin of the terrace is distinctive with a steep bluff on the river side. The bluff when present forms a cutbank in the upper 11 km (7 mi) of the study area.

H-4 Terrace. The H-4 Terrace is the most extensive of the Holocene terraces in the Hanford Reach. The terrace occurs on both sides of the river and many bank-attached and mid-channel islands. The terrace is not present on active low-relief mid-channel bars and areas of river bluffs/cliffs. The terrace tread is situated about 5 m above the low water level of the river and 3 m above the H-5 Terrace.

The H-4 Terrace consists of predominantly compact fine sands and a loose massive fine-sand cap. The compact sand sequence mainly consists of multistory, plane-laminated, fine-sand beds. In some areas, the sequence has been bioturbated and the sands appear massively bedded. The compact sands are primarily floodplain alluvium that was deposited during deceleration of floodwaters as the river over-flowed its banks during periods of high discharge. The loose sand cap primarily consists of eolian sand sheets and dune colonies. On several island/bar complexes, the H-4 Terrace is coarse grained with gravel that ranges from pebble-to-cobble in size. The terrace along most of the Hanford Reach is generally narrow (i.e., less than 100 m wide). The terrace characteristically forms a natural levee above the steep slope on the river-side edge of the terrace landform. In areas where the terrace is narrow (~15 m wide) the terrace consists solely of a natural levee landform.

In several areas, portions of the H-4 Terrace have been partially scoured by lateral erosion leaving several isolated remnants of a small, narrow terrace. All remnants of this terrace occur on the inside bend of the Columbia River in the “Horn” region. The terrace remnants are about 1 m below the H-4 Terrace. The terrace does not appear to be present on the opposite side of the river. The terrace has similar textural characteristics to the H-4 Terrace and geomorphic characteristics to the small isolated terrace remnants between the P-1 and H-1 Terraces.

4.4 COLUMBIA RIVER TERRACES

4.4.2 Holocene Terraces

H-5 Terrace. The H-5 Terrace is the second youngest terrace in the terrace network within the study area. The H-5 Terrace is situated as a step about 1 m above the H-6 Terrace and 2 m above the normal river level. The terrace forms a series of valley remnants along extensive portions of the reach on both sides of the river and bank-attached and mid-channel islands/bars. Although the terrace is not present along river cliffs, bluffs, and cutbanks, narrow benches and minor breaks in slopes occur at the same elevation as the terrace. The margins of the terrace are well defined with a steep ascending slope or minor bluff to the H-4 Terrace and other landforms, and a moderately steep descending slope to the H-6 Terrace. The H-5 Terrace landform has three textural types:

- Gravel textural type consists of gravel that ranges from pebble-to-cobble-boulder in clast size. Treads of the gravel textural type commonly contain mud infilling that is trapped in the spaces among clasts. Fine-grained alluvial caps are rarely observed on treads of this textural type. This textural type is most commonly found on the lower edges of the H-5 Terrace in areas where the terrace is frequently inundated by high river discharges associated with spring run.

- Gravel and sand textural type consists of a basal gravel unit with a capping fine sand unit. The basal gravel unit has similar characteristics to the gravel in the gravel textural type. The capping sand unit is composed of loose to locally compact fine-grained sand that is up to about 1 m thick. The capping sand unit is interpreted to be deposited by a combination of sediments accumulated in overbank environments from periodic river flooding of the terrace and eolian sand sheets and dune colonies migrating across the terrace tread. The capping sand unit is commonly observed on the upper margins of wider segments of the terrace that are protected from erosion during periods of high discharge during river flooding or from high winds that must have frequented the Hanford Reach. The capping sand unit commonly supports varying densities of plant communities (e.g., grasses, junipers).

- Sand textural type consists of fine-grained sediments with predominant grain sizes of fine to silty fine sand. The sand textural type is commonly associated with alternate bars (or opposite bank from the thalweg) or bank-attached islands/slough complexes in the study area. The sand textural type occurs in protected areas marginal to high-discharge channelways where floodwaters reduce flow rate and deposit fine sands. This textural type generally supports abundant grass communities in the study area.

H-6 Terrace. The H-6 Terrace is the lowest and youngest river step in the Columbia River Valley terrace system within the study area. The tread has irregular, undulating surface slopes that gently slope toward the river. At the river's edge, the terrace lies about 1.0 to 1.5 m above normal river level. The terrace is preserved as a series of extensive remnants of highly varying widths (i.e., <5 m to >100 m). The terrace is found on both sides of the river and many of the bank-attached and mid-channel islands/bars in areas of gently sloping riverbanks. The terrace is absent along the portions of the reach with river cliffs, bluffs, and cutbanks, but in these river segments of the reach very narrow erosional benches or "strand lines" occur at the same position above the river as the terrace. The terrace bedforms consist of plane-bedded gravel units with clasts that vary from pebble-to-cobble-boulder in size. The cobble-boulder clasts commonly occur as a lag on the terrace tread. The matrix of the gravelly terrace landform is predominantly well-sorted medium-to-fine sand. The tread gravels commonly contain a mud that was transported by the river and trapped in the spaces among clasts. The muddy gravel supports an ever-increasing density and diversity of vegetation on the riverbanks. The density and variety of vegetation cover along the riverbanks has been increasing since the senior author first started studying the sedimentary deposits and bedforms along the riverbanks in 1968.

4.4 COLUMBIA RIVER TERRACES

4.4.2 Holocene Terraces

H-6 Terrace (Continued)

In the present-day slough areas (i.e., 100-H Area, 100-F Area, Hanford, and Savage Island) and the inside of river bends on the opposite side of the river as the thalweg (e.g., Coyote Rapids, Columbia Horn, and Energy Northwest), the H-6 Terrace is capped by a sedimentary fill that varies in thickness from 30 cm up to about 1.5 m. The lower portion the sedimentary fill is moderately compact fine to silty fine sand and interpreted as overbank alluvium. The upper portion of the fill is loose massive fine to silty fine sand of eolian origin. The sedimentary fill units are present in areas on the terrace distal to the channelways and protected from erosion from flooding during high river stage and eolian dune sands cap the alluvial fill.

5.0 GEOCHRONOLOGY OF LANDFORMS AND SEDIMENTS IN LOWER ELEVATIONS OF THE COLUMBIA RIVER VALLEY

This chapter presents a discussion of the age relationships and age estimates of late Pleistocene and Holocene landforms and sediments investigated within the study area. Age estimates are based on (1) time relationships (correlation) among stratigraphic units and (2) the "absolute" chronology (age) of stratigraphic units or marker horizons. Geochronologic determinations are focused on alluvial deposits of and landforms created by the Columbia River. Dating of other stratigraphic units and landforms has been included in the study to help constrain the age of the alluvial deposits.

Two established dating methods were used in this study: tephrochronology and radiocarbon dating. These methods were selected because:

- The methods are well established in the study of Quaternary sediments and landforms (Noller et al. 2000)
- Fine-grained sediments in overbank and point-bar deposits in the river valley contain organic material amenable to radiocarbon dating.
- Radiocarbon dates from other studies/sources can be readily used to complement radiocarbon-date measurements determined as part of this study.
- Tephra horizons are frequently encountered in sediments that are positioned above, intercalated in, or below the late Pleistocene and Holocene alluvial sediments and landforms throughout the central Columbia Basin.

5.1 TEPHROCHRONOLOGY

Tephra layers are commonly encountered in sedimentary deposits at lower elevations of the Columbia River Valley and form important stratigraphic markers. Tephra horizons important to this study are from Glacier Peak, Mount Mazama (Crater Lake), and Mount St. Helens (Section 1.2 of Part 1). The most common tephra layers in the study area are Mount St. Helens Set S (estimated at 13,000 radiocarbon years before present [rcybp] [Benito and O'Connor 2002]), Glacier Peak (11,250 ± 250 rcybp [Porter 1978, Mehringer et al. 1984]), climactic Mazama (6,845 ± 50 rcybp [Bacon 1983]). These layers represent discrete layers of fine-grained airfall tephra from explosive eruptions of composite volcanoes located in the Cascade Range (Figure 5-1). Ash layers make excellent stratigraphic markers for correlating sedimentary units based on distinct physical and chemical properties of geologic materials from an eruptive event (Mullineaux 1986). Petrologic and geochemical studies have demonstrated that the composition of magmas can be distinguished among volcanoes (Nakagawa and Ohba 2002), and within multiple eruptive events from a single volcano. Volcanic ash layers also make excellent time markers where the age of an ash has been established to another dated sediment or rock type.

This section presents the following discussion:

- The identification of the volcanic sources of ashes in the study based on physical and chemical characteristics of three volcanic ashes
- The role of ashes in establishing chronological control of geomorphic features and sedimentary sequences within the study area.

5.1 TEPHROCHRONOLOGY

5.1.1 Occurrences and Characteristics of Ashes in the Field

Volcanic ashes are well known to the area (e.g., Moody 1977, 1978, 1987; Mullineaux 1972, Mullineaux et al. 1975; Baker et al. 1991). Ash has been found in more than 100 localities within lower elevations of the study area. Ashes are observed in exposures and cores retrieved from drilling operations. The report focuses on three key volcanic ashes to aid in stratigraphic correlation and as time markers (Mount St. Helens Set S, Glacier Peak, and Mazama).

The distribution and general occurrences of the selected ash horizons are illustrated in Figure 5-2 based on information on ashes contained in Table 5-1. These localities were chosen to illustrate the distribution of ash horizons over the river valley and within the study area.

In field exposures, volcanic ash layers form thin horizons (generally less than 20 cm thick and often less than 50 mm thick) that stand out in distinct contrast to bounding sediments due to the very light color of the ash, typically white (7.5YRN8 to 10YR8/1) to light gray (10YR7/1 to 10YR7/2). Texturally, the volcanic ash is fine grained, ranging from sandy silt-clay to silty very fine-to-fine sand (Table 5-2 and Figure 5-3), generally well sorted, and display massive bedding except in areas where the ash has been reworked by surficial processes. Hand lens inspection commonly reveals colorless volcanic shards (felsic glass fragments), crystallites, and lithic fragments. The lower contact of ash layers forms a distinct sharp boundary with underlying sediments. Gradational upper contacts are most common in eolian dune complexes where ash has been reworked by the prevailing winds. The upper contact with overlying fluvial and loessal sediments is typically sharp, but occasionally is gradational with ash rapidly incorporated in the upper sedimentary unit. The ash horizons and boundary sediments typically exhibit evidence of bioturbation from intrusion by animals, insects, and plants.

The ashes are primarily deposited from air fall and mantled the topographic expression of the landscape that existed at the time of the volcanic eruption. The ancient landscape in the study area varied from relatively low relief terrain on terrace steps along the Columbia River Reach to undulating topography on older Holocene and Pleistocene terraces.

The field characteristics used to distinguish these ashes include horizon thickness, color, grain size (grittiness), number of closely spaced eruptive events, and stratigraphic context. A summary of the field characteristics are presented in Table 5-3.

The oldest of the three ashes is Mount St. Helens Set S, and its diagnostic characteristics are multiple eruptive events (typically a couplet to triplet and with several older ash layers commonly present several decimeters below the couplet/triplet), fine-grain size, and association with late Pleistocene glaciofluvial sediments in lower elevations of the river valley. Glacier Peak is recognized by multiple eruptive events (couplet), and the ash commonly has a gritty texture. Mazama is the youngest of the three ashes and is commonly thicker than the other two volcanic ashes (greater than 20 cm in thickness). Mazama ash often displays color variations with the upper portion white (7.5YRN8 to 10YR8/1) to light gray (10YR7/1 to 10YR7/2), and a lower portion having a pinkish (5YR8/3 to 5YR8/4) hue.

The Mount St. Helens 1980 ash layer is also commonly observed in the study area, but is not as important a stratigraphic marker due to the very young age (i.e., May 18, 1980) of the eruptive event. It is distinguished in the field by a single, generally thin (less than 6 mm thick) layer of ash that is exposed at the top of many sedimentary exposures.

Care must be taken when solely using field characteristics for identifying ashes because post-depositional processes may rework the ash and change field characteristics (particularly thickness and textural character).

Table 5-1. Selected tephra localities used in this study. (3 Pages)

Site Number	Location	Sample Number/ Collector	Probable Source[a]	Basis for Identification[b]	Depositional Environment	Reference
1	15/23-15A	C9302/J. T. Lillie	M	A	Talus in Sentinel Gap	Baker et al. 1991; Reidel and Fecht 1994a
2	13/23-4A	--	M	A/F	Sand sheet on lee side of Umtanum Ridge	This study
3	13/23-1D	--	M	A	Capping overbank alluvium in Moran Slough	Greengo 1959
4	13/23-12	--	M	F	Capping overbank alluvium	Brett Lenz personal communication
5	13/24-14	--	M	F	Sand sheet on lee side of Umtanum Ridge	This study
6	13/24-14	--	GP	F	Loess on lower north flank of Umtanum Ridge	This study
7	13/24-12M	KRF-99-114/K. R. Fecht	M	A/F	Capping alluvial plug in abandoned fluvial channel	This study
8	13/25-6E	--	MSH	F	Lee slope of gully eroded into Priest Rapids Bar	This study
9	13/25-7C	--	M	F	Parabolic dune atop channel and overbank alluvial	This study
10	13/25-64	--	M	F	Parabolic dune atop overbank alluvium	This study
11	14/25-32B	--	M	F	Capping overbank alluvium	This study
12	14/25-27H	--	M	F	Dune sand on lee side of Priest Rapids Bar	Reidel and Fecht 1994a
13	14/25-14K	KRF-02-002/K. R. Fecht	GP	A/F	Loess sheet below parabolic dune complex	This study
14	14/26-16E	--	M	F	Parabolic dune atop alluvial gravel	This study
15	14/26-2M	--	M	F	Sand sheet on lee side of gully eroded into White Bluffs escarpment	Reidel and Fecht 1994a
16	14/26-11E	--	M	F	Parabolic dune complex	This study
17	14/26-1F	KRF-02-001/K. R. Fecht	S	A/F	Plane/ripple-laminated sand-dominated glaciofluvial sequence	This study
18	14/26-23N	--	M	F	Sand sheet above interbedded eolian fluvial sands	Reidel et al. 1992
19	14/26-25L	--	M	F	Sand sheet atop undifferentiated gravel	Reidel and Fecht 1994a
20	14/27-29	KRF-01-080/K. R. Fecht	M	A/F	Capping overbank alluvium	Marceau et al. 2003a
21	14/27-32	--	M	F	Sand sheet atop fluvial cap	This study
22	14/27-33	--	M	F	Blowout in dune of lee side of bar	Marceau et al. 2003b
23	14/27-33	KRF-02-003/K. R. Fecht	M	A/F	Capping alluvial plug in abandoned fluvial channel	This study
24	13/26-11B	--	M	F	Blowout in parabolic dune	Reidel and Fecht 1994a
25	13/26-24G	--	S	F	Sand-dominated glaciofluvial sequence	CDA, 1969
26	13/24-29L	--	S	F	Loess sequence	Reidel and Fecht 1994a
27	13/24-34	--	M	F	Eolian sand atop bar in Cold Creek	Reidel and Fecht 1994a
28	13/24-36L	--	S	F	Interbedded sand and silt glaciofluvial sequence in bergmound mound	Fecht and Tallman 1978
29	13/24-36M	--	S	F	Interbedded sand and silt in glaciofluvial sequence in bergmound	Fecht and Tallman 1978
30	13/24-36	RHT-25/A. M. Tallman and K. R. Fecht	S	A/F	Interbedded sand and silt in glaciofluvial sequence in bergmound	Fecht and Tallman 1978; Baker et al. 1991
31	12/25-3C	C6113/K. R. Fecht	S	A/F	Interbedded sand and silt in glaciofluvial sequence in bergmound	Reidel and Fecht 1994a
32	12/25-3J	C9290AB&C/J. T. Lillie	S	A/F	Interbedded sand and silt in glaciofluvial sequence	Baker et al. 1991
33	12/25-2P	BB820-28	S	F	Interbedded sand and silt in glaciofluvial sequence	Baker et al. 1991
34	12/25-2Q	--	S	F	Interbedded sand and silt in glaciofluvial sequence	Reidel and Fecht 1994a
35	12/25-12D	--	S	F	Sand-dominated facies of glaciofluvial sequence	Reidel and Fecht 1994a

Table 5-1. Selected tephra localities used in this study. (3 Pages)

Site Number	Location	Sample Number/ Collector	Probable Source[a]	Basis for Identification[b]	Depositional Environment	Reference
36	12/25-12L	--	S	F	Sand-dominated facies of glaciofluvial sequence	Price and Fecht 1976
37	12/26-7H	--	S	F	Sand-dominated facies of glaciofluvial sequence	Fecht and Weekes 1996
38	12/26-7H	--	S	F	Sand-dominated facies of glaciofluvial sequence	Fecht and Weekes 1996
39	12/26-8E	--	S	F	Sand-dominated facies of glaciofluvial sequence	Fecht and Weekes 1996
40	12/26-9H	--	S	F	Sand-dominated facies of glaciofluvial sequence	Smith 1993
41	12/26-9J	--	S	F	Sand-dominated facies of glaciofluvial sequence	Reidel and Fecht 1994a
42	12/26-10E	--	S	F	Sand-dominated facies of glaciofluvial sequence	Reidel and Fecht 1994a
43	12/26-12D	--	S	F	Sand-dominated facies of glaciofluvial sequence	Reidel and Fecht 1994a
44	12/26-1F	KRF-02-004/K. R. Fecht	S	A	Sand-dominated facies of glaciofluvial sequence	Fecht unpublished geologic mapping
45	12/26-1F	KRF-02-005/K. R. Fecht	S	A	Sand-dominated facies of glaciofluvial sequence	Fecht unpublished geologic mapping
46	12/26-1F	--	S	F	Sand-dominated facies of glaciofluvial sequence	Reidel and Fecht 1994a
47	13/27-28R	C6083/K. R. Fecht	M	A/F	Blowout in parabolic dune atop gravel-dominated facies of glaciofluvial sequence	Reidel and Fecht 1994a
48	12/28-5B	KRF-99-101/K. R. Fecht	M	A/F	Blowout in parabolic dune	This study
49	12/28-3L	BB-891/B. N. Bjornstad	M	A/F	Surficial sediment on White Bluffs escarpment	Baker et al. 1991
50	12/25-30B	C6126, C6127/K. R. Fecht	S	A/F	Gravel-dominated facies of glaciofluvial sequence	Reidel and Fecht 1994a
51	12/25-28B	C6128/K. R. Fecht	S	A/F	Interbedded sand and silt facies in glaciofluvial sequence	Baker et al. 1991
52	12/25-28G	C6123, C6124, C6125/ K. R. Fecht	GP	A	Sidestream alluvial sequence	Reidel and Fecht 1994a
53	12/25-26L	--	S	A/F	Interbedded sand and silt facies of glaciofluvial sequence	Reidel and Fecht 1994b
54	11/26-14K	C9281/J. T. Lillie	S	A/F	Interbedded sand and silt facies of glaciofluvial sequence	Baker et al. 1991
55	11/26-3Q	SRASH-2/S. P. Reidel	M	A	Sidestream alluvium and slope worn debris	Fecht unpublished geologic mapping
56	11/28-18L	--	S	F	Sand-dominated facies of glaciofluvial sequence	Fecht et al. 1999
57	11/28-25L	820-022/B. N. Bjornstad	M	A	Surficial sediments on White Bluffs escarpment	Baker et al. 1991
58	11/28-36L	820-019/B. N. Bjornstad	GP	A	Surficial sediments on White Bluffs escarpment	Baker et al. 1991
59	10/28-2F	--	M	F	Parabolic dune atop fluvial sequence	This study
60	10/28-2K	--	M	F	Capped overbank alluvium on terrace	This study
61	10/28-24-B	--	M	F	Parabolic dune atop fluvial gravel	This study
62	10/28-20D	C6652/K. R. Fecht	M	A/F	Lee side of topographic high in parabolic dune complex	Baker et al. 1991; Fecht et al. 1999
63	10/28-21N	KRF-00-103/K. R. Fecht	M	A/F	Parabolic dune complex	Fecht unpublished geologic mapping
64	9/27-1B	C6463/K. R. Fecht	S	A/F	Interbedded sand and silt facies of glaciofluvial sequence	Reidel and Fecht 1994b
65	9/27-14J	RHT 33, RHT 34/ A. M. Tallman	S	A/F	Interbedded sand and silt facies of glaciofluvial sequence	Baker et al. 1991
66	9/28-194	--	S	F	Interbedded sand and silt facies of glaciofluvial sequence	Reidel and Fecht 1994b
67	9/28-21D	--	S	F	Interbedded sand and silt facies of glaciofluvial sequence	Reidel and Fecht 1994b

Table 5-1. Selected tephra localities used in this study. (3 Pages)

Site Number	Location	Sample Number/ Collector	Probable Source[a]	Basis for Identification[b]	Depositional Environment	Reference
68	9/28-26D	--	M	F	Eolian sheet silty sand on lee side of Badger Mountain	Fecht unpublished geologic mapping
69	9/28-22_	--	S	F	Interbedded sand and silt facies of glaciofluvial sequence	Fecht et al. 1999
70	9/28-27E	--	M	F	Eolian sheet silty sand on lee side of Badger Mountain	Fecht unpublished geologic mapping
71	9/28-10Q	--	M	F	Eolian sheet sand on lee side of glaciofluvial bar	Fecht unpublished geologic mapping
72	9/28-15H	C9233/J. T. Lillie	M	A/F	Capping alluvial plug in abandoned fluvial channel	Baker et al. 1991
73	9/28-15K	--	M	F	Eolian sheet sand overbank alluvium of main stream	Reidel and Fecht 1994b
74	9/28-23D	--	M	F	Capping overbank alluvium of main stream	Rediel and Fecht 1994b
75	9/29-17E	--	M	F	Parabolic dune complex atop fluvial gravel	Fecht unpublished geologic mapping
76	9/28-25L	--	S	F	Interbedded sand and silt facies of glaciofluvial sequence	Reidel and Fecht 1994b
77	9/28-34J	KRF-99-111/K. R. Fecht	S	A/F	Interbedded sand and silt facies of glaciofluvial sequence	Fecht unpublished geologic mapping
78	8/28-1Q	--	S	F	Interbedded sand and silt facies of glaciofluvial sequence	Reidel and Fecht 1994b
79	8/29-6D	--	S	F	Interbedded sand and silt facies of glaciofluvial sequence	Reidel and Fecht 1994b
80	8/29-5D	--	S	F	Interbedded sand and silt facies of glaciofluvial sequence	Reidel and Fecht 1994b
81	9/29-28R	CPP 334	M	A/F	Capping overbank alluvium	Huckleberry et al. 1998; Wakeley et al. 1998
82	8/30-29P	C6099, C6100/K. R. Fecht	S	A/F	Interbedded sand and silt facies of glaciofluvial sequence	Baker et al. 1991 Reidel and Fecht 1994b
83	8/30-30M	C6093 through C6096/ K. R. Fecht	M	A/F	Eolian sheet sand in gully on lee side of Game Farm Hill	Baker et al. 1991
84	15/23-15A	C6671/K. R. Fecht	M	A/F	Talus sentinel gap	Reidel and Fecht 1994a
85	9/28-11B	KRF-05-021/K. R. Fecht	M	A/F	Capping alluvial plug in abandoned fluvial channel	This study
86	13/24-9P	KRF-05-010/K. R. Fecht	M	A/F	Interbedded sidestream alluvial fan and overbank alluvium	This study
87	13/23-125	KRF-05-014/K. R. Fecht	M	A/F	Column at base of Umtanum Ridge	This study

[a] GP – Glacier Peak, M – Mazama, MSH – Mount St. Helens 1980, S – Mount St. Helens Set S.
[b] A – Analytical Methods, F – Field Characteristics.

Table 5-2. Grain size and classification of selected tephra samples (weight %).

Sample No.	Coarse Ash		Fine Ash	Probable Source
	>350 Microns	350 – 44 Microns	<44 Microns	
C6093	2.0	33.7	64.3	Mazama
C6094	2.6	39.7	57.6	Mazama
C6095	0.0	14.2	85.8	Mazama
C6096	0.0	34.9	65.1	Mazama
C6123	0.0	3.8	96.2	Glacier Peak
C6124	1.9	51.4	46.7	Glacier Peak
C6125	0.4	32.7	66.9	Glacier Peak
C6099[a]	22.3	34.4	43.3	Mount St. Helens Set S
C6100	0.1	44.3	55.6	Mount St. Helens Set S
C6113	0.0	32.7	67.3	Mount St. Helens Set S
C6126	0.0	35.4	64.6	Mount St. Helens Set S
C6127	1.5	35.5	63.0	Mount St. Helens Set S
C6128	0.0	36.9	63.1	Mount St. Helens Set S
C6463	0.0	33.1	66.9	Mount St. Helens Set S
	Medium fine to very fine sand		Silt and clay	

[a] Contaminated with host sediment.

Table 5-3. Field characteristics of late Pleistocene and Holocene tephra layers in study area.

Tephra	Color	Eruptive Events	Thickness	Grain Size
Mount St. Helens May 18, 1980	White (7.5 YRN8 to 10YR8/1) to light gray (10YR7/1 to 10YR7/2)	1	Mainly 3 mm to 6 mm, locally accumulates in gullies (maximum observed 15 cm)	Sandy silt to silty very fine sand
Mazama	White (7.5YRN8 to 10YR8/1) to pink (5YR8/3 to 5YR8/4); pink is commonly in lower part of horizon	1	Commonly 15 to 20 cm, locally accumulates in topographic lows (up to 1 m)	Silt
Glacier Peak	White (7.5YRN8 to 10YR8/1)	2	Upper 25 mm to 50 mm; lower 12 mm to 50 mm	Sandy silt to silty very fine sand
Mount St. Helens Set S	White (7.5YRN8 to 10YR8/1)	Mainly 2 in central/southern Columbia Basin (rarely more); mainly 3 in northern Columbia Basin (occasionally more)	Couplet: upper 25 mm to 50 mm (locally up to 15 cm in glaciofluvial channels); lower 6 mm to 12 mm; other units 3 mm to 12 mm	Silt to sandy silt

5.1 TEPHROCHRONOLOGY

5.1.2 Petrologic and Geochemical Characteristics of Ashes

Volcanic ash consists of three primary components: volcanic glass (glass shards and pumice fragments), minerals (phenocrysts), and lithic fragments of preexisting rocks (Sarna-Wojcicki 2000). Glass shards and mineral phenocrysts are comagmatic components of the volcanic ash, whereas the lithic fragments are older surrounding rock debris caught up in the explosive eruption of the volcano. Glass represents the quenched melt of magma during the explosive eruption.

The modal count of major components was determined for several ashes using the 44 to 350 micron size fraction of the ash. The modal count results are presented in Table 5-4. Mazama ash generally has a higher volcanic glass shard content (6% to 17%), whereas Glacier Peak and Mount St. Helens Set S ashes generally have higher percentages of mineral crystals (generally greater than 36%). The modal counts associated with samples C6123 and C6124 have been reworked by fluvial processes of an ephemeral sidestream. The lower ash layer of the Glacier Peak couplet often has a higher abundance of phenocryst crystals than the upper layer. Mount St. Helens Set S ash often has pumice fragments that display evidence of alteration due to surfical processes.

Table 5-4. Abundance of glass shards, pumice fragments, crystals, and lithic fragments in the 44-350 micron fraction.

Sample No.	Modal Count				Probable Source
	Glass Shards	Pumice Fragments	Crystals	Lithic Fragments	
C6093	13.4	61.6	19.0	5.9	Mazama
C6094	14.0	57.1	27.9	1.0	Mazama
C6095	17.2	72.1	8.8	1.9	Mazama
C6096	6.1	62.5	22.0	9.4	Mazama
C6123	14.5	76.3	8.6	0.5	Glacier Peak
C6124	0	4.1	64.8	31.0	Glacier Peak
C6125	0	49.6	40.2	10.2	Glacier Peak
C6099	0.9	40.4	44.4	14.3	Mount St. Helens Set S
C6100	0.7	39.3	42.0	18.0	Mount St. Helens Set S
C6113	0.3	63.6	36.1	0.1	Mount St. Helens Set S
C6126	3.0	59.2	36.5	1.3	Mount St. Helens Set S
C6127	0	44.0	38.0	16.8	Mount St. Helens Set S
C6128	0.5	52.1	46.5	0.9	Mount St. Helens Set S
C6463	0.3	45.3	50.7	3.7	Mount St. Helens Set S

5.1 TEPHROCHRONOLOGY

5.1.2 Petrologic and Geochemical Characteristics of Ashes

The mineral composition of the ferromagnesian or mafic phenocrysts was determined by petrographic examination and supplemented with x-ray diffraction analysis of the 44-350 micron size fraction. The mafic minerals identified included orthophyroxenes (hypersthene), clinopyroxenes (augite), and amphiboles (basaltic, blue-green, and common hornblende; cummingtonite) as dominant mineral groups (Table 5-5). The range of mafic phenocrysts in the greater than 2.95 gm/cm^3 fraction of the analyzed fraction is presented in Table 5-6. Opaque minerals of magnetite and ilmenite were also observed in ash samples. Each of the three volcanic ashes evaluated within this study can be distinguished from one another based on the mineral composition of the mafic phenocrysts. Cummingtonite is abundantly common in phenocrysts of minerals assemblages erupted from Mount St. Helens (Mullineaux et al. 1975) and is diagnostic to Mount St. Helens Set S when compared to mineral assemblages from Mazama and Glacier Peak ashes. Augite is an abundant phenocryst characteristic of ashes from Mount Mazama eruptions (Wilcox 1965). Hornblende and hypersthene predominate in phenocrysts of Glacier Peak ash as found by Powers and Wilcox (1964) and Westgate and Evans (1978). Phenocrysts of cummingtonite and augite are relatively rare in Mazama and Glacier Peak ashes.

The chemical composition of glass shards was determined by direct measurements using EMPA (electron probe micro analyzer) facilities at the University of Rhode Island (Table 5-7) and Washington State University (Table 5-8). The University of Rhode Island facility was used for determining chemical composition of ashes prior to 1989, and the Washington State University facility has been used in subsequent years. Several glass shards ranging in numbers from 3 to 18 were selected for analyses in each sample analyzed. The analytical results indicated that all ashes range in composition from rhyolite to dacite based on the percentage SiO_2, with the lower SiO_2 values dacite and the higher values rhyolite. The ash compositional data were plotted on $Na_2O + K_2O$ versus SiO_2 plots (Figure 5-4). The high silica contents of ash horizons in the study area are appropriate since dacitic and rhyolitic compositions (i.e., calc-alkaline) are commonly associated with violently explosive eruptions that result in widespread airfall ashes (Nakagawa and Ohba 2002).

The major elements measured from glass shards at the University of Rhode Island EMPA facility were compared by K. F. Scheidegger and A. N. Federman of Oregon State University against published data sets for the three key ashes:

- Mazama ash from the climactic eruption 6,850 ± 50 rcybp ago – Powers and Wilcox (1964), Smith and Westgate (1969), and Lemke et al. (1975)

- Glacier Peak ash from the 11,250 ± 250 rcybp eruption – Powers and Wilcox (1964), Smith and Westgate (1969), Smith et al. (1977), and Westgate and Evans (1978).

- Mount St. Helens Set S from 13,000 rcybp eruption – Scheidegger and Federman, unpublished data from S_o.

Overall, Mazama ash tends to have lower SiO_2 values and higher other oxides except for K_2O. Glacier Peak is commonly lower in most oxides except for K_2O, and Mount St. Helens Set S ash tends to be intermediate to low in most oxides compared to Mazama and Glacier Peak. The University of Rhode Island electron microprobe data were provided in the 1980s and display higher variability than the EMPA data sets from Washington State University.

Table 5-5. Mafic phenocrysts in key volcanic ash layers (in %).

Mafic Minerals	BB817	BB820-22	C6083	C6093	C6094	C6095	C6096	C6652	BB820-19	C6123	C6124	C6125	BB820-28	C6099	C6100	C6113	C6126	C6127	C6128	C6463	C9281	C9290A	C9290B	C9290C	RHT-33	RHT-34
Basaltic hornblende	0	0	1	2	1	1	0	0	0	1	2	4	4	0	1	1	2	3	1	3	1	2	2	1	1	1
Blue Green hornblende	0	0	2	0	1	1	1	0	1	0	1	0	0	0	1	1	1	2	0	1	2	1	1	1	0	2
Common hornblende	11	20	50	16	41	30	24	15	52	55	74	51	63	75	65	43	42	55	64	58	48	62	55	57	54	61
Cummingtonite	0	0	0	0	0	0	0	0	0	0	0	0	16	16	16	25	20	14	12	11	19	26	28	27	11	6
Hypersthene	56	53	28	52	40	36	44	56	47	44	23	45	17	9	17	30	35	26	23	27	30	9	14	14	24	20
Augite	33	27	21	29	17	32	31	29	0	0	0	0	0	0	0	0	0	0	0	0	0	0	0	0	0	0
Probable Source*	M	M	M	M	M	M	M	M	GP	GP	GP	GP	S	S	S	S	S	S	S	S	S	S	S	S	S	S

NOTE: M – Mazama, GP – Glacier Peak, S – Mount St Helens Set S.

Table 5-6. Range of mafic (Mg-Fe) phenocrysts (in %) in >2.95 g/cm3 fraction of 44-350 micron split of bulk ash sample from ash samples in the study area.

	Mazama	Glacier Peak	Mount St. Helens Set S
Ash Samples (No.)	8	4	14
Amphiboles			
Basaltic hornblende	0-2	1-4	0-4
Blue-geen hornblende	0-1	0-1	0-3
Common hornblende	9-50	51-74	33-75
Cummingtonite	0	0	6-35
Pyroxenes			
Othropyroxene	36-56	23-47	9-35
Clinopyroxene	17-43	0	0

[a] From K. F. Scheidegger and A. N. Federman of Oregon State University to Rockwell Hanford Operations, Richland, Washington, 1980-1986 (Subcontract SA-475).

Table 5-7. Glass shard chemical composition (University of Rhode Island electron microprobe).

Oxide	Sample Number/Shards Number								
	BB817/10	BB820-22/10	C6083/11	C6093/9	C6094/10	C6095/10	C6096/9	C6652/10	C9302/6
SiO_2	71.32 ± 0.96	71.68 ± 0.43	70.38 ± 3.31	70.34 ± 6.99	70.12 ±1.01	69.71 ± 1.61	70.14 2.37	73.16 ± 0.53	70.82 ± 0.45
Al_2O_3	13.95 ± 0.23	13.95 ± 0.26	14.33 ± 0.70	13.55 ± 0.37	14.04 ±0.70	13.67 ± 0.77	13.77 0.37	13.76 ± 0.17	13.97 ± 0.20
FeO	1.70 ± 0.09	1.80 ± 0.06	1.68 ± 0.22	1.53 ± 0.18	1.87 ± 0.54	1.58 ± 0.16	1.61 0.11	1.88 ± 0.17	1.59 ± 0.12
TiO_2	0.38 ± 0.04	0.40 ± 0.06	0.45 ± 0.05	0.38 ± 0.12	0.40 ± 0.10	0.34 ± 0.05	0.34 0.06	0.34 ± 0.06	0.38 ± 0.03
Na_2O	3.78 ± 0.40	3.85 ± 0.41	3.73 ± 0.58	3.76 ± 0.66	3.89 ± 0.33	3.74 ± 0.36	3.91 0.36	3.22 ± 0.35	3.68 ± 0.31
K_2O	2.80 ± 0.13	2.40 ± 0.72	2.61 ± 0.18	2.52 ± 0.09	2.56 ± 0.12	2.47 ± 0.26	2.59 0.16	2.46 ± 0.22	2.47 ± 0.22
MgO	0.37 ± 0.04	0.38 ± 0.04	0.41 ± 0.04	0.31 ± 0.05	0.39 ± 0.11	0.33 ± 0.07	0.30 0.03	0.40 ± 0.05	0.34 ± 0.03
CaO	1.55 ± 0.12	1.38 ± 0.18	1.37 ± 0.58	1.32 ± 0.18	1.49 ± 0.26	1.40 ± 0.10	1.40 0.10	1.61 ± 0.07	1.42 ± 0.16
MnO	0.04 ± 0.05	0.05 ± 0.04	--	--	--	--	--	0.12 ± 0.03	0.03 ± 0.02
Total	95.87	95.82	94.95	93.71	94.75	93.24	94.06	96.95	94.69
Probable source	Mazama	Mazama	Mazama	Mazama	Mazama	Mazama	Mazama	Mazama	Mazama

Oxide	Sample Number/Shards Number							
	BB820-19/13	C6123/11	C6124/10	BB820-28/3	C6099/8	C6100/10	C6127/10	C6463/10
SiO_2	74.87 ± 0.52	71.58 ± 2.50	72.90 ± 1.32	76.05 ± 0.55	71.66 ± 1.18	72.78 ± 0.82	71.45 ± 1.15	72.26 ± 1.87
Al_2O_3	11.97 ± 0.15	11.98 ± 0.95	11.76 ± 0.94	12.40 ± 1.45	12.64 ± 0.44	12.43 ± 0.38	12.73 ± 0.26	12.53 ± 0.26
FeO	0.79 ± 0.10	0.76 ± 0.20	0.74 ± 0.08	0.80 ± 0.38	0.88 ± 0.14	0.81 ± 0.08	0.91 ± 0.08	0.88 ± 0.15
TiO_2	0.16 ± 0.04	0.15 ± 0.04	0.12 ± 0.03	0.15 ± 0.03	0.10 ± 0.03	0.11 ± 0.03	0.11 ± 0.04	0.12 ± 0.03
Na_2O	3.29 ± 0.38	3.05 ± 0.33	3.06 ± 0.24	1.78 ± 0.10	3.28 ± 0.37	3.03 ± 0.17	3.12 ± 0.25	3.31 ± 0.18
K_2O	2.96 ± 0.30	3.03 ± 0.25	2.91 ± 0.35	2.89 ± 1.12	2.05 ± 0.07	2.15 ± 0.07	2.04 ± 0.09	2.17 ± 0.13
MgO	0.20 ± 0.02	0.18 ± 0.05	0.12 ± 0.03	0.15 ± 0.12	0.18 ± 0.06	0.17 ± 0.02	0.19 ± 0.03	0.17 ± 0.03
CaO	1.00 ± 0.09	1.07 ± 0.14	0.95 ± 0.14	0.86 ± 0.84	1.34 ± 9.26	1.21 ± 0.14	1.25 ± 0.21	1.28 ± 0.09
MnO	0.01 ± 0.03	--	--	0.08 ± 0.02	--	--	--	--
Total	95.25	91.81	102.57	95.16	92.13	92.67	91.74	92.72
Probable source	Glacier Peak	Glacier Peak	Glacier Peak	Mount St. Helens Set S	Mount St. Helens Set S	Mount St. Helens Set S	Mount St. Helens Set S	Mount St. Helens Set S

Oxide	Sample Number/Shards Number						
	C9281/10	C9290A/9	C9290B/5	C9290C/10	RHT-25/9	RHT-33/9	RHT-34/9
SiO_2	73.74 ± 0.59	73.70 ± 0.58	73.66 ± 0.88	73.17 ± 0.20	74.87 ± 1.69	74.99 ± 1.28	74.99 ± 1.14
Al_2O_3	12.86 ± 0.16	12.86 ± 0.13	12.59 ± 0.38	12.77 ± 0.11	13.02 ± 0.45	12.76 ± 0.38	12.95 ± 0.52
FeO	0.86 ± 0.10	0.88 ± 0.11	0.90 ± 0.13	0.86 ± 0.07	0.94 ± 0.09	0.95 ± 0.10	0.91 ± 0.13
TiO_2	0.13 ± 0.03	0.12 ± 0.03	0.12 ± 0.04	0.13 ± 0.04	0.18 ± 0.02	0.16 ± 0.03	0.16 ± 0.03
Na_2O	3.22 ± 0.14	2.94 ± 0.31	2.76 ± 0.33	2.97 ± 0.10	3.81 ± 0.54	4.21 ± 0.35	4.13 ± 0.55
K_2O	2.05 ± 0.02	2.08 ± 0.21	2.14 ± 0.17	2.13 ± 0.14	2.10 ± 0.15	2.09 ± 0.14	2.04 ± 0.24
MgO	0.25 ± 0.02	0.20 ± 0.04	0.21 ± 0.02	0.23 ± 0.02	0.18 ± 0.02	0.17 ± 0.03	0.17 ± 0.03
CaO	1.22 ± 0.10	1.20 ± 0.14	1.14 ± 0.14	1.31 ± 0.09	1.30 ± 0.16	1.17 ± 0.22	1.17 ± 0.15
MnO	0.03 ± 0.03	0.01 ± 0.02	0.02 ± 0.02	0.02 ± 0.03	0.00 ± 0.00	--	--
Total	93.88	94.00	43.54	93.60	96.40	96.49	96.53
Probable source	Mount St. Helens Set S	Mount St. Helens Set S	Mount St. Helens Set S	Mount St. Helens Set S	Mount St. Helens Set S	Mount St. Helens Set S	Mount St. Helens Set S

Table 5-8. Glass shard chemical composition (Washington State University Geoanalytical Laboratory electron microprobe).

Oxide	Sample Number/Shards Number								
	C6671/ 15	KRF 99-101/ 17	KRF 99-111/ 14	KRF 99-114/ 16	KRF 00-103/ 15	KRF 02-003/ 16	KRF-05-010/ 16	KRF-05-014/ 15	KRF-05-021/ 16
SiO_2	73.31 ± 0.25	73.07 ± 0.22	73.46 ± 0.34	73.57 ± 0.18	73.16 ± 0.26	72.99 ± 0.26	73.33 ± 0.26	73.43 ± 0.32	73.46 ± 0.20
Al_2O_3	14.46 ± 0.15	14.55 ± 0.13	14.47 ± 0.16	14.42 ± 0.09	14.50 ± 0.08	14.62 ± 0.16	14.56 ± 0.15	14.43 ± 0.13	14.56 ± 0.14
Fe_2O_3	2.07 ± 0.05	2.18 ± 0.07	2.14 ± 0.08	2.15 ± 0.05	2.15 ± 0.05	2.14 ± 0.06	2.07 ± 0.06	2.06 ± 0.07	2.08 ± 0.05
TiO_2	0.42 ± 0.05	0.42 ± 0.03	0.42 ± 0.02	0.43 ± 0.03	0.42 ± 0.02	0.42 ± 0.02	0.43 ±0.02	0.43 ± 0.03	0.43 ± 0.02
Na_2O	4.66 ± 0.25	4.82 ± 0.09	4.61 ± 0.21	4.48 ± 0.15	4.83 ± 0.18	4.90 ± 0.18	4.57 ± 0.17	4.61 ±0.20	4.40 ± 0.21
K_2O	2.74 ± 0.05	2.71 ± 0.05	2.68 ± 0.08	2.68 ± 0.06	2.66 ± 0.06	2.69 ± 0.09	2.73 ± 0.05	2.72 ± 0.06	2.74 ±0.06
MgO	0.47 ± 0.04	0.46 ± 0.04	0.45 ± 0.04	0.46 ± 0.02	0.48 ± 0.03	0.47 ± 0.05	0.46 ± 0.04	0.48 ± 0.05	0.49 ± 0.03
CaO	1.66 ± 0.05	1.59 ± 0.04	1.58 ± 0.07	1.60 ± 0.06	1.60 ± 0.04	1.56 ± 0.06	1.65 ± 0.06	1.63 ± 0.09	1.66 ±0.05
Cl	0.20 ± 0.02	0.17 ± 0.02	0.16 ± 0.02	0.18 ± 0.01	0.17 ± 0.02	0.18 ± 0.02	0.19 ± 0.02	0.21 ±0.04	0.19 ± 0.02
Total[a]	100	100	100	100	100	100	100	100	100
Probable source	Mazama	Mazama	Mazama	Mazama	Mazama	Mazama	Mazama	Mazama	Mazama
Similarity coefficient[b]	0.99	0.99	0.98+	0.98+	0.99	0.99	0.99	0.99	0.99

[a] Analyses normalized to 100 wt%.
[b] Borchardt et al. (1972), *J. Sed. Petrol.* 42, 301-306.

Oxide	Sample Number/Shards Number				
	SRASH-2/ 17	KRF 02-002/ 17	KRF 02-001/ 18	KRF 02-004/ 18	KRF 02-005/ 16
SiO_2	73.37 ± 0.23	77.65 ± 0.23	77.27 ± 0.46	77.07 ± 0.69	76.96 ± 0.57
Al_2O_3	14.73 ± 0.12	12.53 ± 0.15	13.10 ± 0.24	13.22 ± 0.45	13.26 ± 0.28
Fe_2O_3	2.07 ± 0.05	1.22 ± 0.08	1.30 ± 0.08	1.30 ± 0.10	1.32 ± 0.09
TiO_2	0.43 ± 0.02	0.21 ± 0.02	0.17 ± 0.03	0.19 ± 0.02	0.17 ± 0.02
Na_2O	4.42 ± 0.07	3.52 ± 0.14	4.03 ± 0.20	4.06 ± 0.15	4.07 ± 0.16
K_2O	2.70 ± 0.04	3.18 ± 0.09	2.33 ± 0.13	2.39 ± 0.21	2.33 ± 0.10
MgO	0.44 ± 0.02	0.25 ± 0.02	0.29 ± 0.03	0.29 ± 0.06	0.30 ± 0.04
CaO	1.64 ± 0.05	1.23 ± 0.04	1.39 ± 0.11	1.34 ± 0.17	1.44 ± 0.09
Cl	0.17 ± 0.01	0.18 ± 0.01	0.09 ± 0.02	0.11 ± 0.03	0.10 ± 0.02
Total[a]	100	100	100	100	100
Probable source	Mazama	Glacier Peak	Mount St. Helens Set S	Mount St. Helens Set S	Mount St. Helens Set S
Similarity coefficient[b]	0.97+	0.97+	0.98	0.97	0.98

[a] Analyses normalized to 100 wt%.
[b] Borchardt et al. (1972), *J. Sed. Petrol.* 42, 301-306.

5.1 TEPHROCHRONOLOGY

5.1.3 Volcanic Ash Marker Beds

The three tephras layers from Mount St. Helens Set S, Glacier Peak, and the climactic Mazama can be identified in the study area using physical and chemical characteristics of the ashes as discussed in previous sections. This section presents a discussion on (1) correlation of sedimentary sequences using volcanic ash layers as stratigraphic markers, and (2) age of sedimentary units and landforms based on the known ages of the three eruptive events. The volcanic ashes represent airfall from distal volcanic sources (Figure 5-1) and occur within the study area for distinct stratigraphic units (Figure 5-5) with many ash layers displaying only minor reworking by surfical processes since the original deposition.

Mount St. Helens Set S ash layers are the oldest in age and lowest in stratigraphic profile of the three ashes. The layers occur near or at the top of large-scale cataclysmic glaciofluvial flood sequences within the river valley. The ash layers occur as a distinct couplet or triplet within a thin eolian unit. The layers occur between two separate flooding events and over 20 rhymthites associated with smaller scale glaciofluvial floods, and represent closely spaced eruptions of Mount St. Helens. The ash layers are separated by eolian sediments and occasionally are disrupted by bioturbation or where the ashes have been reworked or eroded by surfical processes. One or two other volcanic ashes thought to be associated with Set S are occasionally found between flood units several meters below the couplet or triplet (Moody 1987, Smith 1993, Fecht and Weekes 1996, this paper). The Set S couplet is ubiquitous to plane-laminated sand and interbedded sand and silt sequences of the glaciofluvial flood sequences throughout the central Columbia Basin. The couplet is occasionally found within eolian sediments between glaciofluvial gravel deposits, mainly in locations protected from extensive erosion (e.g., glaciofluvial flood gravels associated with shoulder bars near the saddle of Gable Mountain and in sidestream channel fill in Dry Creek Valley at distal margins to the glaciofluvial channelways).

In the upper elevations of the river valley, Set S occurs in a variety of surfical deposits, most commonly loess, but also within colluvium, landslide debris, and sidestream alluvium. The ash layers are useful in correlating late Pleistocene-age glaciofluvial sediments (gravel-dominated, sand-dominated, and sand/silt-dominated facies) and loess deposits. Set S has been encountered in numerous exposures and excavations across the river valley (Figure 5-2). By mapping the occurrences of the ash layers across the river valley, one can identify areas of incision into the river valley by fluvial processes constraining the position of the Columbia River in the valley following the large-scale cataclysmic floods. Areas of incision occur in (1) secondary streams of the Columbia (i.e., Yakima, Snake, and Walla Walla Rivers) and sidestreams (e.g., Cold Creek and Dry Creek valleys); (2) several abandoned channelways and broad terraces (P-1 to H-2) in the intermediate and lower elevations of the river valley; and (3) areas of terraces steps (H-3 to H-6) of the lower elevations of the river valley (Figure 4-1).

The Glacier Peak volcanic ash couplet is commonly observed in upper elevations of the river valley where the ash occurs within loess deposits that mantle basaltic ridges. Glacier Peak ash is only occasionally observed in the lower elevations of the river valley. The couplet is observed in overbank deposits of Cold Creek Valley (Figure 5-2 and Table 5-1) and in thin loessal sheets that locally occur between underlying glaciofluvial flood gravels and overlying sand dune colonies (Figure 5-5). Glacier Peak ash layers occurs above 150-m (495-ft) elevation within the river valley. The Glacier Peak ash post-dates large-scale cataclysmic flooding in the river valley. The age of Glacier Peak is 11,250 ± 250 rcybp and thus restricts large-scale flooding of the river valley to less than 11,250 rcybp.

5.1 TEPHROCHRONOLOGY

5.1.3 Volcanic Ash Marker Beds

Mazama volcanic ash is a commonly observed ash in the river valley. It is the thickest of the ash horizons of the late Pleistocene and Holocene ashes in the study area. The ash layer is key to correlating among terraces treads and abandoned channelways in lower elevations of the river valley. Mazama ash occurs in the following Holocene settings on terrace treads (see Figure 5-5):

- In blowouts of eolian dune colonies that occur on many Pleistocene terraces and glaciofluvial flood bars (P-1 and P-X)
- Loessal sands and silts of the upper elevation on basaltic ridges
- In blowouts of eolian dune colonies atop terrace benches (H-1 and H-2)
- Immediately atop alluvial overbank environments associated with H-3 Terraces and an alluvial plug in an abandoned channelway

Since the age of the climactic eruption of Mazama has been determined at 6,845 rcybp, the Mazama ash is an excellent correlation and chronology tool. Terraces P-1, P-X, H-1, and H-2 fluvial and glaciofluvial and associated landforms were created before the Mount Mazama climactic eruption. The presence of Mazama ash at the top of Terrace H-3 and associated channelway plug suggests fluvial aggradation had ceased and a period of river incision had been initiated. Terraces H-4, H-5, and H-6 are landforms created after the Mazama climactic eruption.

5.2 RADIOCARBON GEOCHRONOLOGY

5.2.1 Radiocarbon Analytical Methods and Radiocarbon Dates

Soils and sediments within the river valley typically contain sufficient amounts of organic carbon for measuring radiocarbon content and dating geologic materials. This section reports on the results of radiocarbon dating of soils and sediments collected as part of this study and incorporates radiocarbon dates from several other field investigations along the river reach. Radiocarbon dates are placed in context with the late Pleistocene sedimentary framework and landforms found in the lower elevations of the river valley.

Two analytical methods were used to measure the radiocarbon content of the organic matter in sediment samples: (1) radiometric analysis that measures the radiation emitted by the radioisotope carbon-14 using gas proportional or liquid scintillation systems, and (2) accelerator mass spectrometry (AMS) that uses particle acceleration to sort ions according to their mass and individual ions of carbon-14 are counted on detectors. The radiometric method was used with larger volume sediment samples since this method is relatively simple and less costly. The AMS method was used when insufficient sample size was available for radiometric analysis. The primary analytical laboratories contracted for radiocarbon dating of samples included in this study were Geochron Laboratories located in Cambridge, Massachusetts, and Beta Analytic, Inc. of Miami, Florida.

5.2 RADIOCARBON GEOCHRONOLOGY

5.2.1 Radiocarbon Analytical Methods and Radiocarbon Dates

Sample materials collected for radiocarbon dating included several varieties of organic matter, including mammal bone (mainly from medium to small mammals), fish vertebrae (mainly salmon), mussel shell (mainly *Margaritifera falcate*), charred wood and charcoal, root masses, mammal fecal remains, and bulk soil. Most samples collected in both earlier studies and recent field activities supported cultural studies of ancient human activities along the Columbia River reach. Several samples of bulk soil were collected as part of this study solely for radiocarbon geochronologic dating of late Pleistocene sedimentary units and landforms.

Radiocarbon dating information (sample number and radiocarbon age) and field information (dated material, geologic and cultural context, sample location, and depth below ground surface) were compiled from this study or were extracted from the Hanford Site Archaeological Database maintained by Pacific Northwest National Laboratory (Table 5-9). The geologic context regarding stratigraphic position on the terrace steps and benches (as discussed in Chapter 4.0) was established for each radiocarbon-dated sample in the combined information set. Radiocarbon dates used for each media type were the conventional dates, and no correction factors were applied for environmental effects (e.g., freshwater reservoir effects associated with dating of shell media). Several radiocarbon dates were not included in the final sample set. Dates were excluded if modern age and did not aid in constraining the age of sedimentary units or landforms, or if the sample location did not provide sufficient description to establish an accurate geologic context.

Table 5-9 contains information on 140 radiocarbon dates obtained from the Hanford Site or adjacent mid-Columbia Basin. The dates range in age from 30 ± 50 rcybp to 15,330 ± 60 rcybp, with 83 (approximately 60%) dating to 3,000 radiocarbon years or younger. Materials analyzed included charcoal or charred material (n = 48), mammal bone (n = 36), freshwater mussel shell (n = 32), and bulk soil (n = 24). Samples were taken from three primary soil types: eolian sand (n = 34), point bar alluvium (n = 34), and overbank alluvium (n = 42). The remaining 27 samples, where soil type could be assigned, were from mixed or minor soil types. Not all terraces could be identified with certainty, but where identification was determined near equal samples the majority were obtained from terraces H3 (n = 45) and H4 (n = 22), with minor numbers drawn from H1 (n = 4), H5 (n = 8), and H6 (n = 3). The vast majority of samples derived from a cultural context (n = 103), while 32 were noncultural. The context of five samples could not be determined.

Table 5-9. Radiocarbon dates, Columbia River Basin. (8 Pages)

Laboratory Sample Number	Field Sample Number	Conventional Age B.P.	Material Dated	Geological Context[c]	Location[d]	Cultural[e]	Source
Beta-107583-AMS	801.1	30 ± 50	Charred Material	1.5 m below surface of point bar, fine-grained alluvium	14/27-17C, MC	C	Bjornstad et al. 1998
GX-30149[a]	KRF-03-006	100 ± 50	Mammal bone	84 cm below surface of H5 Terrace, eolian sand in deltaic island	9/29-19J, MC	C	This study
Beta-107580[b]		110 ± 50	Charred material	40 cm below surface of point bar, fine-grained alluvium	14/27-21(G ?), MC	C	Bjornstad et al. 1998
GX-28315-AMS	45BN606-01-12	140 ± 40	Charcoal	80 to 90 cm below surface of H3 Terrace, eolian sand	14/27-29R, RB	C	Marceau and Sharpe 2002a
GX-28314-AMS	45BN606-01-11	150 ± 40	Charcoal	40 to 50 cm below surface of H3 Terrace, eolian sand	14/27-29R, RB	C	Marceau and Sharpe 2002a
GX-25587	KRF-99-24	160 ± 100	Root mass	46 cm below surface of H6 Terrace, overbank alluvium	14/26-11P, RB	NC	This study
GX-26062-AMS	KRF-99-59	190 ± 40	Mammal bone	30 cm below surface of H4 Terrace, eolian cover overlying overbank alluvium	13/24-12F, RB	NC	This study
Beta-92477	800	230 ± 40	Charcoal	1.65 m below surface of point bar, fine-grained alluvium	14/27-17C, MC	NC	Bjornstad et al. 1998
Beta-92906	831.2	230 ± 60	Charred material	1.02 m below surface of point bar, fine-grained alluvium	14/27-21D, MC	C	Bjornstad et al. 1998
Beta-107589-AMS	CB10F1	240 ± 50	Charred material	1.15 m below surface of point bar, fine-grained alluvium	13/27-3R, RB	C	Tamers and Hood 1997
GX-25581	KRF-98-23	250 ± 40	Charcoal	91 cm below surface of point bar, alluvium on modern-day mid-channel island	14/27-17K, MC	C	This study
GX-29273	45BN432/431-01-02	270 ± 50	Charcoal	30 to 40 cm below surface of H3 Terrace, eolian sand	14/27-33G, RB[f]	C	Marceau and Sharpe 2002b
Beta-33039		290 ± 80	Charcoal	0.90 to 1.10 m below surface of H5 (?) Terrace, overbank alluvium	14/26-11D, LB	C	Chatters and Hackenberger 1989
TX-No. 3331		310 ± 40	Charcoal	1.3 to 1.5 m below surface of H6 Terrace, sand levee with alluvial gravel	11/28-2B, RB	C	Rice 1980
Beta-92478	807	310 ± 50	Charred material	75 cm below surface of point bar, fine-grained alluvium	14/27-21G, MC	C	Bjornstad et al. 1998
Beta-107582-AMS	815-F1	310 ± 50	Charred material	1.45 m below surface of point bar, fine-grained alluvium	14/27-21G, MC	C	Bjornstad et al. 1998
GX-29274-AMS	45BN432/431-01-03	310 ± 30	Charcoal	70 to 80 cm below surface of H3 Terrace, eolian sand	14/27-33G, RB[f]	C	Marceau and Sharpe 2002b
Beta-107588-AMS	CB8F3	330 ± 50	Charred material	~3 m below surface of point bar, fine-grained alluvium	13/27-3B, RB	C	Tamers and Hood 1997
Beta-112432-AMS	CB10F2	340 ± 40	Charred material	32 cm below surface of point bar, fine-grained alluvium	13/27-3R, RB	C	Hood 1998
GX-26330	KRF-99-141	410 ± 70	Charcoal	1.20 m below surface of point bar, fine-grained alluvium	13/27-3Q, MC	C	This study
GX-26329	KRF-99-128	420 ± 50	Charcoal	1.32 m below surface of H4 Terrace, overbank alluvium	13/28-32J, LB	C	This study

Table 5-9. Radiocarbon dates, Columbia River Basin. (8 Pages)

Laboratory Sample Number	Field Sample Number	Conventional Age B.P.	Material Dated	Geological Context[c]	Location[d]	Cultural[e]	Source
Beta-112430-AMS	CB8F1	460 ± 50	Charred material	57 cm below surface of point bar, fine-grained alluvium	13/27-3B, RB	C	Hood 1998
Beta-107590-AMS	831-F2	470 ± 50	Organic sediment	1.8 m below surface of point bar, fine-grained alluvium	14/27-21D, MC	C	Bjornstad et al. 1998
GX-32028-AMS	KRF-05-036	470 ± 40	Salmon vertebrae	23 cm below construction modified surface of H3 Terrace, eolian sand	14/27-33G, RB[f]	C	Marceau and Sharpe 2006
Beta-112431-AMS	CB8F4	530 ± 50	Charred material	78 cm below surface of point bar, fine-grained alluvium	13/27-3B, RB	ND	Hood 1998
GX-25583	KRF-99-20	550 ± 40	Mammal bone	46 cm below surface of H6 Terrace, eolian sand atop overbank alluvium remnant	14/26-11H, RB	C	This study
GX-32052	128F2-05-01	570 ± 50	Charcoal	0 to 15 cm below construction modified surface of H3 Terrace, eolian sand	14/27-33G, RB[f]	C	Marceau and Sharpe 2006
GX-25582	KRF-98-24	590 ± 40	Charcoal	2.08 m below surface of point bar on modern-day mid-channel island, fine-grained alluvium	14/27-17K, MC	C	This study
GX-29275-AMS	45BN432/431-01-04	630 ± 30	Mammal bone	80 to 90 cm below surface of H4 Terrace, eolian sand	14/27-33G, RB[f]	C	Marceau and Sharpe 2002b
Beta-92905	907	640 ± 70	Charred material	75 cm below surface of point bar, fine-grained alluvium	14/27-17G, MC	C	Bjornstad et al. 1998
GX-26164-AMS	KRF-99-109	670 ± 40	Salmon vertebrae	33 cm below surface of H4 Terrace, eolian sand above overbank alluvium	14/27-28M, LB	C	This study
GX-31754	KRF-05-017	700 ± 70	Bulk soil	60 to 75 cm below surface of H5 Terrace, overbank alluvium	13/23-12E, RB	NC	This study
Beta-107591-AMS	T800	720 ± 50	Charred material	2.3 m below surface of point bar, fine-grained alluvium	14/27-17C, MC	C	Bjornstad et al. 1998
GX-26165-AMS	KRF-99-110	920 ± 70	Salmon vertebrae	84 cm below surface of H4 Terrace, eolian sand above overbank alluvium	14/27-28P, LB	C	This study
Beta-33036		990 ± 90	Charcoal	1.35 to 1.45 m below surface of H5 (?) Terrace, overbank alluvium	14/26-11D, LB	C	Chatters and Hackenberger 1989
Beta-107584-AMS	804.3	1070 ± 60	Charred material	2.6 m below surface of point bar, fine-grained alluvium	14/27-17C, MC	C	Bjornstad et al. 1998
GX-31802	KRF-05-020	1070 ± 60	Bulk soil	3.05 m below surface of H4 or H3 Terrace, overbank alluvium/eolian sand on top of alluvial gravel	10/28-14H, RB	NC	This study
GX-32027-AMS	KRF-05-035	1080 ± 60	Salmon vertebrae	23 cm below construction modified surface of H3 Terrace, eolian sand	14/27-33G, RB[f]	C	Marceau and Sharpe 2006
Beta-33038		1150 ± 110	Fish bone	2.05 to 2.15 m below surface of H5 (?) Terrace, overbank alluvium	14/26-11D, LB	C	Chatters and Hackenberger 1989
GX-28316-AMS	45BN606-01-13	1200 ± 40	Mammal bone	60 to 70 cm below surface of H3 Terrace, mixed eolian sand and alluvium silt	14-27-29R, RB	C	Marceau and Sharpe 2002a

Table 5-9. Radiocarbon dates, Columbia River Basin. (8 Pages)

Laboratory Sample Number	Field Sample Number	Conventional Age B.P.	Material Dated	Geological Context[c]	Location[d]	Cultural[e]	Source
GX-26328	KRF-99-117	1210 ± 50	Charcoal	1.55 m below surface of H4 Terrace, contact between eolian cap and overbank alluvium	10/28-2P, RB	C	This study
GX-25580-AMS	KRF-98-18	1320 ± 40	Charcoal	2.29 m below surface of point bar, fine-grained alluvium	14/27-17R, MC	C	This study
Beta-33035		1370 ± 160	Charcoal	1.15 to 1.25 m below surface of H5 (?) Terrace, overbank alluvium	14/26-11D, LB	C	Chatters and Hackenberger 1989
GX-28425-AMS	HT2001007-01-03	1450 ± 40	Mammal bone	50 to 60 cm below surface in giant current ripple complex, eolian sand	14/26-22D, RB	C	Marceau and Sharpe 2002a
Beta-92473	1-806-1	1550 ± 40	Charcoal	~1.8 m below surface of point bar, fine-grained alluvium	14/27-17G, MC	C	Bjornstad et al. 1998
Beta-92475	3-806-1	1570 ± 50	Charcoal	~1.6 m below surface of point bar, fine-grained alluvium	14/27-17G, MC	NC	Bjornstad et al. 1998
Beta-133287-AMS	LOCKEF371599	1600 ± 40	Charred material	~5 m below surface of point bar, fine-grained alluvium	14/27-21(G ?), MC	C	Wright 1999
Beta-92904-AMS	906A-1	1670 ± 60	Charcoal	2.6 m below surface of point bar, fine-grained alluvium	14/27-21D, MC	C	Bjornstad et al. 1998
Beta-134469	LOCKEF141598	1720 ± 40	Charred material	Point bar, fine-grained alluvium	14/27-21(G ?), MC	C	Not determined
GX-28424-AMS	HT2001007-01-02	1760 ± 50	Mammal bone	50 to 60 cm below surface in giant current ripple complex, eolian sand	14/26-22D, RB	C	Marceau and Sharpe 2002a
GX-26059-AMS	KRF-99-52	1780 ± 40	Mammal bone	99 cm below surface of H5 Terrace, overbank alluvium	14/27-20D, RB	NC	This study
GX-31751	KRF-05-013	1780 ± 80	Bulk soil	1.00 to 1.14 m below surface of alluvial fan cut into H3 Terrace, alluvial fan debris	13/24-9P, RB	NC	This study
GX-26331-AMS	KRF-99-142	1800 ± 40	Mammal bone	1.83 m below surface of H3 Terrace, mixed overbank alluvium or eolian sand	13/27-24N, RB	C	This study
GX-31728	KRF-05-009	1830 ± 130	Bulk soil	8 to 13 cm below surface of H1 Terrace, eolian dune cap	14/26-25E, MC	NC	This study
Beta-92474	2-806-1	1840 ± 50	Charcoal	~1.8 m below surface of point bar, fine-grained alluvium	14/27-21D, MC	C	Bjornstad et al. 1998
WSU-1421		1840 ± 50	Shell	1.6 to 2.0 m below surface of H4 Terrace, soil ???	14/26-28M, RB	C	Rice 1973
GX-26332-AMS	KRF-99-143	1890 ± 40	Mammal bone	1.83 m below surface of H3 Terrace, overbank alluvium or eolian deposit	13/27-24N, RB	C	This study
Beta-107581-AMS		1910 ± 50	Charred material	1.9 m below surface of point bar, fine-grained alluvium	14/27-21(G ?), MC	C	Tamers and Hood 1997
GX-26163-AMS	KRF-99-108	1930 ± 60	Shell	46 cm below surface of H4 Terrace, eolian sand above overbank alluvium	14/27-28M, LB	C	This study
Beta-92476	4-806-1	1940 ± 40	Charcoal	2.45 m below surface of point bar, fine-grained alluvium	14/27-21D, MC	NC	Bjornstad et al. 1998
Beta-107585-AMS	810.1	1950 ± 50	Charred material	4.35 m below surface of point bar, fine-grained alluvium	14/27-21G, MC	C	Bjornstad et al. 1998

Table 5-9. Radiocarbon dates, Columbia River Basin. (8 Pages)

Laboratory Sample Number	Field Sample Number	Conventional Age B.P.	Material Dated	Geological Context[c]	Location[d]	Cultural[e]	Source
GX-31727-AMS	KRF-05-008	1980 ± 40	Bulk soil	41 to 46 cm below surface of H1 Terrace, eolian dune cap	14/26-25E, MC	NC	This study
GX-28309-AMS	45BN606-01-06	1990 ± 40	Mammal bone	80 to 90 cm below surface of H3, soil mixed eolian sand and alluvium silt	14/27-29R, RB	C	Marceau and Sharpe 2002a
GX-31753	KRF-05-016	2030 ± 70	Bulk soil	1.73 to 1.88 m below surface of H5 Terrace, overbank alluvium	13/23-12E, RB	NC	This study
GX-26064-AMS	KRF-99-94	2040 ± 30	Mammal bone	1.32 m below surface of H4 Terrace, overbank alluvium	14/26-15F, LB	NC	This study
Beta-133286-AMS	LOCKEF171599	2090 ± 40	Charred material	3.15 m below surface of point bar, fine-grained alluvium	14/27-21(G ?), MC	C	Wright 1999
Beta-44112		2100 ± 90	Mammal tooth enamel	Blowout in parabolic dune colony, eolian sand		C	Chatters et al. 1995
GX-26161-AMS	KRF-99-104	2100 ± 40	Shell	82 cm below surface of H3 (?) Terrace, colluvium atop overbank alluvium	14/27-21P, LB	ND	This study
Beta-92903-AMS	804.1	2130 ± 60	Charred material	Base of cutbank on point bar, fine-grained alluvium	14/27-21C, MC	NC	Bjornstad et al. 1998
GX-26211	KRF-99-66	2130 ± 120	Shell	36 cm below surface of H4 Terrace, overbank alluvium	14/26-28M, RB	C	This study
GX-28304-AMS	45BN606-01-01	2180 ± 40	Mammal bone	90 cm to 1.00 m below surface of H3 Terrace, overbank alluvium	14/27-29R, RB	C	Marceau and Sharpe 2002a
GX-26213-AMS	KRF-99-105	2190 ± 40	Mammal bone	1.24 m below surface in colluvium and slopewash	14/27-21P, LB	ND	This study
GX-31801	KRF-05-019	2210 ± 50	Organic soil	3.05 m below surface of H4 or H3 Terrace, overbank alluvium/eolian cap	10/28-2L, RB	C	This study
GX-26063-AMS	KRF-99-68	2220 ± 50	Shell	1.02 m below surface of H4 Terrace, overbank alluvium	14/26-28M, RB	C	This study
Beta-134468	LOCKEF131998	2470 ± 40	Charred material	Point bar, fine-grained alluvium	14-27-21(G ?), MC	C	???
GX-28332-AMS	45BN606-01-19	2470 ± 40	Mammal bone	1.10 to 1.20 m below surface of H3 Terrace, overbank alluvium	14/27-29R, RB	C	Marceau and Sharpe 2002a
GX-28312	45BN606-01-09	2480 ± 30	Mammal bone	90 cm to 1.00 m below surface of H3 Terrace, overbank alluvium	14/27-29R, RB	C	Marceau and Sharpe 2002a
GX-31752	KRF-05-015	2560 ± 70	Bulk soil	2.84 to 3.00 m below surface of H5 Terrace, overbank alluvium	13/23-12E, RB	NC	This study
GX-28305-AMS	45BN606-01-02	2610 ± 30	Mammal bone	90 cm to 1.00 m below surface of H3 Terrace, overbank alluvium	14/27-29R, RB	C	Marceau and Sharpe 2002a
GX-28320-AMS	45BN606-01-17	2610 ± 40	Charcoal	90 cm to 1.00 m below surface of H3 Terrace, overbank alluvium	14-27-29R, RB	C	Marceau and Sharpe 2002a
GX-28426-AMS	HT2001007-01-05	2640 ± 50	Mammal bone	40 to 50 cm below surface in giant current ripple complex, eolian sand	14/26-22D, RB	C	Marceau and Sharpe 2002a
GX-28323-AMS	45BN606-01-20	2750 ± 30	Mammal bone	90 cm to 1.00 m below surface of H3 Terrace, overbank alluvium	14-27-29R, RB	C	Marceau and Sharpe 2002a

Table 5-9. Radiocarbon dates, Columbia River Basin. (8 Pages)

Laboratory Sample Number	Field Sample Number	Conventional Age B.P.	Material Dated	Geological Context[c]	Location[d]	Cultural[e]	Source
Beta-107587	CB1F1	2850 ± 50	Charred material	1.45 m below surface of point bar, fine-grained alluvium		C	Tamers and Hood 1997
GX-28307-AMS	45BN606-01-04	2860 ± 40	Mammal bone	30 to 40 cm below surface of H3 Terrace, mixed eolian sand and alluvial silt	14/27-29R, RB	C	Marceau and Sharpe 2002a
GX-26335-AMS	KRF-99-147	2990 ± 40	Salmon vertebrae	15 cm below surface of H4 Terrace point bar, fine-grained alluvium	13/27-25C, MC	C	This study
GX-31726-AMS	KRF-05-007	3200 ± 40	Bulk soil	53 to 58 cm below surface of H1 Terrace, eolian dune cap	14/26-25E, MC	NC	This study
GX-26333-AMS	KRF-99-144	3460 ± 40	Mammal bone	58 cm below surface of H4 Terrace on bank-attached island, overbank alluvium	13/27-25C, RB	C	This study
GX-28423-AMS	HT2001007-01-01	3550 ± 40	Mammal bone	75 to 85 cm below surface in giant current ripple complex, eolian sand	14/26-22D, RB	C	Marceau and Sharpe 2002a
GX-30145-AMS	KRF-03-002	3730 ± 60	Shell	1.02 m below surface of H4 Terrace, reworked overbank alluvium	10/28-12N, LB	NC	This study
Beta-33041		3850 ± 130	Bulk soil	1.18 to 1.27 m below surface of H4 or H3 Terrace, overbank alluvium	14/26-11D, LB	C	Chatters and Hackenberger 1989
GX-31299-AMS	128F2-04-2	3870 ± 40	Mammal bone	90 cm to 1.05 m below surface of H3 Terrace, mixed eolian sand and alluvial silt	14/27-33G, RB[f]	C	This study
GX-26217	KRF-99-125	3990 ± 130	Shell	53 cm below surface of H4 Terrace, overbank alluvium	13/27-24N, LB	C	This study
GX-26160	KRF-99-100	4050 ± 220	Shell	25 cm below surface of H3 Terrace, eolian sand above Mazama tephra	13/28-31G, RB	C	This study
GX-26162-AMS	KRF-99-107	4060 ± 40	Shell	84 cm below surface of H4 Terrace, contact between eolian sand and overbank alluvium	14-27-28M, LB	C	This study
GX-26214-AMS	KRF-99-106	4100 ± 40	Shell	1.24 m below surface in colluvium and slopewash	14/27-21P, LB	ND	This study
GX-31298-AMS	128F2-04-1	4160 ± 40	Mammal bone	50 to 60 cm below surface of H3 Terrace, eolian sand	14/27-33G, RB[f]	C	This study
GX-31800	KRF-05-018	4270 ± 110	Bulk soil	3.60 m below surface of H4 or H3 Terrace, overbank alluvium/eolian cap	10/28-2L, RB	NC	This study
GX-26216-AMS	KRF-99-116	4460 ± 40	Mammal bone	69 cm below surface of H3 Terrace, eolian sand atop overbank alluvium	10/28-2P, RB	C	This study
GX-26219-AMS	KRF-99-127	4590 ± 40	Shell	1.45 m below surface of H4 Terrace, overbank alluvium	13/27-24N, LB	C	This study
GX-25586	KRF-99-23	4610 ± 40	Shell	1.07 m below surface of H4 Terrace, overbank alluvium	14/26-14F, RB	C	This study
GX-26066	KRF-99-96	4720 ± 310	Shell	46 cm below surface of H3 Terrace, near top of overbank alluvium	13/25-3D, LB	C	This study
GX-26218	KRF-99-126	4780 ± 60	Shell	1.12 m below surface of H4 Terrace, overbank alluvium	13/27-24N, LB	C	This study

Table 5-9. Radiocarbon dates, Columbia River Basin. (8 Pages)

Laboratory Sample Number	Field Sample Number	Conventional Age B.P.	Material Dated	Geological Context[c]	Location[d]	Cultural[e]	Source
GX-31723	KRF-05-004	4780 ± 150	Bulk soil	1.27 m below surface of H5 Terrace, mixed eolian/alluvium deposit	14/27-20D, RB	NC	This study
GX-26334	KRF-99-146	4840 ± 60	Shell	Base of slump on top of terrace, shell from H4 Terrace?	13/27-25C, MC	C	This study
GX-25584	KRF-99-21	4860 ± 190	Shell	46 cm below surface of H4 Terrace, overbank alluvium	13/25-3K, RB	C	This study
GX-28429	HT2001007-01-06	4880 ± 80	Shell	2 to 20 cm below surface in giant current ripple complex, eolian sand/ slopewash	14/26-22D, RB	C	Marceau and Sharpe 2002a
GX-25585-AMS	KRF-99-22	4900 ± 40	Shell	91 cm below surface of H4 Terrace, overbank alluvium	13/25-3K, RB	C	This study
GX-28427-AMS	HT2001001-01-07	4945 ± 40	Mammal bone	60 to 70 cm below surface in giant current ripple complex, eolian sand/ slopewash	14/26-22D, RB	C	Marceau and Sharpe 2002a
GX-26212-AMS	KRF-99-103	5000 ± 40	Shell	1.30 m below surface of H3 (?) Terrace, colluvium atop overbank alluvium	14/27-21P, LB	ND	This study
GX-31725-AMS	KRF-05-006	5060 ± 40	Bulk soil	84 to 89 cm below surface of H1 Terrace, eolian dune cap	14/26-25E, MC	NC	This study
GX-31722	KRF-05-003	5830 ± 200	Bulk soil	1.98 cm below surface of H5 Terrace, mixed eolian/alluvium deposit	14/27-20D, RB	NC	This study
GX-28428	HT2001007-01-04	5880 ± 70	Shell	20 to 30 cm below surface in giant current ripple complex, eolian sand/ slopewash	14/26-22D, RB	C	Marceau and Sharpe 2002a
GX-31750	KRF-05-012	5900 ± 200	Bulk soil	1.60 to 1.75 m below surface of alluvial fan cut into H3 Terrace, alluvial fan debris	13/24-9P, RB	NC	This study
GX-31660/31661	KRF-05-002	6190 ± 230	Bulk soil	60 cm above gravel base of H4 Terrace, overbank alluvium	13/25-3K, RB	NC	This study
GX-26057	KRF-99-84	6310 ± 170	Shell	30 cm below surface of H3 Terrace, overbank alluvium	13/27-23N, RB	C	This study
Beta-194766-AMS	45BN135#1	6310 ± 40	Mammal bone	Within H5 point bar, capping eolian sand	14/27-29K, MC (?)	C	Hood 2004
GX-31749	KRF-05-011	6390 ± 220	Bulk soil	3.15 to 3.30 m below surface of alluvial fan cut into H3 Terrace, alluvial fan debris	13/24-9P, RB	NC	This study
GX-26055	KRF-99-82	6550 ± 260	Shell	69 cm below surface of H3 Terrace, overbank alluvium	13/27-23N, RB	C	This study
GX-26058	KRF-99-85	6840 ± 100	Shell	15 cm below surface of H3 Terrace, overbank alluvium	13/27-23N, RB	C	This study
GX-31658/31659	KRF-05-001	6840 ± 200	Bulk soil	30 cm above gravel base of H4 Terrace, overbank alluvium	13/25-3K, RB	NC	This study
GX-30147	KRF-03-004	6980 ± 60	Shell	30 cm below surface of H3 (?) Terrace, eolian dune sand atop bench – stratigraphically below Mazama tephra	10/28-23A, RB	C	This study
GX-31655	KRF-04-075-1	6990 ± 130	Bulk soil	1.5 m below surface in organic soil at top of alluvial plug in ancient channelway, 2 cm below Mazama ash	13/24-12M, MC	NC	This study

Table 5-9. Radiocarbon dates, Columbia River Basin. (8 Pages)

Laboratory Sample Number	Field Sample Number	Conventional Age B.P.	Material Dated	Geological Context[c]	Location[d]	Cultural[e]	Source
GX-31656	KRF-04-075-2	7010 ± 160	Bulk soil	1.5 m below surface in organic soil at top of alluvial plug in ancient channelway, 2 cm below Mazama ash	13/24-12M, MC	NC	This study
GX-26215	KRF-99-115	7090 ± 130	Shell	69 cm below surface of H3 Terrace, eolian sand atop overbank alluvium	10/28-2P, RB	C	This study
GX-26056	KRF-99-83	7330 ± 110	Shell	46 cm below surface of H3 Terrace, overbank alluvium	13/27-23N, RB	C	This study
GX-26065	KRF-99-95	7710 ± 340	Shell	In blowout surface of H3 Terrace, atop overbank alluvium	14/26-16R, RB	C	This study
Beta-33040		7880 ± 110	Shell	1.18 to 1.27 m below surface of H4 or H3 Terrace, overbank alluvium	14/26-11D, LB	C	Chatters and Hackenberger 1989
GX-26159	KRF-99-99	7960 ± 210	Shell	25 cm below surface of H3 Terrace, overbank alluvium (projected below Mazama tephra)	13/28-31G, RB	C	This study
UCR-3807		8130 ± 40	Bone	H3 Terrace, overbank alluvium	12/29-27N, RB	C	Taylor et al. 1998
GX-32054	128F2-05-03	8270 ± 100	Shell	1.00 m below construction modified surface of H3 Terrace, eolian sand	14/27-33G, RB[f]	C	Marceau and Sharpe 2006
UCR-3476		8410 ± 60	Bone	H3 Terrace, overbank alluvium	12/29-27N, RB	C	Taylor et al. 1998
Beta-133993		8410 ± 40	Bone	H3 Terrace, overbank alluvium	12/29-27N, RB	C	Taylor et al, 1998
GX-31300	128F2-04-3	8650 ± 110	Shell	60 to 70 cm below surface of H3 Terrace, eolian sand	14/27-33G, RB	C	This study
GX-29272	45BN432/431-01-01	8860 ± 80	Shell	80 to 90 cm below surface of H3 Terrace, overbank alluvium	14/27-33G, RB[f]	C	Marceau and Sharpe 2002b
	WW-1626	9010 ± 50	Organic Soil	20 cm below surface of H3 Terrace, overbank alluvium	12/29-27N, RB	NC	Wakeley et al. 1998
GX-32055-AMS	128F2-0504	9360 ± 60	Bulk soil	1.00 m below construction modified surface of H3 Terrace, eolian sand	14-27-33G, RB[f]	C	Marceau and Sharpe 2006
	WW-1727	12460 ± 50	Organic Soil	~2.25 m below surface of H3 Terrace, overbank alluvium	12/29-27N, RB	NC	Wakeley et al. 1998

Table 5-9. Radiocarbon dates, Columbia River Basin. (8 Pages)

Laboratory Sample Number	Field Sample Number	Conventional Age B.P.	Material Dated	Geological Context[c]	Location[d]	Cultural[e]	Source
GX-31657-AMS	KRF-04-076	12790 ± 90	Bulk soil	2.00 m below surface In alluvial sand plug overlying fluvial gravel	13/24-12M, MC	NC	This study
	WW-1738	14560 ± 50	Organic soil	~3.20 m below surface of H3 Terrace, overbank alluvium	12/29-27N, RB	NC	Wakeley et al. 1998
	WW-1737	15330 ± 60	Organic soil	~3.05 m below surface of H3 Terrace, overbank alluvium	12/29-27N, RB	NC	Wakeley et al. 1998

[a] Geochron dates are based on the Libby half-life (5,570) for carbon-14. The error is ±1. The modern standard is 95% of the activity of the National Bureau of Standards' oxalic acid. All dates are carbon-13 corrected.

[b] Beta dates are based on the Libby half-life (5,568) for carbon-14. The error is ±1. The modern standard is 95% of the activity of the National Bureau of Standards' oxalic acid. All dates are carbon-13 corrected.

[c] Depths mainly from source study, geologic context from this study.

[d] Location is based on rectangular system for subdivision of public land (township, range, section, 1/4 1/4 section, and left bank [LB], right bank [RB], mid-channel [MC].

[e] Cultural (C), non-cultural (NC), not determined (ND).

[f] Location designated in table as RB in modern river platform could be a MC bar in ancestral river pattern.

5.2 RADIOCARBON GEOCHRONOLOGY

5.2.2 Radiocarbon Dates of Sedimentary Units and Landforms

This section presents a discussion of the age of sedimentary units and landforms of late Pleistocene and Holocene age based on radiocarbon dating. Age dating focused on steps/benches in the terrace system and downstream accretionary bedforms of the island/bar complexes. The discussion uses information compiled in Table 5-9 and field notes prepared during geologic mapping of the study area. Radiocarbon dates were placed within a stratigraphic position (i.e., basal gravel, overbank alluvium, or capping eolian veneer). Further refinement of stratigraphic units is not possible with the field data collected due to (1) bioturbation that extensively disrupted and destroyed internal bedding, and (2) limited lateral continuity of bedding due to erosion, poor sediment exposure, and inundation of terraces by dam-improved reservoirs.

The age of sediments and landforms on the P-x, P-1, H-1, and H-2 Terraces are not well constrained by radiocarbon dates, primarily because coarse gravel material that dominates the sediments on the terraces contains very little organic material. Radiocarbon dates from these terraces are from eolian sediments that cap the sedimentary sequence and landforms. The eolian sediments form relatively stable sand sheets or migrating dune colonies that post-date alluvial sedimentation on these terraces. The oldest date of eolian sediments from these terraces is 5,060 ± 40 rcybp (GX-31725-AMS). This date is significantly younger than the age of Mazama ash that is commonly found in eolian sequences capping the terraces.

Radiocarbon dating focused primarily on terrace steps H-3, H-4, H-5, and H-6 because of the abundance of cultural features and prevalence of organic material on these terraces. Dates from these terrace steps were collected from fine-grained sediments that are found in overbank alluvium and eolian caps atop gravel treads.

Radiocarbon dates from the overbank alluvial of the H-3 Terrace range from at least 9,360 ± 60 (GX-32055-AMS) to 6,840 ± 100 rcybp (GX-26058). The older age is from an eolian sand sheet that caps the H-3 gravel tread in the sloughs river segment. The oldest age of an alluvial cap from the study area is 8,860 ± 80 (GX-29272) from shell collected near the base of the cap in the sloughs river segment. The bones of Kennewick Man were originally entombed in the base part of the H-3 Terrace before being scattered along the modern day right riverbank in the Clover Island river segment. The 6,840 ± 100 rcybp date is from a shell midden located near the top of the overbank alluvial. The alluvial cap is situated uncomformably on top of alluvial gravel. The alluvial gravel of the H-3 Terrace that underlies the overbank alluvium has not been sampled for radiocarbon dating. The age of the alluvial gravel must be older than the overbank alluvium or greater than 9,360 ± 60 rcybp.

Eolian sand/silts dominate the upper part of the fine-grained sequence on the H-3 step. The eolian sediments range in age from 6,980 ± 60 rcybp (GX-30147) to the present. The oldest date of the eolian cap was collected within 15 cm from the base of the Mazama ash (dated at 6,850 ± 250 rcybp). Mazama ash is commonly found in wind-blown sediments of the H-3 Terrace and often occurs within 20 cm of the contact between the overbank alluvium and capping eolian sediments. The oldest radiocarbon date is from a shell midden near the base of the eolian section. The eolian processes on the terrace have continued to the present, based on the thickness of the eolian deposits (often up to 50 cm) and the occurrence of Mount St. Helens ash from the May 18, 1980, eruption that occurs near the top of the eolian cap and is actively being reworked into modern dunes.

5.2 RADIOCARBON GEOCHRONOLOGY

5.2.2 Radiocarbon Dates of Sedimentary Units and Landforms

The H-4 Terrace, like the H-3 Terrace, consists of a basal gravel, overbank alluvium, and eolian cap. The gravel has not been dated, but must have been deposited following the entrenchment of the Columbia River into the bed. Thus, the H-3 gravel is younger than the H-3 overbank alluvium, or 6,840 ± 100 rcybp. The gravel is older than the overlying overbank alluvium of the H-4 Terrace or older than 4,900 ± 40 rcybp (GX-25585-AMS). The overbank alluviuim rests unconformably on the gravel. The overbank allluvium ranges in age from 4,900 ± 40 rcybp to 2040 ± 30 (GX-26064-AMS). The bounding ages of overbank alluvium were dated from mollusk shell and mammal bone, respectively. The eolian section on the H-4 Terrace becomes the dominant sediment type by 1,930 ± 60 rcybp (GX-26163-AMS) after a gradational transition from overbank-dominated sediment. Eolian processes have been active on the H-4 Terrace from 1,930 ± 60 rcybp up to the present day (190 ± 40 rcybp [GX-26062-AMS]).

The H-5 Terrace forms a distinct landform in the downward-stepping terrace system; however, the age of this landform has been difficult to determine based on the wide variation in ages. As with the two previous terraces, the basal gravel has not been dated. The primary organic materials sampled from the alluvium are bulk soil and mammal bone. Bulk soil samples are dated at 4,780 ± 150 (GX-31723) and 2,560 ± 70 (GX-31752) rcbp. These dates overlap the period of deposition of the overbank alluvium in the H-4 Terrace. A mammal bone was dated at 1,780 ± 40 (GX-26059-AMS) rcybp. The age of the alluvial cap has been assigned to 1,780 ± 40 rcybp, as the bulk soil dates appear too old to be representative of the H-5 Terrace. Further field work is needed to constrain the age of the overbank alluvium on the H-5 Terrace. The eolian cap has a single radiocarbon date of 100 ± 50 rcybp (GX-30149). The date is from 84 cm below the terrace surface. The thickness and young age of the eolian sand is expected in the area of the right bank of the Sloughs river segment, since the segment has migrating sand from winds trending northeasterly along the regional wind direction and winds parallel to the river created by topographic relief of the White Bluffs. The Sloughs areas has an ample supply of sand to support migrating dune colonies that are forming thick eolian caps over terrace treads.

The H-6 Terrace is the youngest of the terrace steps and could be considered part of the modern streambed as it is inundated almost annually during high-stage flow. This terrace forms a distinct geomorphic feature, although not as dominant a landform as the upper terrace benches (i.e., H-3 and H-4 Terraces). The gravel of this step has not been dated. Radiocarbon dates are available from alluvial and eolian sediments. The dates come from isolated exposures that are remnants of more extensive deposition and were partially eroded by the Columbia River. Field mapping and radiocarbon dates from these remnants indicate a complex relationship between overbank alluvium and the eolian cap. Eolian and alluvial sediments are intercalated throughout the reach. Overbank alluvium dominates in the Vernita and Wooded Island river sections, whereas eolian sediments are more prevalent in the Horn river segment. The age of the fine-grained remnants are between 310 ± 40 (TX-3331) and 160 ± 100 (GX-25587) rcybp. Fine-grained sediments continue to accumulate in the modern-day channel area around the older erosional remnants on the terrace. Most accumulation of fine-grained sediments occur in slough areas and other areas distal to channel flow.

5.2 RADIOCARBON GEOCHRONOLOGY

5.2.2 Radiocarbon Dates of Sedimentary Units and Landforms

The second area of focus for age dating is the downstream accretionary bedforms on island/bar complexes. The age of the bedforms have been determined for the major bar forms (i.e., mid-channel and bank-attached) in the study area. The oldest and most continuous record of the accretionary bedforms is from Locke Island with over 20 radiocarbon dates. The dates range from 2,470 ± 40 (Beta-134468) to modern day (30 ± 50 [Beta-107583-AMS] rcybp). The low-angle cross-bedding bedforms decrease in age upsection. Cutbanks at the downstream terminus of most overbank accretionary bedforms have cultural charred material dating less than 600 rcybp (Table 5-9).

The mid-channel and bank-attached island/bar complexes have terrace steps that are positioned at the same elevation as several of the lower three downward-stepping terraces (H-4, H-5, and H-6) on adjacent banks of the Columbia River. The depositional bedforms on all three steps of the largest bank-attached bars (Savage Island) are similar to bedforms on the terraces along the left and right riverbanks. For the smaller bank-attached and mid-channel bars primary lithofacies is low-angle cross-bedding with occasional horizontal laminations in the lowest steps. The lithofacies are almost totally associated with the downstream accretionary bedforms, with the exception of several minor lateral and upstream accretionary bedforms. The bank-attached and mid-channel island/bar complexes have age dates that span the range of late H-3 Terraces (oldest island/bar date of 2,470 ± 40 rcybp [Beta-134468]) through the H-6 Terrace (youngest island/bar date of 30 ± 50 rcybp [Beta-107583-AMS]). The steps on the island/bar complexes appear to be of similar age as their corresponding terraces on the main left and right riverbanks.

6.0 CHARACTERISTICS OF THE POST-GLACIAL COLUMBIA RIVER

This section presents the evolution of the Columbia River from the end of cataclysmic glaciofluvial flooding to the present-day river conditions, and an initial evaluation of the stability of the river channel based on current river flow conditions. The discussion of the evolution of the river utilizes the information presented in Chapter 4 on bedforms, landforms, and environmental interpretations and their association with terrace steps.

6.1 RIVER METAMORPHOSIS

Between 15,700 and 13,500 years before present during the late Pleistocene, much of eastern Washington was subjected to cataclysmic flooding from sudden outbursts from Glacial Lake Missoula that flowed through a network of channelways (a series of coulees named by J. H. Bretz as the Channeled Scabland) and into the structural basins of south-central Washington (Bretz et al. 1956, Baker et al. 1991, Booth et al. 2004). Within the Pasco Basin and study area, the inflow of colossal floodwaters exceeded the outflow at Wallula Gap that is located several kilometers downstream of the study area. This resulted in the temporary impoundment of floodwaters in the basin. The initial flooding, temporary lake impoundment, and draining floodwaters resulted in a sequence of gravel-dominated facies in main channel areas, sand-dominated facies adjacent to main channelways, and interbedded sand and silt facies that are found away from main channels along basin margins and backflooded environments in tributary valleys (Baker et al. 1991). These sediments and associated landforms from large-scale flooding are major components of Relief Generation III. Large-scale floods ended about 13,500 years before present as the Cordilleran Ice Sheet, along with its major ice lobes Okanagon and Purcell Trench, began rapidly retreating northward.

The remaining part of this section focuses on the evolution of the Columbia River since the end of the large-scale outburst floods. The discussion of the river environment is discussed in terms of environmental interpretations and continuity of the bedforms and landforms of seven downward-stepping terraces in the river valley.

The uppermost bench (P-1 Terrace) of the terrace system is dominated by GBL with CHL architectural elements and is associated with a braided stream environment with an extensive network of migrating large-scale bars and channels. The GBL and CHL architectural elements represent sediments transported by ice-sheet meltwaters and periodic small-scale outburst floods from the last stages of Glacial Lake Missoula and other ice margin lakes (e.g., glacial lakes Columbia 1 and 2, Priest Lake, Elk) as the Cordilleran Ice Sheet continued to rapidly retreat northward. Point bars have been mapped at several bends in channelways and at the downstream end of land masses where channelways merge. The braided stream is contained in a single channelway in the northern and southern parts of the study area, but narrower anastomosing channelways were formed in the central portion of the study area (Figure 6-1). The age of the channel gravel on the P-1 Terrace post-dates Mount St. Helens Set S ash (or post 13,000 years in age) and several post-ash, large-scale floods. The gravel also transcends the eruption of Glacier Peak ash (11,250 ± 250 rcybp) as the tephra is not found atop the P-1 Terrace at any location in the study area.

6.1 RIVER METAMORPHOSIS

The river channel at the end of P-1 Terrace underwent several planform changes due to reduced discharge and decreased sediment influx in the Columbia River as the continental ice sheet continued back- and down-wasting. The changes in flow and bedload resulted in a narrower river channel throughout the study area and abandonment of channelways in the anastomosing channel area. As the Columbia River entrenched into the river bed, gravel necks aggraded plugs at the head end of the channel that blocked off the southern channelways around Gable Mountain. With the southern channelways blocked and abandoned, the Columbia River was diverted into the two northernmost channels. With further river entrenchment, the N-Channel was abandoned. The resulting planform after the anastomosing of channelways were abandoned was a single river channel through the river within the study area.

The formation of a single river channel planform marks the transition from the P-1 Terrace to the H-1 Terrace (Figure 6-2). The single channelway closely follows the present-day path of the Columbia River. The river channel is narrower than the river during the time spanned by the P-1 Terrace. The river on the H-1 Terrace was a shallow braided stream with smaller scale bedforms/elements (GBM and CHM) compared to bedforms on the P-1 Terrace. The gravel deposited on the H-1 Terrace represents a river system still influenced by glacial debris from the backwasting of the continental ice sheet. The river flow and load was significantly reduced from the river on the P-1 Terrace. The age of the H-1 Terrace is not well constrained in the study area. It is younger than the P-1 Terrace and Glacier Peak ash (11,250 ± 250 rcybp) and older than the overbank alluvium on H-3; this is greater than 9,360 rcybp.

The H-2 Terrace is similar in character to the H-1 Terrace with a braided river system that continues to be dominated by the GBM and CHM elements. SB becomes an abundant element on the H-2 Terrace, as sandy bars are commonly found on the inside of channel bends and the downstream end of gravel bars. The river channel during the time of the H-2 Terrace was narrower than the H-1 Terrace and further entrenched into the valley floor as the Columbia River continued to adjust to lower flow rates and reduced sediment load at the end of the Ice Age. The age of the H-2 Terrace is constrained by the same dates as the H-1 Terrace (post-Glacier Peak ash [11,250 ± 250 rcybp]) and overbank alluvium on the H-3 Terrace (about 9,360 rcybp). The H-2 Terrace by its entrenched position into the H-1 Terrace is younger than H-1. H-2 Terrace sediment accumulation ended with the Columbia River initiating another cycle of river rejuvenation and entrenchment into the river bed.

The H-3 through H-6 Terraces form a set of narrow, downward-stepping benches. The planform for the Columbia River changed from a broad braided stream to a narrow entrenched straight stream with a single, sinuous thalweg and with alternating (bank-attached) and mid-channel bars (Figure 6-3). This change in planform ended the influence of meltwaters from the ice sheet and removal of the glacial debris that choked much of the upper Columbia River drainage basin. This new planform starting with the H-3 Terrace marked the beginning of a post-glacial Columbia River. The main channel was formed mainly of CHM elements with occasional GBM and SB elements. The bank-attached and mid-channel bars typically consist of GBM and DA elements. Secondary channelways sedimentation often have high-energy course deposits (CHM and GBM elements) and low-energy slackwater slough sand and silt (SB and CH [FF] elements).

Channel margins are well defined and are commonly bounded by overbank alluvium and levees (mainly FF and LV elements with minor CR/CS elements.). The terrace steps indicate cycles of (1) river rejuvenation with channel entrenchment and (2) sediment accumulation and hydraulic molding of bedforms.

6.1 RIVER METAMORPHOSIS

During the start of the river occupation at the level of the H-3 Terrace, the Columbia River started entrenching into bedrock along most of the river bed within the study area. The river incised into basaltic bedrock in the upstream part of the study area (i.e., from Sentinel Gap river segment [RM 406] through the Umtanum Ridge river segment [RM 392]). Basalt outcrops formed prominent topographic highs in the river bed from Priest Rapids that remained in the channel until inundated by the reservoir behind Priest Rapids Dam. Below the Umtanum Ridge river segment, the Columbia River entrenched into mudstone/conglomerate of the Ringold Formation. Many of the bank-attached and mid-channel bars from Coyote Rapids downstream to the confluence of the Snake are relatively stable bedforms. The stability is due to resistant erosional remnants of the Ringold formation that form the core of the bars.

The cyclic pattern of the terraces indicates Columbia River episodes of erosional entrenchment followed by periods of sediment accumulation. The ages associated with four river cycles are as follows:

1	Sediment accumulation on H-3 Terrace	~9,360 to 6,800 rcybp
2	River entrenchment into H-3 Terrace	6,800 to 4,900 rcybp
3	Sediment accumulation on H-4 Terrace	4,900 to 2,100 rcybp
4	River entrenchment into H-4 Terrace	2,100 to 1,800 rcybp
5	Sediment accumulation on H-5 Terrace	(est) 1,800 to 1,200 rcybp
6	River entrenchment into H-5 Terrace	1,200 to 500 rcybp
7	Sediment accumulation on H-6 Terrace	500 to 300 rcybp
8	Erosion on H-6 Terrace	300 to 30 rcybp
9	Sediment reaccumulation on H-6 Terrace	30 years to present

6.2 RIVER STABILITY

Fluvial processes continually act on the streambed and banks of perennial streams with erosional scour occurring in one area of the stream and sediment deposition in another. Therefore, streambeds and stream banks are never completely and totally stable. This section investigates and assesses the degree of stability of the streambed and banks of the Columbia River within the study area. The discussion focuses on changes observed in the river channel and establishes several long-term average rates of change. The discussion is presented in terms of the following stream aspects: channel pattern, vertical stability (aggradation and degradation), and lateral stability (bank erosion and avulsion).

6.2.1 Channel Pattern

The channel pattern or planform of the Columbia River evolved following inundation of the river valley by meltwaters from late Pleistocene, large-scale cataclysmic flooding. At cessation of large-scale flooding, the river planform formed an anastomosing stream pattern that subsequently transformed to a braided stream planform. Both types of planforms were shallow fluvial systems with poorly defined banklines and subject to channel migration. The last stage of metamorphosis of the Columbia River was the change to the straight stream planform of the modern-day river. The straight stream planform has persisted in south-central Washington since the Columbia River occupied the streambed of the H-3 Terrace for 9,360 rcybp. Since the river has evolved into the straight channel planform, migration of the thalweg has largely been restricted to back-and-forth sinuous movement within the existing river channel. The river during this time has entrenched into the streambed. The entrenched stream channel and relatively limited changes in hydrologic and climatic cycles over the past 10,000 years indicate that the straight channel planform is the stable channel pattern of the Columbia River for the present and will likely be the stable planform until the next major change in climate/river hydrology or tectonism.

6.2 RIVER STABILITY

6.2.1 Channel Pattern

Within the river channel, a sinuous thalweg has been mapped on the streambed based on bathymetric data. The bathymetric data along with surface mapping of bedforms/landforms were used to delineate a network of alternate bars (i.e., right and left bank-attached island/bar complexes). The stability of the thalweg can be assessed based on changes observed within the stream channel. A thalweg change manifests itself through scouring of alternate bars as the thalweg and alternate bars migrate downstream. Inspection of historic aerial photos and topographic maps of the river indicate a low rate of alternate bar migration in the river channel over historic times. The "persistence" of island/bar complexes in the river channel has been observed by Hall (1968) and the senior author (unpublished data). Minor changes to alternate bars (bank-attached island/bar complexes) and mid-channel island/bar complexes indicate the thalweg has undergone relatively minor shifts within the channel over the last century. These minor changes are another indication that the straight planform of the Columbia River is a relatively stable channel pattern. The relatively fixed position of thalweg and alternate bars in the river channel is in part due to the entrenchment into resistant bedrock. The resistant bedrock is a key factor that controls the rate of shifting of the thalweg in the channel and the aggradation/degradation of alternate bars.

Entrenchment of the Columbia River into its streambed has reduced the likelihood of morphological changes to the existing straight channel planform under the current climatic/hydrologic conditions. Rapid channel changes due to stream avulsion are severely limited due to the relatively narrow floodplain and height of the land adjacent to the floodplain that is well above the 100-year flood level.

6.2.2 Vertical Stability

The Columbia River, as an entrenched straight stream, has been actively eroding into the streambed during the late Pleistocene and much of the Holocene. The rate of streambed erosion is a function of stream power and the characteristics of the geologic materials in the bed.

The streambed of the Columbia River consists of alluvial bedforms that are migrating over bedrock. Alluvial bedforms are best observed in riffles and in shallow pools where transient bedforms are typically aggraded and molded during low-stage flow, and sediments scoured and transported downstream during high-stage flow during the spring freshet. In pools the alluvial bedforms and bedrock are typically armored with a lag of cobbles from the transport and deposition of Holocene alluvium and boulders that are remnants of Pleistocene glaciofluvial sediments. The large clast size of gravel material on the streambed is relatively stable (i.e., clasts are not likely to be eroded from the stream bed and transported downstream) except at high-stage flow where the flow exceeds 100 cm/sec.

From the upstream boundary of the study area to about RM 396, the streambed is eroded into bedrock that is composed of basalt. Erosion into bedrock is due to a combination of uplift of the Yakima Folds (i.e., Saddle Mountains and Umtanum Ridge structures) and entrenchment of the Columbia River into the streambed as the river seeks its base level. Below RM 396 and throughout most the remainder of the study area, the streambed is scoured into resistant alluvial sediments of the Ringold Formation (members of Wooded Island and Taylor Flat). At the river bend near RM 336 the river impinges on basalt bedrock along the north flank of a small doubly plunging anticline. Here, the river is redirected eastward along the axis of the Pasco syncline where the river has entrenched back into resistant alluvial sediments until encountering basalt at Wallula Gap in the Horse Heaven Hills downstream for the study area.

6.2 RIVER STABILITY

6.2.2 Vertical Stability

The paired downward-stepping terrace system along the riverbanks suggests the river has undergone cycles of erosional scouring interrupted by periods of sediment aggradation within the streambed. These paired terraces can be used to determine the rate of channel entrenchment. Using the well-defined terraces located along the Hanford Reach, an average entrenchment rate can be calculated based on the difference in height between the alluvial caps mantling the H-3 and H-6 Terraces (approximately 6 m) divided by the age difference between the two terraces (approximately 10,000 years). The average entrenchment rate over the past 10,000 years is 0.6 mm/yr over most of the Hanford Reach. This rate is relatively low. The low rate is in part due to the resistance and competence of geologic materials in the streambed and the low gradient in this part of the river system.

6.2.3 Lateral Stability

Lateral stability is a function of stream power and the properties of the geologic materials along the bankline. The bankline separates bedforms/landforms of the river channel from the floodplain environment and other geologic units. The lateral stability of the bankline may be affected by the composition of the bank materials, the type and density of plant communities, planform of the river segment (e.g., straight or bend), and stresses placed on the bank from geomorphic landforms and tributary streams.

The materials along the banklines are important to the stability of the Columbia River. The materials are mainly composed of the following:

- Basaltic and resistant alluvial bedrock (as discussed above).
- Terrace gravels including upper terraces (P-x through H-2 Terraces) that are armored with cobble-boulder clasts, and lower terraces (H-3 through H-6 Terraces) with armored cobble-pebble clast treads and capped by overbank alluvium.
- Engineered dikes/levees armored with large boulder-size riprap of basalt and other artificially constructed banks.

The bedrock, coarse-grained terraces, and cohesive alluvial caps found along the riverbank are relatively resistant to erosion by fluvial processes within overbank environments of straight segments of the Columbia River. In places where the riverbanks along straight river segments consist of basaltic and resistant alluvial bedrock, hydraulic processes of the Columbia River have had little impact on the riverbanks, and lateral erosion of banks is minimal. In areas where the channel is bounded by a floodplain, the riverbanks typically contain a series of downward-stepping terraces (i.e., H-3 through H-6 Terraces). The lower terrace steps are often inundated by Columbia River floods (Figure 6-4) and yet, along much of the river, the steps have survived for thousands of years of repeated hydraulic stresses from high-stage flow. Preservation of these terraces, particularly the younger two terraces (H-5 and H-6 Terraces), is a good indication that little lateral erosion has occurred in most areas of the floodplain. The persistence of all four or most of the paired terraces along major portions of the riverbanks suggests the lateral encroachment of the Columbia River beyond the limits of the main channel in straight river segments has been generally minimal over the past 10,000 years.

6.2 RIVER STABILITY

6.2.3 Lateral Stability

Cutbanks are common features observed along the river reach in the fine-grained alluvial sediments within downstream accretionary bedforms. The bedforms were aggraded during periods of high-stage flow and later scoured laterally during lower stage flow. The lateral scour undercut the riverbanks creating local scarps. The scarps form almost vertical faces that often expose the complete thickness of the alluvial cap. The direction of flow during sediment aggradation has been mainly parallel to the banks, whereas the flow was directed into the bank during periods of lateral erosional scour. Active cutbanks are observed at the downstream end of many bank-attached and mid-channel island/bar complexes. The presence of cutbanks is evidence that lateral erosion is an active process along the banks of many island/bar complexes in the modern-day Columbia River.

Extensive scouring of overbank alluvium that caps the H-6 Terrace has been observed in several areas along the reach. Examples of this erosion are found above Coyote Rapids on the left bank (RM 384), at the Horn on the right bank (RM375.5), and opposite Homestead Island on the right bank (RM 352). At these localities, only small isolated remnants of the alluvial cap remain above the gravel tread. The floodplain has been scoured up to 1.5 km along the river, and the bank has receded as much as 150 m due to lateral erosion. In areas of maximum lateral erosion, the bankline has receded back into the H5 and H-4 Terraces. This extensive lateral scouring of the terrace steps is the result of very large-scale flooding of the Columbia River. The age of the flood post-dates the deposition of the alluvial cap of the H-6 Terrace (i.e., 160 rcyb or between 1745 and 1805 A.D.) and pre-dates the early historic evidence (i.e., aerial photography in 1930s) along the reach.

Scouring of the H-6 Terrace likely occurred during the 1894 flood (maximum flow of 20,954 m^3/sec [740,000 ft^3/sec]) (Wood 1954) or other floods of similar very-high flow.

At river bends or meanders, the outside bank is more susceptible to lateral erosion than other areas of the river bankline. This is due to stream power being directed into the riverbank. In river bends where the channel is entrenched into basaltic bedrock (i.e., at Umtanum Ridge [RM 396] and near Bateman Island [RM 334]) the extent of lateral erosion is very low based on the fact that the point of inflection of the bend has remained essentially in a fixed position for at least the past 10,000 years. In other river bends, where the outside bank consists of resistant alluvium of the Ringold Formation, the outer bank shows evidence of lateral erosion of at least several centimeters per year. The most active area of lateral erosion occurs along the left bank in the Horn segment between RM 376 to RM 371.5. The Columbia River has scoured into the outer bank undercutting the Ringold Formation, forming the prominent 150-m-high escarpment of the White Bluffs. Based on the inferred position of the river channel that was reconstructed from remnants of paired terrace steps (i.e., H-3 through H-6 Terraces), the average rate of lateral erosion at the Horn has been 30 cm/yr over the past 10,000 years. The growth and shift of the river bend at the Horn indicates a rotational pattern similar to rotational patterns described by Brice (1964). The inflection point at the bend has slowly migrated downstream approximately 5.5 km from a point established at the end of large-scale Pleistocene cataclysmic flooding. The inflection point has rotated approximately 40 degrees clockwise about a pivot point that is located inland from the right bank.

6.2 RIVER STABILITY

6.2.3 Lateral Stability

Minor stream inflections in the direction of water flow occur extensively throughout the river channel. These inflections cause flow to be diverted and directed toward the riverbanks. The flow inflections in the channel are attributed to the presence of geomorphic landforms or tributary streams, including:

- Bank-attached island/bar complexes (e.g., Yeager Island [RM 390], Homestead Island [RM 352], and Nelson Island [RM 340]) that cause flow to be directed to the opposite bank
- Mid-channel island/bar complexes (e.g., 100-D Island [RM 377], Johnson Island [RM 346], and Seagull Island [RM 340]) that force flow to be diverted around the landform and often toward both riverbanks
- Riffles (e.g., Upper Priest Rapids [RM 406], Coyote Rapids [RM 382), and Sloughs surface ripples [RM 368.5]) that are shallows in the river that spread the flow laterally toward the riverbanks
- Tributary stream deltas and flow (e.g., ephemeral stream in Sourdough Canyon [RM 400.5], Yakima River [RM 335], and Snake River [RM 325]) that push the Columbia River flow toward the opposite bank
- Landslides (e.g., Locke Island landslide complex [near RM 372.5]) that have entered the river channel force flow to the opposite bank or bank of intervening island/bar complexes (e.g., left bank of Locke Island).

Minor flow inflections have had little impact on sediment deposition or erosional scour on the banks of the Columbia River and island/bar complexes, except for several local areas of the river where the inflections are noticeable in the channel and riverbanks. Riverbanks most significantly impacted are associated with the recent irrigation-induced Locke Island landslide and the long-term encroachment of the Yakima River delta. The Locke Island landslide has engulfed much of the river channel (up to 213 m) between the left bank of the Columbia River and the Locke Island island/bar complex (Bjornstad et. al 1998). The flow rate through the channel has increased due to the constriction and the flow has been redirected into the left bank of Locke Island causing lateral scour and recession of the bank. The lateral erosion rate has been as much as 16 m per year (Bjornstad et. al., 1998). At the confluence of the Yakima River, the delta has been encroaching on the Columbia River channel since the end of large-scale cataclysmic flooding. The confluence of the Yakima River has moved 11.2 km downstream in the last 12,000 years, and over the past 10,000 years the delta has migrated into the Columbia River channel near RM 334. Here the encroachment of the Yakima River delta and flow has resulted in a shift of the thalweg of the Columbia River from outside of the bend (right riverbank) in the Columbia River to the inside (left bank). The channel of the Columbia River has adjusted laterally approximately 1 km into the left riverbank.

Engineered riprap dikes have been constructed along portions of the riverbank in the cities of Kennewick, Pasco, and Richland for flood control. The dikes were constructed to heights that extend above the H-3 Terrace. The surfaces of the dikes are composed of large boulder-size riprap of basalt. The basaltic material is of sufficient size and density such that the dikes have not affected by hydraulic processes of the Columbia River. The banklines of the river have remained essentially unchanged along segments of the Columbia River where dikes have been constructed. These areas of the riverbank show no recent evidence of lateral erosion by the river.

6.2 RIVER STABILITY

6.2.3 Lateral Stability

Artificial banks were constructed along short segments of the riverbank to support reactor operations in the 100 Areas, municipal activities at the Hanford town site, and laboratory and fuel fabrication operations in the 300 Area. These banks, constructed of native sand and gravel, were derived from recontouring of land adjacent to the riverbanks. The artificial banks in several of these areas were constructed up to the river channel and, therefore, are subject to hydraulic processes of the Columbia River and lateral erosion during periods of high-stage flow. Inspection of the steep artificial banks suggests the banks are relatively stable with no noticeable lateral erosion into or sloughing of the artificial bank. The artificial banks have retained the relatively steep slopes since construction in the 1940s through 1960s.

Many riverbanks other than the steepest slopes (e.g., margins of Pleistocene expansion and channel bars, and White Bluffs) are covered with vegetation including grasses, shrubs, and occasionally trees. The plant communities consist of well-established upland and riparian vegetation. The density of vegetation has increased on the lower banks (i.e., riparian areas) since construction of flood control dams and storage reservoirs on the upper Columbia River. The increase in vegetation is largely due to controlled discharges from the upper Columbia that has affected sediment aggradation and degradation in the study area. Stream power has been significantly reduced (approximately 50%) that has resulted in reduced erosion along the riverbanks, increased deposition of fine-grained sediment in interstitial spaces among gravel clasts and mantling gravel treads, and creation of an ideal environment for establishing plant growth. An increase in the density of vegetation, particularly riparian vegetation, reduces the potential for stream erosion and increases the stability of the stream bank.

6.2.4 Assessment of River Stability

The Columbia River is the major perennial stream that drains about 670,000 km^2 (259,000 mi^2) of the continental interior of the Pacific Northwest. The dynamic hydraulic processes acting on the channel and overbank environment have continuously molded and shaped the river valley since cessation of large-scale cataclysmic flooding in the late Pleistocene. Field mapping has revealed that the streambed of the Columbia River over the past 10,000 years has both aggraded sediments creating an extensive network of fluvial bedforms and eroded a complex series of channelways, island/bar complexes, and escarpments.

Bedforms formed in the streambed as a result of sediment accumulation are grouped into three categories. The categories are distinguished based on the bedform position in either the channel or floodplain and the length of time the bedform has remained "stationary" in the streambed. Bedforms include those identified over the past 10,000 years, but with emphasis on the modern-day river:

- Channel bedforms (primary architectural elements CHM, GBM, and SB; minor element FF) that are transient features that commonly deposited during low-stage flow and eroded at high-stage flow. These bedforms are modern-day features that are generally retained in channelways from 1 to 100(?) years before being eroded, re-entrained into the flow, and sediments transported downstream.

- Channel bedforms (primary architectural element DA) that are relatively "fixed" in the channelway, but are continually molded and typically prograde downstream as accretionary bedforms. The bedforms occur in the modern-day channel, but were initially formed in many cases more than 2,000 years ago. The bedforms are actively aggrading sediments. Bedforms in this category typically persist the river channel for more than 100 years.

6.2 RIVER STABILITY

6.2.4 Assessment of River Stability

- Floodplain bedforms (primary architectural elements LV and FF, and minor CR, CS, and CH(FF)) capping gravel treads (H-3 through H-6 Terraces) that formed a series of paired downward-steeping terraces. The overbank alluvium aggraded during the sediment accumulation phase of the deposition/erosion cycles that characterize the Columbia River throughout the Holocene. The bedforms occur on the terrace steps on both sides of the river along extensive portions of the river valley. Sedimentation in the Columbia River associated with the H-3 Terrace started about 10,000 years ago, followed by sediment deposition on the H-4, H-5, and H-6 Terraces, respectively. The H-6 Terrace is associated with the modern-day floodplain of the Columbia River.

Erosional scouring of the river valley has been observed during the field mapping phase of this study and is largely expressed in the form of unconformities within the stratigraphic sequences and presence of erosional escarpments. The erosional features found in the study area are summarized in the following categories:

- Small-scale erosional scarps that occur as active cutbanks and are commonly associated with fluvial bedforms in architectural elements DA, FF, and LV. The scarps occur throughout channel and floodplain of the modern-day Columbia River, but are generally restricted to less than 3 m in height and often less than 200 m in length.

- Large-scale erosional scarps that form present prominent landforms and result from scouring older geologic materials. Examples in the study area include scarps composed of Columbia River basalt in the Sentinel Gap, Priest Rapids and Umtanum Ridge river segments; scarps of alluvial sediments from scouring of the Ringold Formation and debris from ancient and modern-day landslides along the White Bluffs in the Horn, Sloughs, and Wooded Island river segments; and steep slopes carved into the glaciofluvial flood bars in the Umtanum and N-channel river segments. These scarps vary from several meters to over 50 m in height and often extend over one kilometer along the river.

- Terrace flights (H-3 through H-6) are evidence of several cycles of sediment accumulation interrupted by river entrenchment. The terraces are paired landforms that are 1 to 3 m in height and are exposed along most riverbanks where there a floodplain is present. Elsewhere, the land bordering the river channel is above the level impacted by high-stage flow. The treads of the downward-steeping benches are trend parallel (same horizontal gradient) to the modern-day uncontrolled river channel and represent a net entrenchment into the streambed over the last 10,000 years.

The field mapping and aerial photo analysis of the modern-day river within south-central Washington have shown the river to a dynamic system based on the occurrence of aggrades bedforms in channelways and the floodplains, and scouring along the stream bed and riverbanks. The general rate of sediment aggradation along the streambed has remained relatively constant for many bedforms (architectural elements CHM, GBM, SB, and DA). There are several bedforms that have increased in density, including:

- GBM below the channel constriction between Locke Island and the Locke Island landslide in the Horn river segment

- SB downstream of landslides that have entered the river from irrigation-induced mass wasting of the White Bluffs that occur in the Sloughs and Wooded Island river segments

- FF and CH(FF) capping the H-6 Terrace tread with a corresponding increase in the density of plant communities that occur in most river segments.

6.2 RIVER STABILITY

6.2.4 Assessment of River Stability

Scouring of the riverbanks has been observed several localized areas of the river valley including:

- Undercutting of the White Bluffs in the Horn river segment
- Lateral erosion of the H-6 Terrace at the left bank above Coyote Rapids, right bank at the Horn, and across from Homestead Island
- Small cutbanks that are common to most island/bar complexes.

Overall, changes in the streambed from sediment accumulation and erosional scouring are relatively minor, and the geologic materials are mostly being transferred slowly through the study without much overall net change in accumulation or degradation of material. The riverbanks (natural and engineered) are stable except for short segments that have undergone lateral scour. The most active banks for lateral erosion in along the White Bluffs that are receding at a long-term average rate of 30 cm/yr. The stream forms a straight river system that was established 10,000 years ago and continues a long-term low rate in streambed incision of 0.6 mm/yr. The morphological pattern has not significantly changed over climatic/hydrologic conditions that have existed over the past 10,000 years. In addition, the river has sufficiently entrenched into the streambed to preclude significant channel avulsion. The conclusion of the assessment is that the Columbia River over the 137-km segment of the study is a stable stream system. It is expected to remain stable even under the controlled conditions imposed on the hydrologic conditions of the river by the network of dams and reservoirs that operate in the upper Columbia River basin.

7.0 SUMMARY AND CONCLUSIONS

This section summaries key results and conclusions of this study of sediments and bedforms in the lower slopes of the Columbia River valley from Sentinel Gap (RM 410) to the confluence of the Snake River (RM 325).

- The history of the Columbia River in the river valley is preserved within a series of seven downward-stepping terraces. The terraces are incised into the stream bed forming erosional terraces that are continuous along extensive portions of the river valley. The terraces occur on adjacent river banks at the same elevation creating paired terraces. The terraces have been designated in descending order: P-1, H-1 through H-6.

- The terraces represent cycles of sediment accumulation and river rejuvenation (erosion through lateral planation and incision) along the valley floor. Such landforms are common to many mid-latitude, continental river systems in post-glacial times. The cycles in the four lowest (i.e., H-3 through H-6 Terraces) reflect changes in fluvial processes in the upper river basin and are likely associated with climatic changes.

- The planform of the Columbia River changed significantly over the late Pleistocene and Holocene based on river position, lithofacies, architectural elements, and geomorphic features. The morphological classification of the Columbia River is based on examination of terraces and classification changes from the end of Pleistocene large-scale cataclysmic flooding to the modern-day river. The progressive changes in planform from a glacial to the modern river are as follows:

  – Shallow, broad anastomosing (multiple-channel) stream with large-scale braided network of bars and channelways (P-1 Terrace)

  – Shallow single-channel braided stream with network of moderate-scale bars and channelways (H-1 and H-2 Terraces)

  – Shallow to entrenched straight stream with a channel containing a sinuous thalweg and bank-attached (alternate) and mid-channel bars, and an overbank environment with a floodplain and levees (H-3 Terrace)

  – Entrenched straight stream with a channel containing a sinuous thalweg and bank-attached (alternate) and mid-channel bars, and an overbank environment with a floodplain and levees (H-4 through H-6 Terraces).

  The changes observed in the planform reflect the transition from a glacial climate to a warmer post-glacial climatic period.

- The Columbia River from the time of the H-1 Terrace to present day occupies only a small part of the river valley and appears too small to have eroded the valley. The stream is underfit for the river valley. Most of the extensive erosion of the valley occurred during the Pleistocene when the river had very high discharges due to large outburst floods from Glacial Lake Missoula.

- The Columbia River has transported mainly pebble-cobble gravel with some suspended material from the time the river occupied the P-1 Terrace through the present system. The dominance of gravel classifies the river as a bedload fluvial system.

- The course of the Columbia River is controlled by the geologic structure of the landscape. The river segment between Sentinel Gap (RM 410) and Umtanum Ridge (RM 396) is eroded into basalt and transects the Saddle Mountains anticline at Sentinel Gap. The portion of the river forms an antecedent stream. At Umtanum Ridge the river abuts against the basaltic ridge and bends eastward into the central Pasco Basin where the river course follows near axis of the Wahluke and Pasco synclines to the downstream end of the study area (RM 325). This segment of the river follows a course created by the slope and configuration of the surface and based on structural controls. Downstream from Umtanum Ridge, the river forms a consequent stream.

- Artifacts of ancient man have been observed on most terraces with abundant artifacts found on the lower four steps (H-3 through H-6). The overbank alluvium of the H-3 Terrace is likely host sediment for Kennewick Man. The oldest evidence found in the study area is lithic fragments (1) at a point bar near the downstream end of the N-channel and (2) on a mid-channel bar in the China Bar area (RM 390). Both of the older sites are located far inland form the present-day Columbia River. The artifacts rest on the surface of fluvial bars on the H-1 Terrace.

- The architectural elements change as the river planform evolved. The GBL and CBL elements dominate the P-1 Terrace and represent sediment accumulation from small-scale outburst floods and meltwater from backwasting of the continental ice sheet during the late glacial period. The GBM and CHM elements are most extensive in the H-1 and H-2 Terraces with the SB element increasing on the H-2 Terrace. The sedimentary deposits accumulate in a fluvial environment of discharge and bedload that were significantly higher than today, but less than the P-1 Terrace period. The lower four steps have principally GB and SB elements in the channel and mainly FF and LV elements in the floodplain. The river during the last steps deposited sediments mainly by floods associated with high spring runoff from melting of the snowpack in the upper river basin.

- The age of the terraces were estimated based on radiocarbon and tephrochronology dating methods primary from the study area, as well as constraints from other published papers. The age of the fluvial sediments along with erosional cycles follow:

1	Sediment accumulation on H-3 Terrace	9,360 to 6,800 rcybp
2	River entrenchment into H-3 Terrace	6,800 to 4,900 rcybp
3	Sediment accumulation on H-4 Terrace	4,900 to 2,100 rcybp
4	River entrenchment into H-4 Terrace	2,100 to 1,800 rcybp
5	Sediment accumulation on H-5 Terrace	(est) 1,800 to 1,200 rcybp
6	River entrenchment into H-5 Terrace	1,200 to 500 rcybp
7	Sediment acscumulation on H-6 Terrace	500 to 300 rcybp
8	Erosion on H-6 Terrace	300 to 30 rcybp
9	Sediment reaccumulation on H-6 Terrace	30 years to present

- The modern Columbia River channel is relatively stable based on:

  - Preservation of a set of downward-stepping terraces along extensive portions of the river valley.

  - Entrenchment of the river channel into resistant bedrock (basalt and mudstone/conglomerate) over most of the river channel.

  - The river is incising at an average rate of 0.6 mm/yr using the H-3 through H-6 Terrace treads.

  - Establishment of vegetation communities along the river banks.

  - Reduced stream power due to regulated flow within the river basin that is controlled by a network of dams and storage reservoirs.

  - River banks have sufficient height above 100-year flood to prevent major channel avulsion.

- Geologic processes that could locally impact the stability in local parts of the channel include:

  - Undercutting of White Bluffs near the Horn as a result of hydraulic erosion. The river has been undercutting the bluffs at the Horn at an average rate of 30 cm/yr in the Holocene.

  - Irrigation-induced landslides have encroached into the river channel, resulting in increased stresses mainly along river banks and bank-attached/mid-channel bars and erosion of the banks (e.g., Locke Island).

  - Artificial river banks constructed along short segments of the river may be subject to higher rates of erosion than naturally occurring banks.

  - The prograding delta of the Yakima River into the right bank of the Columbia River channel has created stresses on the left bank of the trunk stream. The long term effect will be a minor shift of the Columbia River channel to the left bank.

8.0 REFERENCES

Bacon, C. R., 1983, "Eruptive History of Mount Mazama and Crater Lake Caldera, Cascade Range, U.S.A.," *Journal of Volcanology and Geothermal Research*, Vol. 18, pp. 57-115.

Baker, V. R., 1973, *Paleohydrology and Sedimentology of Lake Missoula Flooding in Eastern Washington*, Geological Society of America Special Paper 144, Boulder, Colorado, 79 p.

Baker, V. R., B. N. Bjornstad, A. J. Busacca, K. R. Fecht, E. P. Kiver, V. L. Moody, J. G. Rigby, D. F. Stradling, and A. M. Tallman, 1991, "Quaternary Geology of the Columbia Plateau," *The Geology of North America*, Vol. K-2, "Quaternary Nonglacial Geology, Conterminous United States," Geological Society of America, Boulder, Colorado, pp. 215-250.

Benito, G. and J. E. O'Connor, 2002, "Number and Size of Last-Glacial Missoula Floods in the Columbia River Valley Between the Pasco Basin, Washington, and Portland, Oregon," *Geological Society of America Bulletin*, Vol. 115, No. 5, pp. 624-638.

Bjornstad, B. N., K. R. Fecht, and C. J. Pluhar, 2001, "Long History of Pre-Wisconsin, Ice-Age Floods: Evidence from Southeastern Washington State," *Journal of Geology*, Vol. 109, pp. 695-713.

Bjornstad, B. N., N. A. Cadoret, P. R. Nickens, and M. K. Wright, 1998, *Monitoring Bank Erosion at the Locke Island Archaeological National Register District: Summary of 1996/1997 Field Activities*, PNNL-11970, Pacific Northwest National Laboratory, Richland, Washington.

Booth, D. B., K. G. Troost, J. J. Clague, and R. B. Waitt, 2004, "he Cordilleran Ice Sheet," Chapter 2 in A.Gillespie, S. C. Porter, and B. Atwater (eds.), *The Quaternary Period in the United States: International Union for Quaternary Research*, Elsevier Press, p. 17-43 (Reprint).

Bridge, J. S., 1985, "Paleochannel Patterns Inferred from Alluvial Deposits: A Critical Evaluation," *Journal of Sedimentary Petrology*, Vol. 55, pp. 579-589.

Bretz, J. H., H. T. U. Smith, and G. E. Neff, 1956, *Channel Scabland of Washington – New Data and Interpretations*, Geological Society of America, Vol. 67, pp. 957-1049.

Brice, J. C., 1964, *Channel Patterns and Terraces of the Loups Rivers in Nebraska*, U.S. Geological Survey Professional Paper 442-D, Boulder, Colorado.

Chatters, J. C., H. A. Gard, and P. E. Minthorn, 1992, Fiscal Year 1991 Report on Archaeological Surveys of the 100 Areas, Hanford Site, Washington, PNL 8143, Richland, Washington.

Fecht, K. R. and D. C. Weekes, 1996, *Geologic Inspection of the Sedimentary Sequence at the Environmental Restoration Disposal Facility*, BHI-00230, Bechtel Hanford, Inc., Richland, Washington, 17 p.

Fecht, K. R., S. P. Reidel, and A. M. Tallman, 1987, "Paleodrainage of the Columbia River System in the Columbia Plateau of Washington State – A Summary," in J. E. Schuster (ed.), *Selected Papers on the Geology of Washington*, Bulletin 77, Division of Geology and Eastern Sciences, Olympia, Washington.

Fecht, K. R., T. E. Marceau, B. N. Bjornstad, D. G. Horton, G. V. Last, R. E. Peterson, S. P. Reidel, and M. M. Valenta, 2004, *Late Pleistocene- and Holocene-Age Columbia River Sediments and Bedforms: Hanford Reach Area, Washington – Part 1*, BHI-01648, Rev. 0, Bechtel Hanford, Inc., Richland, Washington.

Friedman, G. M., 1962, "On Sorting, Sorting Coefficients, and the Log Normality of the Grain-Size Distributions of Sandstones," *Journal of Geology*, Vol. 70, pp. 737-753.

Griffiths, J. C., 1967, *Scientific Method in the Analysis of Sediments*, McGraw-Hill Book Company, New York, New York.

Hall, B., 1968, *Persistence of River Bars, Columbia River at Hanford, Washington*, U.S. Army Corps of Engineers, Seattle District, Seattle, Washington.

Inman, D. L., 1949, "Sorting of Sediments in the Light of Fluid Mechanics," *Journal of Sedimentary Petrology*, Vol. 19, pp. 51-70.

LeMaitre, R. W. (ed.), 1989, *A Classification of Igneous Rocks and Glossary of Terms*, Blackwell Scientific Publications, Oxford, England, 193 p.

Lemke, R. W., M. R. Mudge, R. E. Wilcox, and H. A. Power, 1975, "Geologic Setting of the Glacier Peak and Mazama Ash-Bed Markers in West-Central Montana," *U.S. Geological Survey Bulletin*, 1395-H, 31 p.

Miall, A. D., 1978, "Lithofacies Types and Vertical Profile Models in Braided River Deposits: A Summary," in A. D. Miall (ed.), *Fluvial Sedimentology*, Canadian Society of Petroleum Geology Memoir 5, pp. 543-576.

Miall, A. D., 1996, *The Geology of Fluvial Deposits, Sedimentary Facies, Basin Analysis, and Petroleum Geology*, Springer-Verlag Press, Berlin, Germany, 582 p.

Marceau, T. E. and J. J. Sharpe, 2002a, *Excavation Report for Archaeological Site 45-BN-888 and 45-BN-606 on the Hanford Site, Richland, Washington*, BHI-01645, Bechtel Hanford, Inc., Richland, Washington.

Marceau, T. E. and J. J. Sharpe, 2002b, *Report of Archaeological Excavations Conducted at UPR-100-F-2 on the Hanford Site, Washington*, BHI-01649, Bechtel Hanford, Inc., Richland, Washington.

Mehringer, P. J., J. C. Shepard, and F. F. Foit, 1984, "The Age of Glacier Peak Tephra in West-Central Montana," *Quaternary Researc*h, Vol. 21, pp. 36-41.

Moody, U. L., 1977, "Correlation of Flood Deposits Containing St. Helens Set S Ashes and Stratigraphic Position of St. Helens Set J and Glacier Peak Ashes, Central Washington," *Geological Society of America*, Abstracts with Program, Vol. 9, No. 7, p. 1098-1099.

Moody, U. L. 1978, "Microstratigraphy, Paleoecology, and Tephrachronology of the Lind Coulee Site, Central Washington," PhD dissertation, Washington State University, Pullman, Washington, 273 p.

Moody, U. L. 1987, "Late Quarternary Stratigraphy of the Channeled Scabland and Adjacent Area," PhD dissertation, University of Idaho, Moscow, Idaho, 419 p.

Mullineaux, D. R., 1986, "Summary of Pre-1980 Tephra-Fall Deposits Erupted from Mount St. Helens, Washington State, U.S.A.," *Bulletin Volcanologique*, Vol. 48, pp. 17-26.

Mullineaux, D. R., J. H. Hyde, and M. Rubin, 1972, "Preliminary Assessment of Upper Pleistocene and Holocene Pumicious Tephra from Mount St. Helens, Southern Washington," *Geological Society of America*, Abstracts with Program, Vol. 4, No. 3, pp. 204-205.

Mullineaux, D. R., J. H. Hyde, and M. Rubin, 1975, "Widespread Late Glacial and Postglacial Tephra Deposits from Mount St. Helens Volcano Washington," *Journal of Research of the U.S. Geological Survey*, Vol. 3, pp. 329-335.

Nakagawa, M. and T. Ohba, 2002, "Minerals in Volcanic Ash 1: Primary Minerals and Volcanic Glass," *Global Environmental Research*, Vol. 6, No. 2, pp. 41-51.

Newcomb, R. C., J. R. Strand, and F. J. Frank, 1972, *Geology and Ground-Water Characteristics of the Hanford Reservation of the Atomic Energy Commission, Washington*, U.S. Geological Survey Professional Paper 717, Washington, D.C.

Noller, J. S., J. M. Sowers, and W. R. Lettis (eds.), 2000, *Quaternary Geochronology Methods and Applications*, AGU Reference Shelf 4, American Geophysical Union, Washington, D.C., 482 p.

Porter, S. C., 1978, "Glacier Peak Tephra in North Cascade Range, Washington, Stratigraphy, Distribution, and Relationship to Late-Glacial Events," *Quaternary Research*, Vol. 10, pp. 30-41.

Powers, H. A. and R. E. Wilcox, 1964, "Volcanic Ash from Mount Mazama (Crater Lake) and from Glacier Peak," *Science*, Vol. 144, pp. 1334-1336.

PSPL, 1982, "Skagit/Hanford Nuclear Project," *Preliminary Safety Analysis Report*, Amendment 23, Puget Sound Power and Light Company, Bellevue, Washington.

Quinn, R. R., 1982, "Variations in Atmospheric Circulation, Mount St. Helens Eruptions," 1980, in Keller, S.A.C. (ed.), *Mount St. Helens: One Year Later*, Eastern Washington University Press, Cheney, Washington.

Reidel, S. P., N. P. Campbell, K. R. Fecht, and K. A. Lindsey, 1994, "Late Cenozoic Structure and Stratigraphy of South-Central Washington," in R. Lasmanis and E. Cheney (eds.), *Second Symposium on the Geology of Washington*, Washington Division of Geology and Earth Resources Bulletin 80, pp. 159-180.

Rice, D. G., 1983, *Cultural Resources at Hanford WPPSS and US DOE, Richland, Washington*, Report prepared for Washington Public Power Supply System, Richland, Washington.

Sarna-Wojcicki, A., 2000, "Tephrochronology," in Noller, J. S., J. M. Sowers, and W. R. Lettis (eds.), *Quaternary Geochronology Methods and Applications*, AGU Reference Shelf 4, American Geophysical Union, Washington, D.C.

Smith, D. G. W. and J. A. Westgate, 1969, "Electron Microprobe Technique for Characterizing Pyroclastic Deposits," *Earth and Planetary Sciences Letters*, Vol. 5, pp. 313-319.

Smith, G. A., 1993, "Missoula Flood Dynamics and Magnitudes Inferred from Sedimentology of Slack-Water Deposits on the Columbia Plateau, Washington," *Geological Society of America Bulletin*, Vol. 105, pp. 77-100.

Smith, H. W., R. Okazaki, and C. R. Knowles, 1977, "Electron Microprobe Data for Tephra Attributed to Glacier Peak, Washington," *Quaternary Research*, Vol. 7, pp. 197-206.

Taylor, R. E., D. L. Kirner, J. R. Southon, and J. C. Chatters, 1998, Letter to *Science*, "Radiocarbon Dates of Kennewick Man, *Science*, Vol. 280, pp. 1171-1172.

Waitt, R. B., 1980, "About Forty Last-Glacial Lake Missoula Jökulhlaups Through Southern Washington," *Journal of Geology*, Vol. 88, pp. 653-679.

Waitt, R. B., 1980, "Cordilleran Icesheet and Lake Missoula Catastrophic Floods, Columbia River Valley, Chelan to Walla Walla, *Guidebook for West Coast Friends of the Pleistocene Field Conference*.

Waitt, R. B., 1985, "Case of Periodic, Colossal Jökulhlaups from Pleistocene Glacial Lake Missoula," *Geological Society of America Bulletin*, Vol. 96, pp. 1271-1286.

Wakeley, L. P. et al., 1998, G*eologic, Geochronologic and Historical Investigations of the Discovery Site of Ancient Remains in Columbia Park, Kennewick, Washington*, U.S. Army Corps of Engineers, Technical Report GL-98-13, Waterways Experiment Station, Vicksburg, Mississippi.

WCC, 1981, "Task D3. Quaternary Sediments Study of the Pasco Basin and Adjacent Areas," Woodward-Clyde Consultants, Report to Washington Public Power Supply System, Richland, Washington.

Westgate, J. A. and M. E. Evans, 1978, "Compositional Variability of Glacier Peak Tephra and Its Stratigraphic Significances," *Canadian Journal of Earth Sciences*, Vol. 15, pp. 1554-1567.

Wilcox, R. E., 1965, "Volcanic Ash Chronology," Wright, H. E. and D. G. Frey (eds.), *The Quaternary of the United States*, Princeton University Press, New Jersey, pp. 807-816.

Woods, V. W., 1954, *A Summary of Columbia River Hydrographic Information Pertinent to Hanford Works 1894-to-1954*, HW-30347, General Electric Company, Richland, Washington, 40 p.

APPENDIX A

FIGURES

Figure 4-1. Map depicting distribution of major relief generations and geologic units in the Columbia River Valley in south-central Washington.

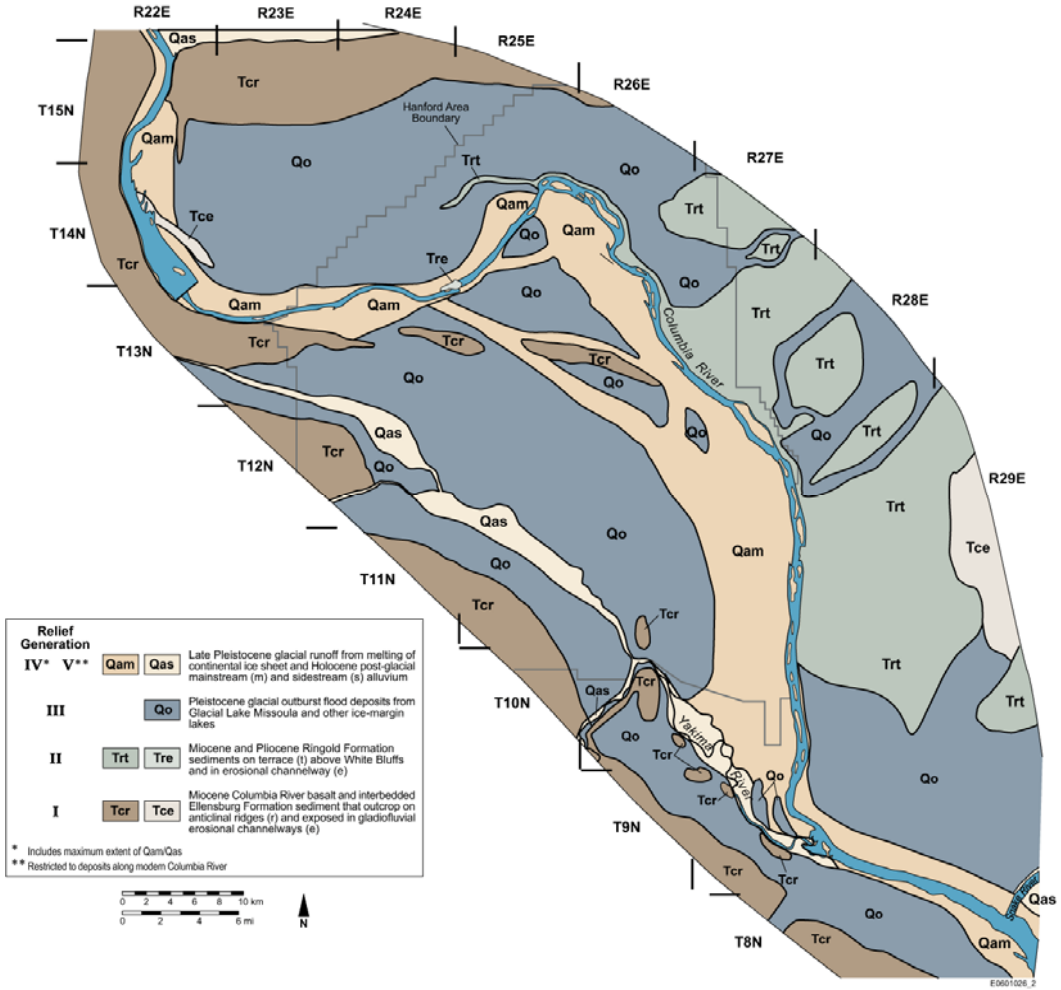

Figure 4-2. Geologic cross-section across Coumbia River Valley at RM 330.

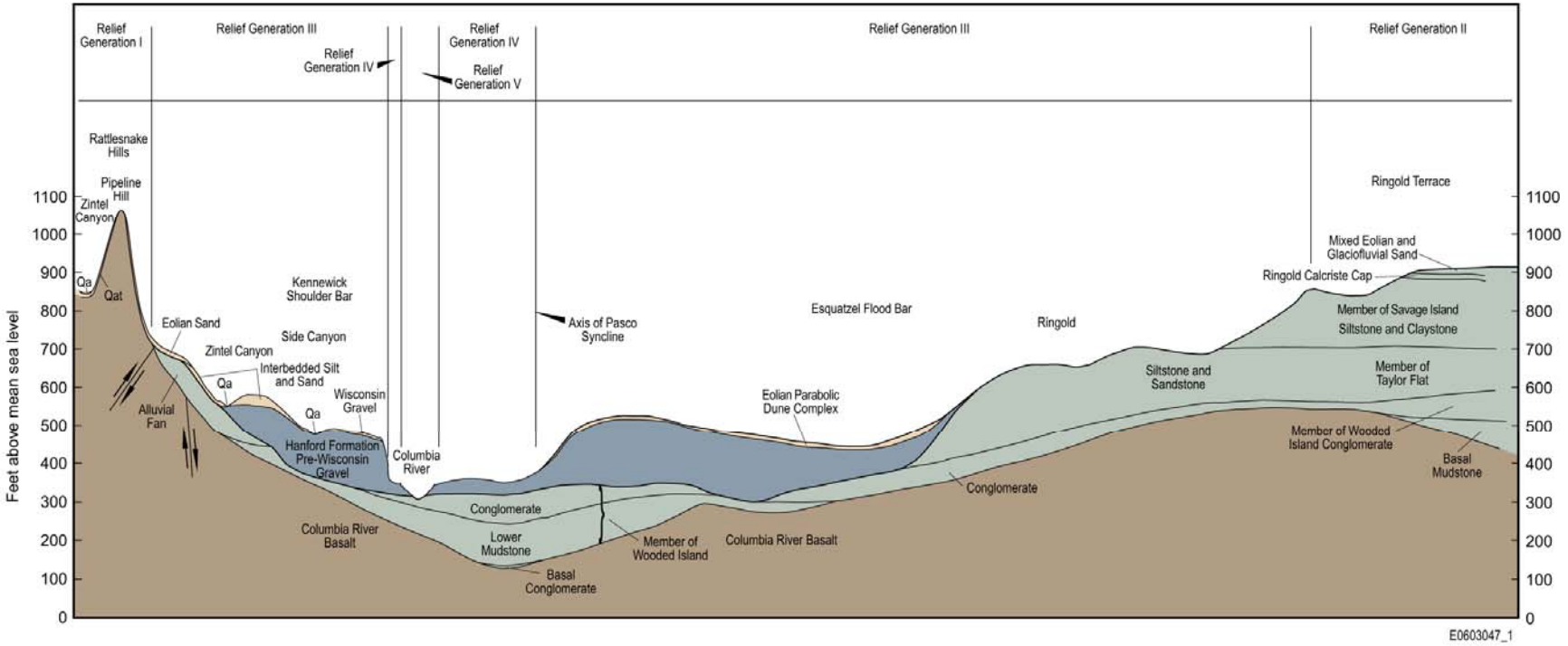

Figure 4-3. Diagram of terrace benches addressed in this study.

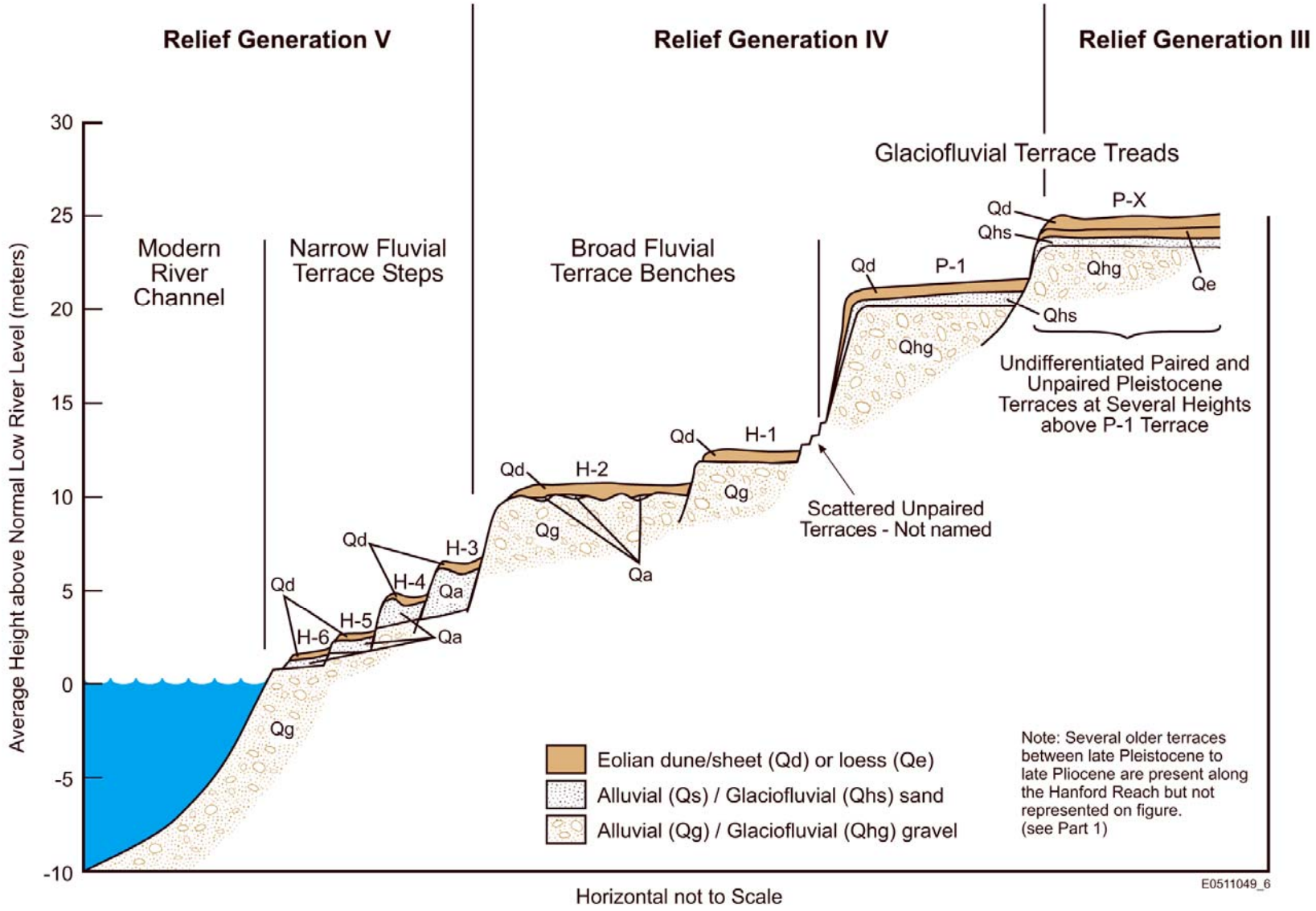

Figure 4-4. Summary of left- and right-bank terraces in Columbia Valley from Sentinel Gap to confluence of Snake River.

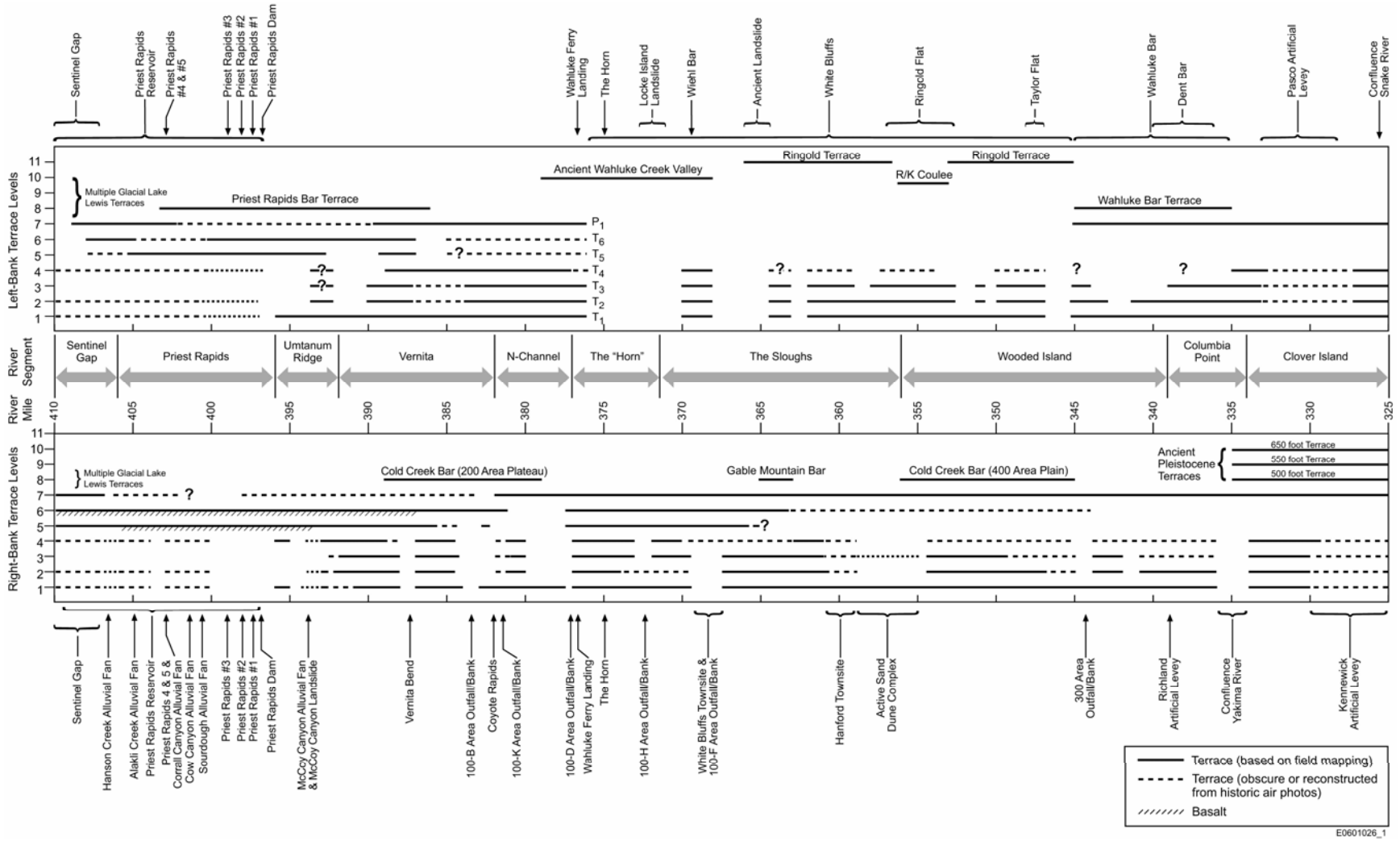

Figure 4-5. Pebble-cobble southwest face upstream of Wooded Island.

Figure 4-6. Cobble-boulder southwest face upstream of Wooded Island.

Figure 5-1. Cascade volcanoes with ash planes discussed in this study.

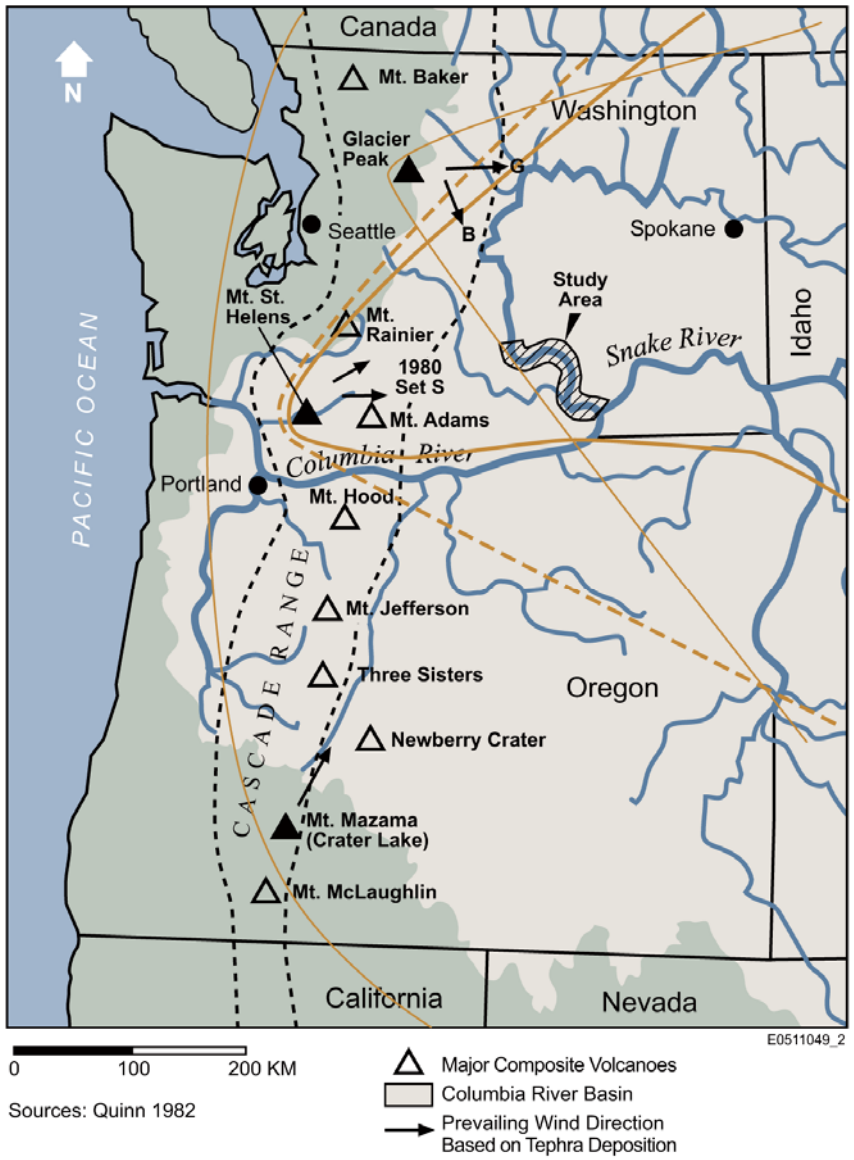

Figure 5-2. General geologic map of the study area depicting selected ash localities.

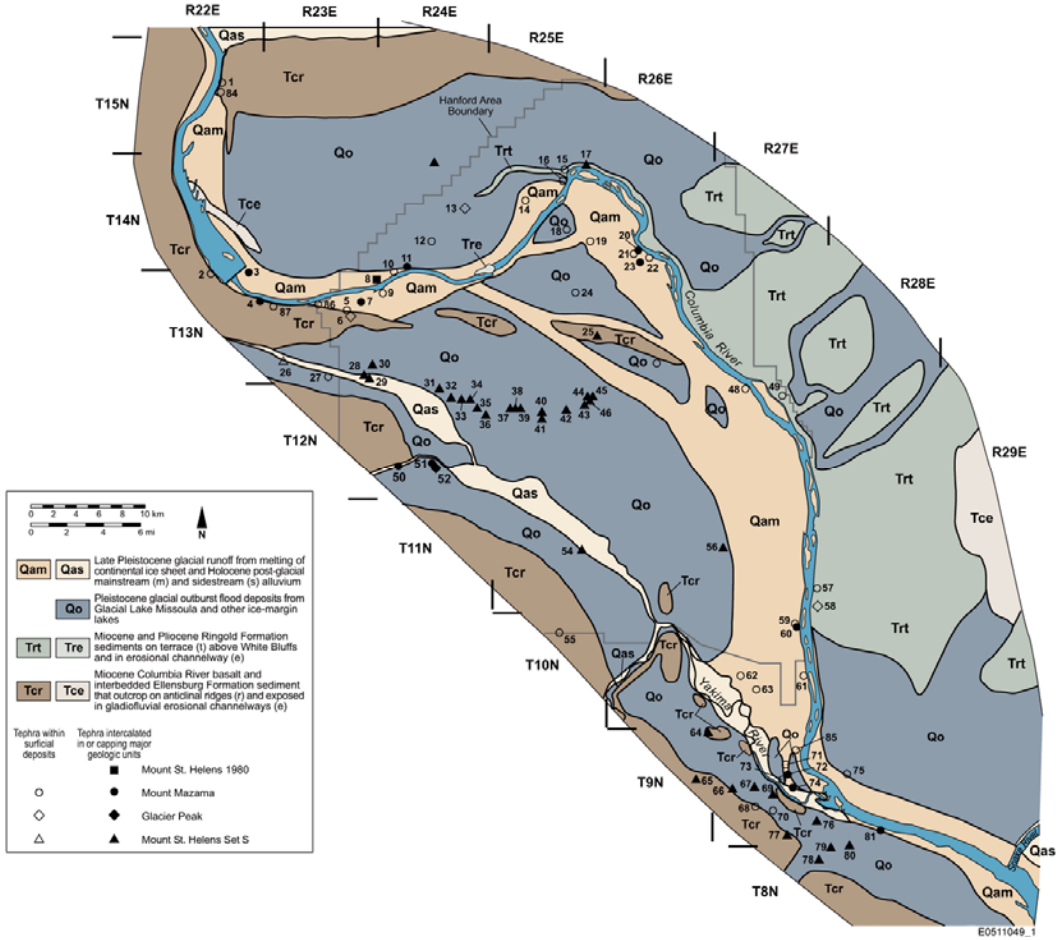

Figure 5-3. Histogram of grain size of selected tephra samples.

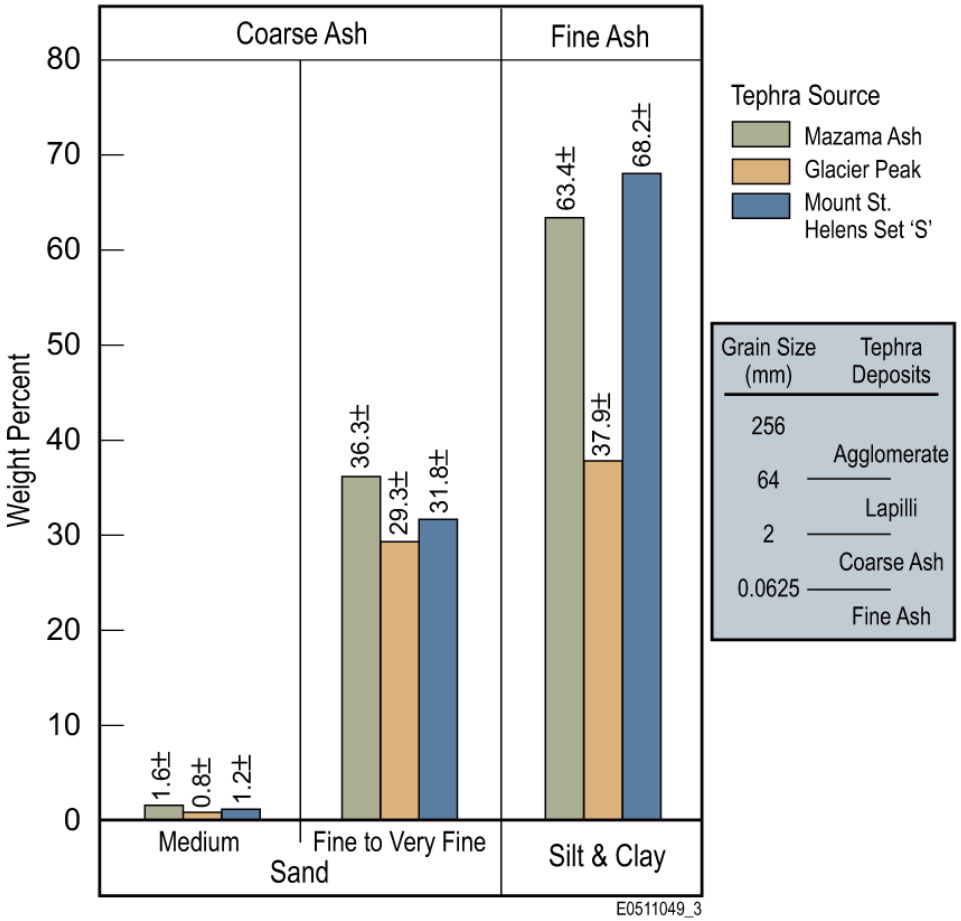

Figure 5-4. Chemical classification of glass shards from Washington State University (a) and from University of Rhode Island (b), using total alkali versus silica. Classification scheme based on LeMaitre 1989.

(a)

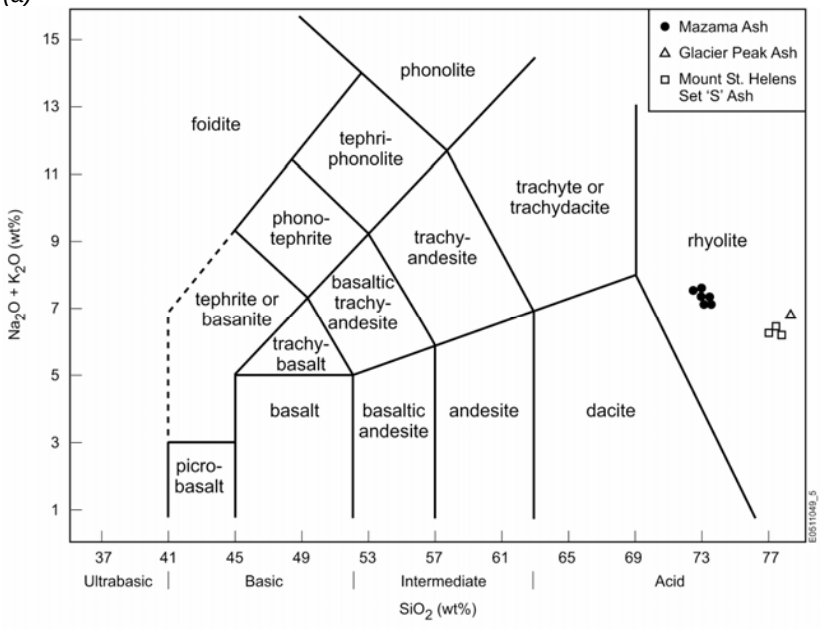

(b)

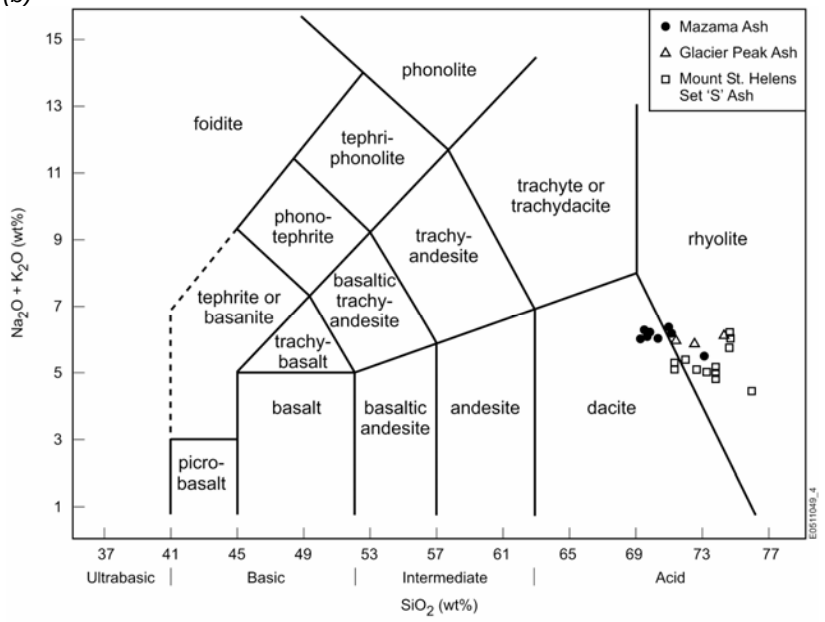

Figure 5-5. Stratigraphic position of Mazama, Glacier Peak, and St. Helens Set S in the lower elevations of the river valley.

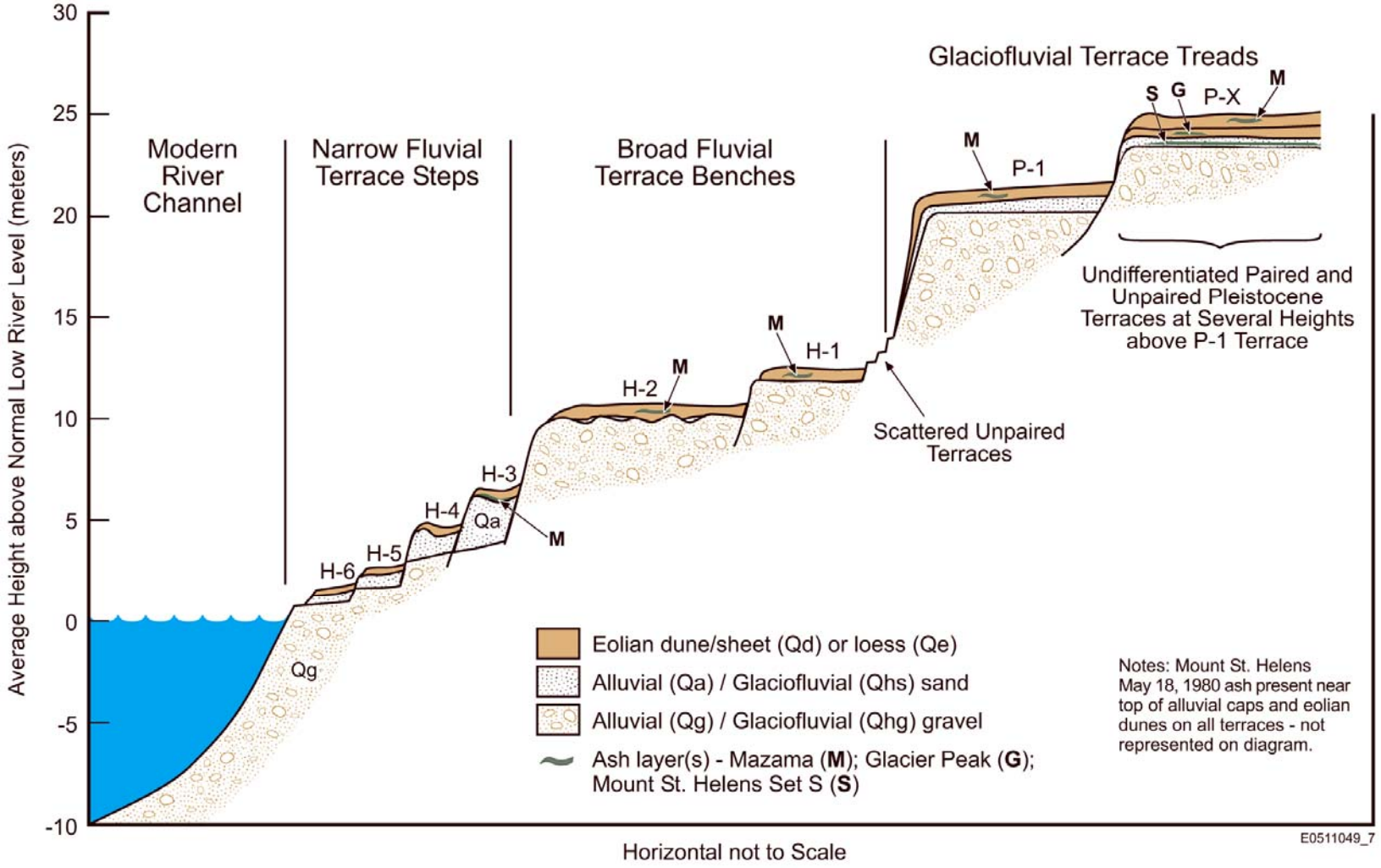

Figure 6-1. Columbia River during late Pleistocene time (post-large-scale glaciofluvial flooding).

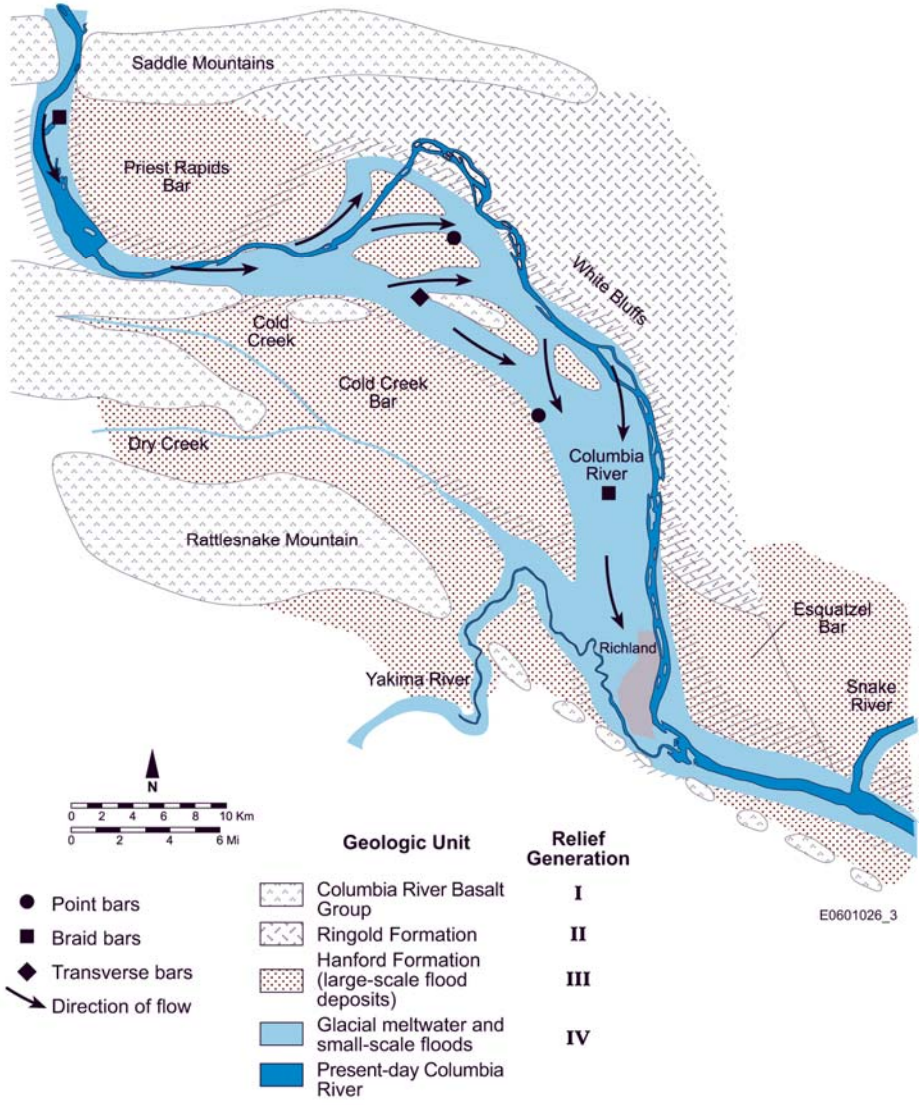

Figure 6-2. Columbia River during early Holocene (H-1 and H-2 Terraces).

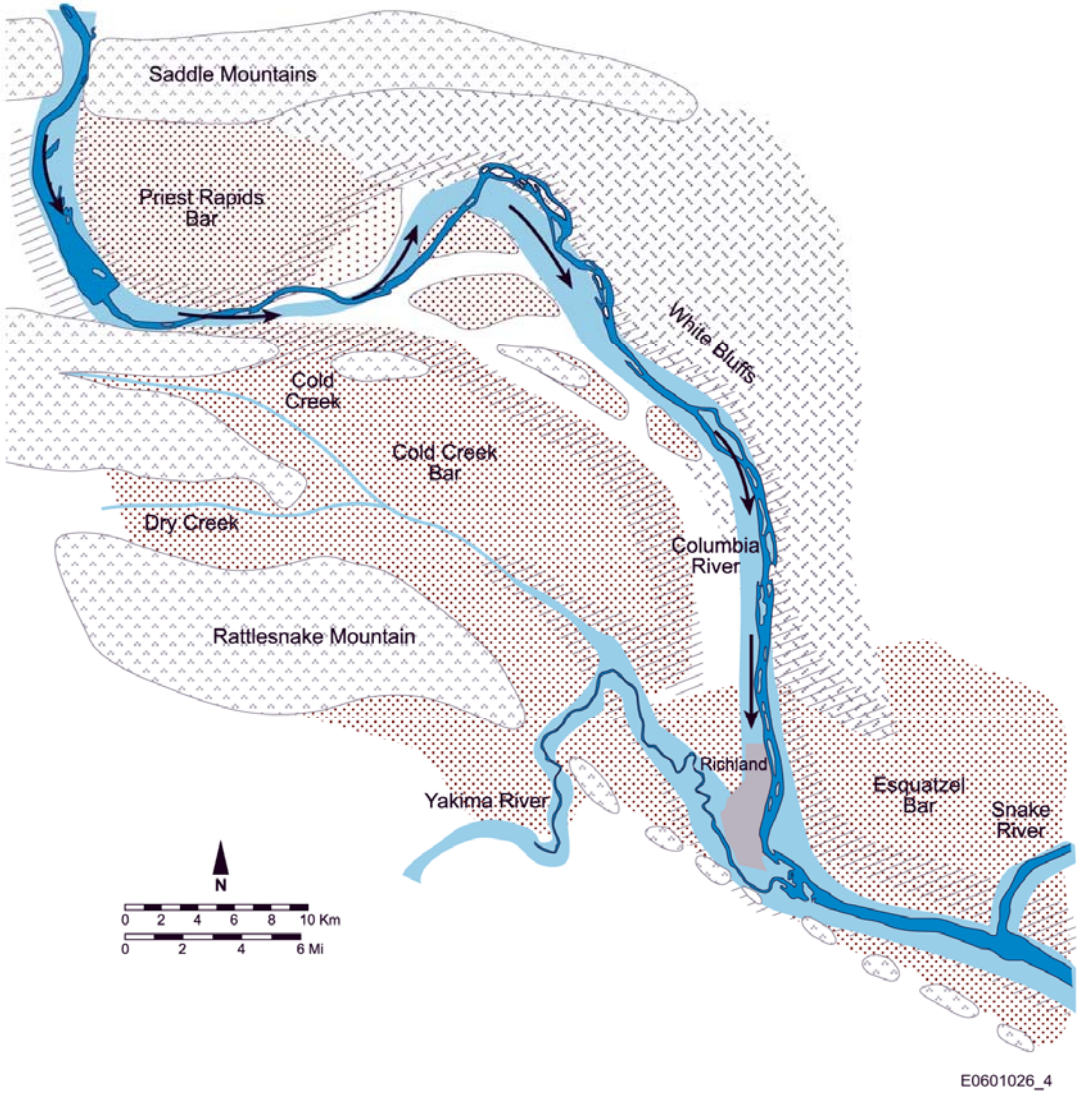

Figure 6-3. Columbia River during the mid to late Holocene (H-3 through H-6 Terraces).

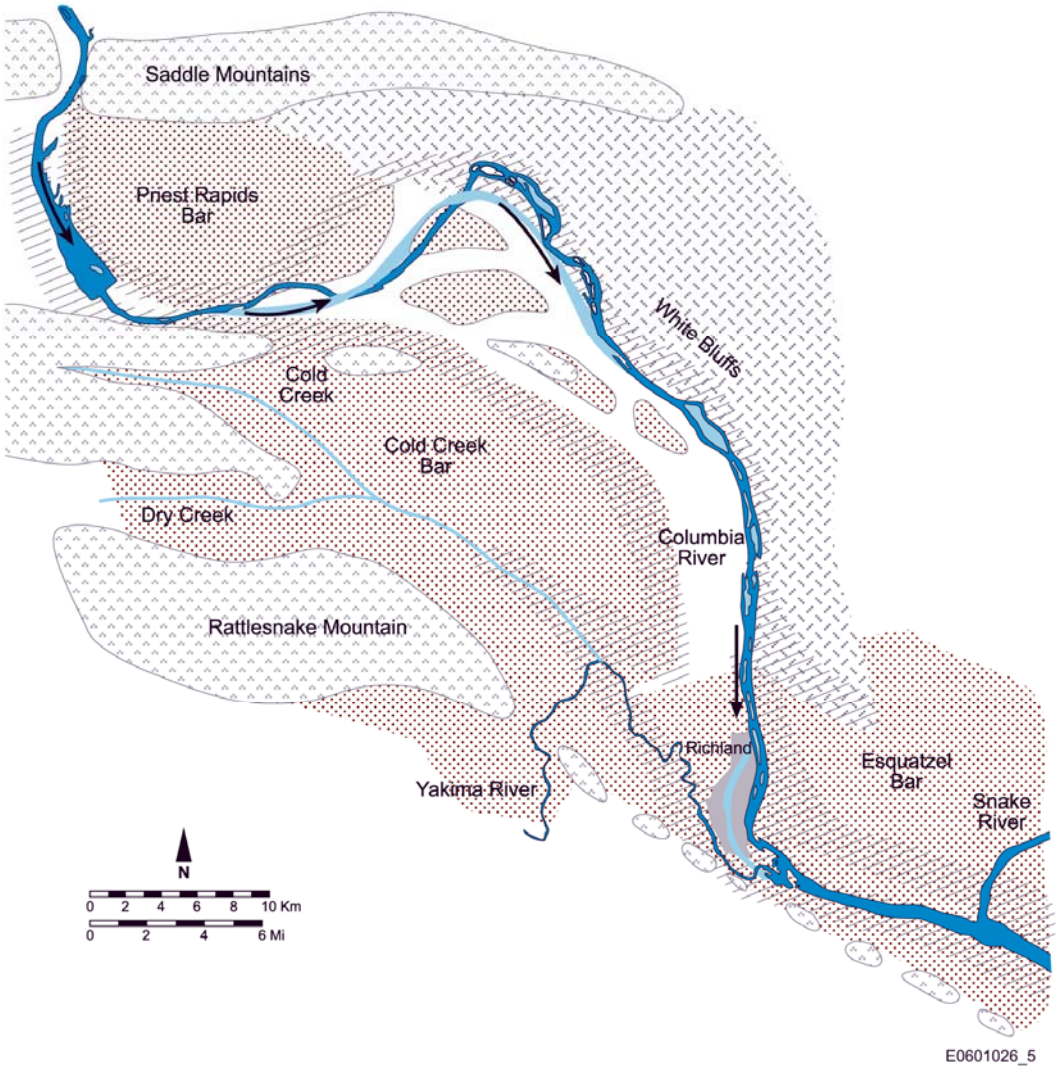

Figure 6-4. Flow rate required to inundated lower fluvial terraces along Hanford Reach.

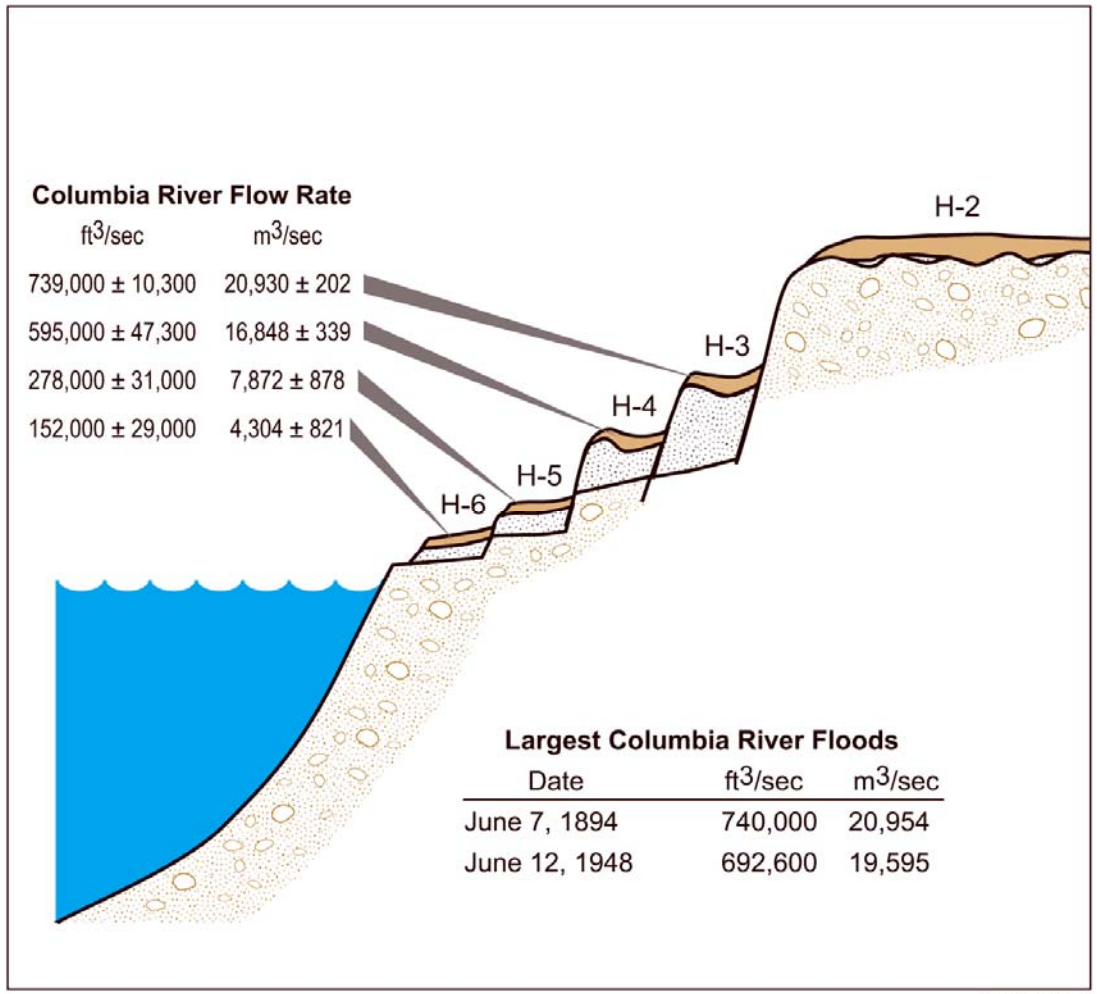

DISTRIBUTION

U.S. Department of Energy, Richland Operations Office

RL Reading Room	H2-53

Washington Closure Hanford

K. R. Fecht (5)	H9-01
K. A. Gano	H9-03
T. E. Marceau (5)	H9-23
J. J. Sharpe	H0-23
D. D. Teel	H9-04
J. E. Thomson	H0-23
Records and Document Control	H0-30
Hanford Technical Library	P8-55

WCH-R & DC mjp 03/29/06

WCH-46
Rev. 0
OU: N/A
TSD: N/A
ERA: N/A

STANDARD APPROVAL PAGE

Title: Late Pleistocene- and Holocene-Age Columbia River Sediments and Bedforms: Hanford Reach Area, Washington – Part 2

Author Name: K. R. Fecht
T. E. Marceau

Approval: J. E. Thomson, Risk Assessment Manager

Signature

3/27/06
Date

The approval signature on this page indicates that this document has been authorized for information release to the public through appropriate channels. No other forms or signatures are required to document this information release.

Geologic Atlas Series

E0507029